AD-A084 936 PISA UNIV (ITALY) INST OF AERONAUTICS F/G 20/11
THE FATIGUE CRACK GROWTH UNDER VARIABLE AMPLITUDE LOADING IN SU--ETC(U)
NOV 79 A SALVETTI, G CAVALLINI, L LAZZERI DA-ERO-78-G-107
UNCLASSIFIED NL

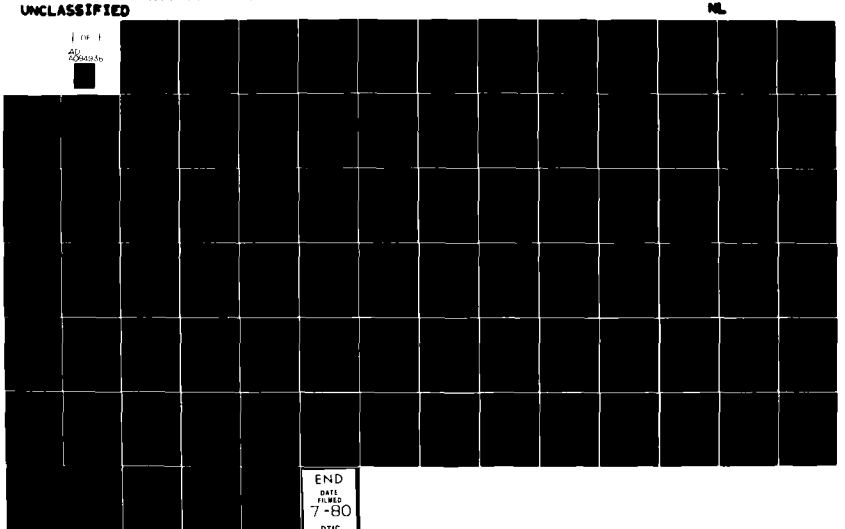

END
DATE FILMED
7-80
DTIC

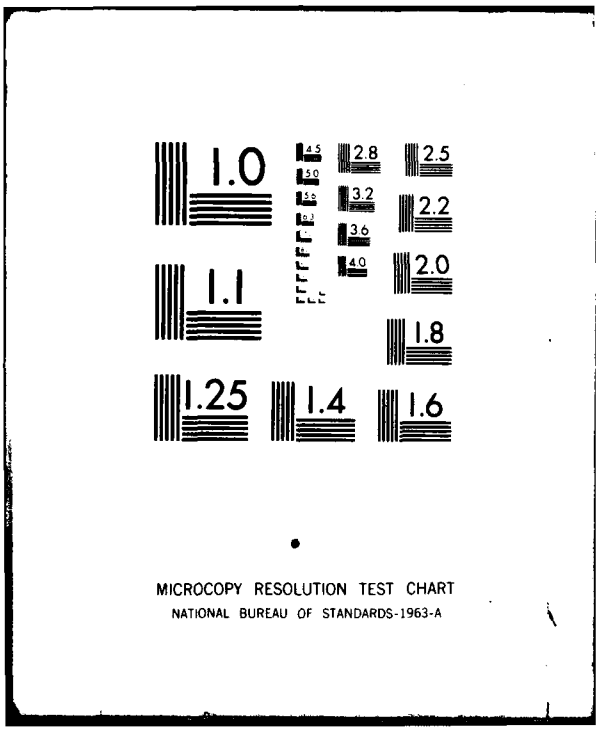
1.0
1.1
1.25
1.4
1.6
1.8
2.0
2.2
2.5
2.8
3.2
3.6
4.0
4.5
5.0
5.6
6.3
MICROCOPY RESOLUTION TEST CHART
NATIONAL BUREAU OF STANDARDS-1963-A

AD

THE FATIGUE CRACK GROWTH UNDER VARIABLE AMPLITUDE LOADING IN BUILT-UP STRUCTURES

1st Annual Technical Report

By

A. SALVETTI - Principal Investigator
G. CAVALLINI and L. LAZZERI

November 1979

EUROPEAN RESEARCH OFFICE

United States Army

London England

LEVEL II

GRANT NUMBER DA-ERO 78-G-107

Istituto di Aeronautica
Università di Pisa
Italy

AD

THE FATIGUE CRACK GROWTH UNDER VARIABLE AMPLITUDE LOADING IN BUILT-UP STRUCTURES

1st Annual Technical Report

By

A. SALVETTI - Principal Investigator
G. CAVALLINI and L. LAZZERI

November 1979

EUROPEAN RESEARCH OFFICE

United States Army

London England

GRANT NUMBER DA-ERO 78-G-107

Istituto di Aeronautica
Università di Pisa
Italy

UNCLASSIFIED

SECURITY CLASSIFICATION OF THIS PAGE (When Data Entered)

R&D 2600 MC/AN

REPORT DOCUMENTATION PAGE

READ INSTRUCTIONS BEFORE COMPLETING FORM

1 REPORT NUMBER

2 GOVT ACCESSION NO. AD-A084 936

3 RECIPIENT'S CATALOG NUMBER

4. TITLE (and Subtitle)

The Fatigue Crack Growth Under Variable Amplitude Loading in Built-up Structures.

5 TYPE OF REPORT & PERIOD COVERED
1st Annual Tech. Report
Sept 78 - Oct 79

6. PERFORMING ORG. REPORT NUMBER

7. AUTHOR(s)

A. Salvetti L. Lazzeri
G. Cavallini

8. CONTRACT OR GRANT NUMBER(s)

DAERO-78-G-107

9. PERFORMING ORGANIZATION NAME AND ADDRESS

Instituto di Aeronautica
Universita di Pisa

10. PROGRAM ELEMENT, PROJECT, TASK AREA & WORK UNIT NUMBERS

6.11.02A1T161102BH57-06

11. CONTROLLING OFFICE NAME AND ADDRESS

USARSG(E)
BOX 65
FPO NY 09510

12. REPORT DATE
Nov 79

13. NUMBER OF PAGES
76

14. MONITORING AGENCY NAME & ADDRESS (if different from Controlling Office)

Annual t . . . rept. no. 1,
Sep 78 - Oct 79

15. SECURITY CLASS. (of this report)

UNCLASSIFIED

15a. DECLASSIFICATION/DOWNGRADING SCHEDULE

16. DISTRIBUTION STATEMENT (of this Report)

Approved for Public Release, Distribution Unlimited

17. DISTRIBUTION STATEMENT (of the abstract entered in Block 20, if different from Report)

18. SUPPLEMENTARY NOTES

19. KEY WORDS (Continue on reverse side if necessary and identify by block number)

Crack Growth (U) Stringer-sheet friction (U) fatigue crack (U) amplitude loads (U) crack propagation (U) fastener-flexibility (U)

20. ABSTRACT (Continue on reverse side if necessary and identify by block number)

The object of this investigation is the development of a reliable procedure for evaluating the growth of a crack in a built-up structure under realistic loading conditions.

To this end tests have been conducted on stiffened and unstiffened panels to monitor the growth of a crack both under constant and variable amplitude loads.

PTO

DD FORM 1 JAN 73 1473 EDITION OF 1 NOV 65 IS OBSOLETE

UNCLASSIFIED

SECURITY CLASSIFICATION OF THIS PAGE (When Data Entered)

401046 LB

The test data has been evaluated on the basis of a deep theoretical analysis which has allowed us to reach significant results on the following main topics:

- influence of the fastener flexibility and stringer-sheet friction forces on fatigue crack propagation in stiffened panels,

- reliability of existing methods for predicting the growth of a crack under loading conditions in plain sheets.

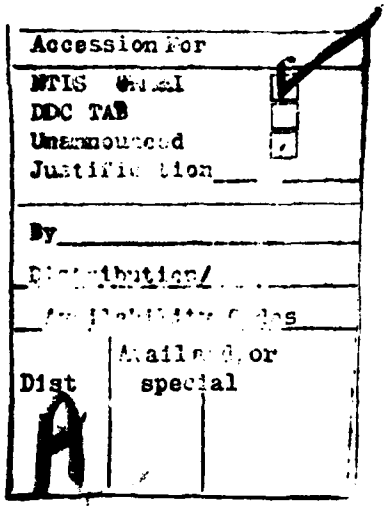

SUMMARY

Research aimed at developing reliable methods to predict the growth of a crack in aircraft built-up structures under realistic load conditions is current being carried out at the Institute of Aeronautics of the University of Pisa under the three-year research contract DA-ERO-78-G-107.

This paper presents the results obtained in the course of the first year. Such results concern two main topics, namely

- *prediction of crack growth in riveted stiffened panels under constant amplitude loading*
- *prediction of crack growth in plain sheets under variable amplitude loading.*

With regard to the first topic, the results concern mainly the evaluation of rivet flexibility and friction forces between the stringer and sheet cover. Such quantities have been obtained by analysis of crack growth test data by means of a SKESA computer program developed ad hoc, which establishes them by searching for the best regression by correlating the crack rate with the stress intensity factor.

As far as the second topic is concerned, a rationale has been developed and implemented in a CADAV computer program to evaluate existing methods for computing crack growth under variable amplitude loading. Attention has been focused on four methods, namely: non-interactive, Wheeler, Bell-Eidinoff and Willenborg methods.

Tests have been performed both atconstant and variable amplitude loading. Constant amplitude test data has been used to obtain reference K-rate relationships. Variable amplitude test data obtained utilizing a FALSTAFF spectrum, has been compared with prediction by means of the CADAV which classifies the methods on the basis of a statistical criterion.

TABLE OF CONTENTS

SUMMARY	Page	III
LIST OF ILLUSTRATIONS	"	V
LIST OF TABLES	"	VIII
LIST OF SYMBOLS	"	IX
1. INTRODUCTION	"	1
2. BRIEF STATEMENT OF THE BASIS OF THE RESEARCH	"	1
3. CRACK GROWTH IN RIVETED STIFFENED PANELS UNDER CONSTANT AMPLITIDE LOADING	"	4
3.1. THE INFLUENCE OF FASTENER FLEXIBILITY AND FRICTION FORCES ON THE FATIGUE CRACK GROWTH PHENOMENON	"	4
3.2. FASTENER FLEXIBILITY AND FRICTION FORCES EVALUATION PROCEDURE	"	5
3.3. EXPERIMENTAL CRACK GROWTH DATA	"	7
3.4. CRACK GROWTH DATA ANALYSIS	"	8
3.5. LIMITS OF THE PRESENT ANALYSIS	"	11
4. EVALUATION OF EXISTING METHODS FOR PREDICTING CRACK GROWTH UNDER VARIABLE AMPLITUDE LOADING	"	13
4.1. THE RATIONALE OF THE PRESENT APPROACH	"	15
4.2. EXPERIMENTAL RESULTS AND ANALYSIS	"	17
4.2.1. CONSTANT AMPLITUDE	"	17
4.2.2. VARIABLE AMPLITUDE LOADING	"	18
5. CONCLUSIONS	"	20
REFERENCES	"	23
APPENDIX 1	"	25
APPENDIX 2	"	27
FIGURES	"	29
TABLES	"	67

LIST OF ILLUSTRATIONS

Figures

Fig. 1.	Typical anomalies in K-rate relationships in stiffened panels due to errors both in SIF and da/dn computation	Page	29
Fig. 2.	Rationale for evaluating fastener flexibility and friction forces from test data	"	30
Fig. 3.	Simplified method for predicting rivet flexibility	"	31
Fig. 4.	Idealization of the friction forces by means of fictitious rivets	"	32
Fig. 5a.	Crack growth data for stiffened panels riveted with countersunk rivets. New series tests	"	33
Fig. 5a.	Continued	"	34
Fig. 5b.	Crack growth data for stiffened panels riveted with round head rivets. New series tests	"	35
Fig. 6a.	Influence of the friction forces on the stress intensity factor as computed by SKESA	"	36
Fig. 6b.	Influence of the rivet flexibility on the stress intensity factor as computed by SKESA	"	37
Fig. 7a.	Test CRIC-8: shape of da/dn vs.ΔK for different values of ξ and η. The dots correspond to couples of values da/dn,ΔK as obtained by spline and K modules. The continuous line is the best-fit curve	"	38
Fig. 7a.	Continued	"	39
Fig. 7a.	Continued	"	40
Fig. 7a.	Continued	"	41
Fig. 7a.	Continued	"	42
Fig. 7b.	Test CRIC-5: da/dn vs.ΔK for different values of ξ and η, plotted as explained in Fig.7a. In this case small loop-type anomalies are present also at the higher values of F_{DATA}	"	43
Fig. 7b.	Continued	"	44
Fig. 7b.	Continued	"	45
Fig. 7b.	Continued	"	46
Fig. 7b.	Continued	"	47
Fig. 7c.	Test CRIC-1: da/dn vs.ΔK for different values of ξ and η, plotted as explained in Fig.7a.In this case loop-type anomalies are present also at the higher values of F_{DATA}	"	48

Fig. 7c.	Continued ..... Page	49
Fig. 7c.	Continued ..... "	50
Fig. 7c.	Continued ..... "	51
Fig. 7c.	Continued ..... "	52
Fig. 8a.	F_{DATA} versus ξ and η for different stiffened panels.The results well depict the different situations found in the present investigation. Test CRIC-9 and CRIC-8 curves are representative of crack rate data which correlate fairly well with Paris law (negligible anomalies in K-rate relationships $\bar{\xi}$ and $\bar{\eta}$). Test CRIC-1 and CRIC-5 are representative of the worst correlations (small but not negligible anomalies at $\bar{\xi}$ and $\bar{\eta}$)"	53
Fig. 8a.	Continued ..... "	54
Fig. 8b.	Standard deviation σ versus ξ and η for different stiffened panels. The same considerations of Fig.8a can be applied ..... "	55
Fig. 8b.	Continued ..... "	56
Fig. 9	Log $\bar{\xi}$ distribution.The curve A is relevant to $\bar{\eta}$ = 0.14.The median value is ξ_2= 0.49 ($\bar{\xi}$=0.686) and the standard deviation is σ_2=0.219 (σ=0.307). The results indicate that the flexibilities found with this approach are noteworthy lower than those predicted by Fig.3 or Douglas formula. The curve B has been obtained considering all the $\bar{\xi}$ belonging to the same population irrespective of the values of $\bar{\eta}$	57
Fig. 10	Errors found in ξ evaluation due to errors in the spline module. Within range of pratical interest $0.2 \leq \xi_2 \leq 0.8$ the absolute error is lower than 0.06 and the relative error is lower than 12%	58
Fig. 11	Typical errors of the spline interpolation technique.The curve with equidistant points is representative of the present approach. The curve with thickened points given an idea of potential improvements that can be obtained by a modified test technique which provides more information in the neighbourhood of maximum and minimum points ..... "	59
Fig. 12	Fatigue crack propagation under spectrum loading. Approach Logic ..... "	60
Fig. 13	Regression analysis on experimental data for evaluating Forman's law ..... "	61
Fig. 14	Regression analysis on experimental data for evaluating Forman's law.Best-fit straigth lines for data relevant to R=cost. ..... "	62

Fig. 15 Lognormal cumulative distributions of the variable n_{ex}/n_c for two ranges of damage growth Page 63

Fig. 16 Comparison of test data with prediction ..... " 64

Fig. 17 Fatigue crack propagation under spectrum loading flat panel.FASLATFF spectrum ..... " 65

Fig. 18 Fatigue crack propagation under spectrum loading stiffened panels. FALSTAFF spectrum ..... " 66

LIST OF TABLES

Tables

Tab.I	Main characteristics of the stiffened panels. Old series tests	Page	67
Tab.II	Main characteristics of the stiffened panels. New series tests	"	68
Tab.III	Results of new series tests	"	69
Tab.III	Continued	"	70
Tab.III	Continued	"	71
Tab.III	Continued	"	72
Tab.III	Continued	"	73
Tab.III	Continued	"	74
Tab.IVa	Optimum values of ξ and η for countersunk rivets tests	"	75
Tab.IVb	Optimum values of ξ and η parameters for round head rivets tests	"	76

LIST OF SYMBOLS

a - Half-crack length, mm.

A_r - Rivet shank cross sectional area, mm^2

da/dn - Crack growth rate, mm/cycle

d - Rivet diameter, mm.

E_c - Sheet Young's modulus, Kg/mm^2

E_r - Rivet Young's modulus, Kg/mm^2

E_s - Stiffener Young's modulus, Kg/mm^2

F_{DATA} - Statistical parameter of regression

K - Stress intensity factor, Kg/mm$^{3/2}$

n - Number of load cycles

P - Rivet load, Kg.

P_f - Fictitious rivet friction load, Kg.

R - Stress ratio

SIF - Stress Intensity Factor, Kg/mm$^{3/2}$

S_{MAX} - Maximum stress of load cycle

S_{MIN} - Minimum stress of load cycle

S_y - Yielding stress, Kg/mm^2

t_c - Sheet thickness, mm.

t_s - Stiffener thickness, mm.

η - Friction parameter

$\bar{\eta}$ - Optimum friction parameter

Δ - Rivet deflection, mm.

ΔK - Stress intensity factor range, Kg/mm$^{3/2}$

ξ - Flexibility parameter

$\bar{\xi}$ - Optimum flexibility parameter

σ - Standard deviation

1 - INTRODUCTION

This paper presents the first year's results of an investigation carried out at the Institute of Aeronautics, Pisa University, under contract DA-ERO-78-G-107.

The objective of this investigation is the development of a reliable procedure for evaluating the growth of a crack in a built-up structure under realistic loading conditions.

To this end tests have been conducted on stiffened and unstiffened panels to monitor the growth of a crack both under constant and variable amplitude loads.

The test data has been evaluated on the basis of a deep theoretical analysis which has allowed us to reach significant results on the following main topics:

- influence of the fastener flexibility and stringer-sheet friction forces on fatigue crack propagation in stiffened panels
- reliability of existing methods for predicting the growth of a crack under loading conditions in plain sheets.

2 - BRIEF STATEMENT OF THE BASIS OF THE RESEARCH.

The need for investigation into crack growth in riveted built-up structures under variable amplitude loading, springs from two main causes, namely the uncertainty surrounding the computational methods of the stress intensity factor and the complexity of the crack growth interaction effects caused by load amplitude variations.

The uncertainty surrounding the K values has to be ascribed mainly to the difficulty of assessing the actual values of the mutual forces existing in the junction between the stringers and the sheet cover, (junction forces).

For a given structure geometry, the junction forces depend on such quantities as the rivet-hole deformation and the friction

between stringer-skin contacting surfaces. Only rough approximations are currently available for such quantities and therefore the stress intensity values computed are affected by errors that may be sufficiently large as far as the crack length, the structure geometry and load level are concerned.

As a consequence of the above, the basic problem of computing the crack growth under constant amplitude loading also involves uncertainty in the case of a stiffened structures.

To overcome the problem knowledge on the junction forces must be improved to such an extent as to compute the stress intensity factor with an accuracy comparable to that reached in the evaluation of K in plane sheets.

As far as the second cause is concerned, the role of the interaction effects in fatigue crack growth problems is well documented, ref.|1|.

One such problem which can be taken as an example is the implementation of reliable crack growth prediction methods, one of the biggest problems in damage tolerant structure design.

The research effort in this area has given rise to very promising results and certain important prediction methods are currently available,|2,3,4,5|.

However, the overall picture of damage accumulation during crack growth under variable amplitude loading is still insufficiently clear and further investigation is required to improve the reliability of crack growth prediction methods.

The production of experimental data on crack growth under load sequences representative of airplane operations must be considered of particular significance in this respect.

Further, as all the existing methods derive their experimental evidence mainly from tests performed on sheet specimens, there is a need for crack growth data drawn from tests on representative airplane structures under realistic loading conditions.

In conclusion, the success of the search for a reliable method to predict crack growth in stiffened structures under variable

amplitude loading depends upon the solution of two related problems, namely,

- further insight into the problem of the evaluation of junction forces to produce a reliable K computational approach and
- critical evaluation of the state-of-the-art crack growth prediction methods for variable amplitude loading through the comparison of a set of experimental crack growth data representative of operational activity as far as load sequences and specimen configurations are concerned.

In connection with the first problem mentioned above significant results can be obtained by suitable analysis of constant amplitude crack growth data.

The second problem can be conveniently dealt with in two successive stages.

In the first stage, by keeping the specimens to be tested as simple as possible (viz. plane sheets for which SIF solutions are well known), the reliability of existing prediction methods can be assessed against crack growth data obtained from different load spectra.

In a second stage, the capability of the most promising prediction methods is further exploited in relation to crack growth data drawn from complex structures (built-up structures) under spectrum loading representative of the operational activity.

In the present report the results obtained in the first year of the research will be presented.

Such results refer to the following main topics:

a_1 - constant amplitude fatigue tests on stiffened panels,

a_2 - development and implementation of a rationale to obtain information on the junction forces (fastener flexibility and friction forces) from the crack growth data in stiffened panels,

b_1 - crack growth tests under variable amplitude loading in plain sheets,

b_2 - development and implementation of a rationale to evaluate the reliability of existing prediction methods of crack growth under variable amplitude loading.

3 - CRACK GROWTH IN RIVETED STIFFENED PANELS UNDER CONSTANT AMPLITUDE LOADING.

In the present section, attention will be focused on the results obtained up to now concerning the improvement of fatigue crack growth prediction techniques in riveted stiffened structures under constant amplitude loading.

Research in this area has been mainly devoted to assessing the influences of fastener flexibility and stiffener sheet cover friction forces on the SIF and to develop and substantiate a rationale to obtain a reliable evaluation of such quantities.

3.1 - THE INFLUENCE OF FASTENER FLEXIBILITY AND FRICTION FORCES ON THE FATIGUE CRACK GROWTH PHENOMENON.

As explained above, to effectively predict fatigue crack growth in a built-up structure, it is necessary to evaluate fastener flexibility and the junction friction forces.

A lot of information on both the above mentioned points can be deduced by comparing the expected K-rate relationship and the relationship based on crack growth test data and K values computed on the basis of selected fastener behaviour (elastic,or elastoplastic behaviour with a selected value of flexibility) and given friction forces.

Fig.1 gives a qualitative indication on the way the information can be obtained from the said comparison. In the upper part of the figure typical data obtained from a plain sheet test is shown.Here both the crack rate da/dn and the stress intensity factor K are increasing functions of the crack length a. Therefore, the relationship between da/dn and K is biunivocal and each point of the curve corresponds to an single value of the crack length.

In the case of stiffened panels, both da/dn and K show maxima and minima according to variations in the crack length, so that the same point of the da/dn versus K curve may correspond to more than one value of the crack length.

In these conditions, anomalies of the da/dn-K curve are possible due to errors or in the computational methods for K (central part of the figure) or in the evaluation of da/dn (lower part of the figure).

In all cases, the da/dn-K curve is no longer a single value relationship and takes on the different shapes shown in a qualitative way in the central and lower part of Fig.1.

These anomalies in the da/dn-K curves can be profitably used to gather information on junction forces (fastener and friction forces), if a highly accurate procedure is available to compute da/dn. In such conditions all the anomalies in da/dn-K curves obtained by processing crack growth test data can be traced back to errors in the SIF computational approach. Since the only significant causes of error in the computation of the SIF can be ascribed to an incorrect value selection of the fastener flexibility and friction forces, it is possible in principle to establish that the "best values" of both these quantities are those which eliminate or minimize such anomalies.

A first application of this concept was shown in references 6 and 7, utilizing a very rough approximation for the computation of the stress intensity factor, namely a zero-friction, rigid-fastener idealization.

The anomalies of the da/dn-ΔK curves so obtained allowed us to establish a qualitative classification of the influences of different parameters (rivet types, stiffener types and materials) on the fatigue crack growth in riveted stiffened structures.

3.2 - FASTENER FLEXIBILITY AND FRICTION FORCES EVALUATION PROCEDURE.

To obtain a quantitative assessment of these influences the

following rationale (Fig.2) has been developed. Crack growth data is obtained by testing stiffened panels under constant amplitude. The da/dn fatigue crack propagation rate is then calculated with a spline function interpolation method (Appendix 1). The stress intensity factor is computed using displacement compatibility methods obtained by modifiyng the original Poe approach by taking fastener elastic flexibility and plasticity into account and by allowing for the influence of friction between sheet and stringer. Rivet flexibility in the elastic range is taken into account by means of a parameter ξ which is the ratio between the actual flexibility and a computed value.

In the present research the computed values have been obtained on the basis of the simplified theory as summarized in Fig.3 and of the Swift formula, ref.|8|.

The fastener load which starts significant plastic deformation is calculated on the basis of simple lap joint tests.

The friction forces have been simulated by a set of fictitious rigid-perfectly plastic fasteners placed between the actual fasteners.

The first fictitious fastener is placed half way between the first and the second rivet, the second fictitious fastener between the second and the third rivet and so on as shown in Fig.4. The fastener load P_f, in correspondence with which sliding takes place, is considered a variable to be determined.

For each couple of values ξ and P_f the stress intensity factor is computed for all the crack lengths relevant to the test under examination.

The da/dn crack rate computed by means of the spline approach is correlated with ΔK obtained following the above mentioned procedure. A best-fit analysis is then carried out utilizing a Paris K-rate relationship. The best-fit is then evaluated through such statistical quantities as the standard deviation, correlation coefficient and F-data. The best values of ξ and P_f are then determined when extremum conditions (minimum for standard deviation and maximum for the other two quantities) are found.Obviously,

only one statistical quantity could be used to obtain the best values of ξ and P_f but redundant information is felt to be useful.

This rationale has been implemented by means of the SKESA computer program based on three main modules, namely the spline module, the stress intensity module, and the best-fit statistical evaluation module.

By means of such a computer program the a-n test data is processed until the best combination of ξ and P_f is found.

3.3 - EXPERIMENTAL CRACK GROWTH DATA.

The rationale described in the previous section was applied by means of the SKESA computer program to a set of a-n data obtained by constant amplitude crack propagation tests.

The main characteristics of the stiffened panels are shown in Tab.I and Tab.II. All the panels are stiffened by straps of the same material as the sheet cover riveted with countersunk or round head rivets. Both 2024-T3 and 7075-T6 aluminum alloys were used in the panel construction.

The stiffened panels of Tab.I differ regarding the geometric configuration, the type of rivet and the material. The panels of Tab.II differ only as far as the type of rivet is concerned.

The panels of Tab.I were tested in the course of previous research and the relevant test data has already been utilized for preliminary analys s of the crack growth phenomenon as outlined in ref.|6,7|.

The panels of Tab.II were tested in the course of the present investigation to obtain further data. The tests were performed with an improved testing technique (see Appendix 2) based on a servo controlled loading machine and on measurement of the successive crack tip positions obtained by means of a sliding microscope which allowed us an absolute error on the crack length no higher than .1 mm. and pratically no error on the number of cycles. The results of such tests, which are given in Tab.III and plotted

in figs 5a and 5b, can also be profitably used to check how the accuracy of the crack length and load measurement can influence the scatter of the phenomenon.

3.4 - CRACK GROWTH DATA ANALYSIS.

All the a-n data relevant to the panels in Tab.I and II have been analyzed utilizing the SKESA computer program.

The elastic flexibility of the rivets has been evaluated by means of a parameter given by:

$$\xi_i = \frac{dP/d\Delta \cdot E_r d}{F_i(\lambda_i, \mu_i)}$$

where the first factor of the numerator is the actual flexibility (see figs 2,3) and the denominator, part of the $1/E_r d$ factor, is a reference value of the flexibility function of the non dimensional geometric ratios λ_i and the Young moduli ratios μ_i.

Two different types of function F_i have been selected for the purposes of the present analysis, namely the function F_1, defined in the lower box of Fig.3 which corresponds to ξ_1, and the function

$$F_2 = 5 + 0.8 \frac{E_r}{E_s} \frac{d}{t_s} + 0.8 \frac{E_r}{E_c} \frac{d}{t_c}$$

which corresponds to ξ_2 obtained from ref. 8 and referred to hereafter as the Douglas flexibility formula.

The plastic range of the load-displacement relationship is accounted for by a very slow slope linear variation starting from a load $\bar{P}$ which depends on the shape and dimensions of the rivets.

The fictitious rivets which simulate the friction forces have been represented by the sliding force P_f (see Fig.2) by means of the parameter

$$\eta = \frac{P_f}{S_y A_r}$$

where S_y is the yielding stress of the rivet material and A_r the rivet shank cross section area.

Therefore, η embodies the scatter due to the variability both in the normal force and in the friction coefficient.

To illustrate the type of data processing performed by means of the SKESA computer program, some typical results are shown in figs 6a to 8b.

Fig.6a shows the influence of the friction forces on the computed values of the SIF. Fig.6b shows the influence of flexibility on the same quantity.

Fig.7 describes how the shape of the da/dn- ΔK curve modifies with varying ξ and η.

Each plot shows da/dn (obtained by test data and the spline module) as a function of ΔK (obtained by the SIF module for selected values of ξ and η), together with the best fit curve computed forcing the da/dn-ΔK to conform to a Paris[1] type K-rate relationship.

Lastly, figs 8a and 8b show typical plots of F-data and standard deviation, σ, as a function of ξ and η; such plots are used to obtain the best values of ξ and η, namely the values $\bar{\xi}$ and $\bar{\eta}$, which maximize (minimize) F-data (the standard deviation).

To contain the computational efforts within acceptable limits, only a relatively small number of values of the variables ξ and η were used to draw such plots.

The couple of values $\bar{\xi}, \bar{\eta}$ which gives extremum conditions among the values selected for ξ and η, was assumed to be the best values of ξ and η without trying a better allocation of the extrema by means of some extrapolation-interpolation technique.

In this way all the values which lie in a given range around the selected values of ξ and η are considered equivalent.

---

(1) *The Paris type K-rate relationship has been selected instead of other types of relationships (Forman or Collipriest), since it works accurately in the ΔK range typical of the present test data.*

This approach is felt to be adequate for present purposes since $\bar{\xi}$ and $\bar{\eta}$, being random variables, can be characterized by their statistic distributions. And, if one tries to determine such distributions simply through histograms, he only needs to know how many values of the random variable lie within each interval selected to construct the histogram.

On the basis of such considerations, as far as η is concerned, after preliminary trials the following values were considered sufficient:

$$\eta_1 = 0,\ \eta_2 = 0.07,\ \eta_3 = 0.014,\ \eta_4 = 0.021$$

which correspond to sliding forces of

$$P_{f1} = 0,\ P_{f2} = 20,\ P_{f3} = 40,\ \text{and}\ P_{f4} = 60\ \text{Kg},$$

on the basis of a rivet diameter of 1/8 and $S_y = 36\ \text{Kg/mm}^2$.

In this way each value η_i can be considered to represent all the values lying approximately in the interval

$$\eta_i - 0.035 \leq \eta \leq \eta_i + 0.035$$

As far as the selection of the variables ξ is concerned, in a first trial we worked with three values of ξ, namely

$$\xi_1 = 0.3 \quad \xi = 0.7 \quad \xi_3 = 1$$

By inspection of the diagram obtained with such values a preliminary rough allocation of the maximum of F-data was obtained.

From such an inspection it was found that ξ is scattered within an interval ranging approximately from 0.1 to 1.

As a consequence of the above, a knowledge of $\bar{\xi}$ within a interval $\bar{\xi} \pm 0.05$ was considered adequate for the purpose of the present investigation.

Calculations were then carried out in the neighborhood of the first approximation best value of ξ with the steps in ξ which

allowed us to locate $\bar{\xi}$ with the said approximation.

The results of the data processing is summarized in Tables IVa and IVb.

Tab.IVa shows the best values $\bar{\xi}$ and $\bar{\eta}$ obtained in the case of stiffened panels with countersunk rivets; tab.IVb gives the same quantities for the stiffened panels with round head rivets.

As far as the countersunk rivet data is concerned, the scatter in $\bar{\eta}$ is negligible and the vast majority of values fall in the interval $0.105 \leq \bar{\eta} \leq 0.175$ and they have been assigned the value $\bar{\eta} = 0.14$.

For such data it was possible to obtain the cumulative distribution of $\bar{\xi}$. Log-normal distribution of such a variable is given in Fig.9.

As far as the data relevant to round head rivets is concerned, a wider scatter in $\bar{\eta}$ has been found and the present data does not allow us to drawn conclusions in term of the distribution of such random variables.

Further data must be collected to obtain a clear picture of the phenomenon.

3.5 - LIMITS OF THE PRESENT ANALYSIS.

The results summarized in the previous section have two limitations. The first one, which is inherent in the data processing system, stems from the accuracy with which the spline module works.

As already explained, the logic of the present approach is to ascribe any anomaly in the K-rate relationship to K evaluation and to determine the best values of flexibility and friction by minimizing such anomalies. But, if anomalies in the K-rate relationships stem from errors in da/dn computation procedure, the best-fit technique tries to eliminate such anomalies by modifying ξ and η.

As a consequence of the above, it is necessary to guarantee negligible errors in the output of the spline module.

However, it is difficult to quantify the accuracy of the method and one must rely mainly on checks performed utilizing comparison

with known functions.

As explained in appendix 1, this was the way used in the evaluation of the spline method.

Good results were obtained by applying the spline module to known functions which present the typical trend of a-n data found in stiffened panels, and by comparing the spline derivatives with the analytical ones.

However, examination of the results in terms of da/dn versus K as in the examples in Fig.7, gave rise to some doubts with respect to the method used to assess the accuracy of the spline module.

It was decided to proceed to a further evaluation based on the following methods.

A Paris K-rate relationship is numerically integrated utilizing SIF solutions corresponding to stiffened panels with different rivet flexibilities.

The a-n data so obtained is then utilized as input to the SKESA computer program.

In such a way, since the actual value of the flexibility is known and since the errors induced by the integration are negligible, the difference between the actual flexibility and that computed by SKESA, can be used to quantify the error in the spline module.

Fig.10 shows the results of such an investigation. As can be observed, errors up to 10% in $\bar{\xi}$ are to be found; such errors are always on the same side and the computed solution is stiffer than the real one. Fig.11 shows a comparison between a typical da/dn-a curve as computed by the spline module and the actual values of such a function.

The spline module fails to reproduce da/dn accurately only in the two zones of maximum and minimum predicting a lower rate in the zone of the maximum and a higher rate in the zone of the minimum.

Improvement in the spline module output might be obtained by thickening the points to be interpolated in the neighbourhood of the points of extremum.

Preliminary results of such an approach,of which a typical example can be seen in Fig.11, indicate that such a way is practicable even if no well founded rule of thickening is at present available.

The second limitation stems from the nature of the scatter in the parameters $\bar{\xi}$ and $\bar{\eta}$. Since flexibility and friction are random variables, different fasteners in the same stiffened panel should be assigned different values of ξ and η in K computation.Obviously such a point of view can hardly be implemented within the limits of acceptable computer times.

The present approach which is based on constant values of ξ and η for a given panel, gives on the contrary weighted averages of such quantities which can be effectively used to compute the SIF and therefore the crack growth rate.

Notwithstanding such limitations, the approach implemented in the SKESA computer program can be considered an effective device for analysis of crack growth data in stiffened panels in order to obtain an engineering evaluation of the fastener flexibility and friction forces.

4 - EVALUATION OF EXISTING METHODS FOR PREDICTING CRACK GROWTH UNDER VARIABLE AMPLITUDE LOADING.

As explained in section 2, the next step in the investigation concerns evaluation of existing methods for predicting crack growth under variable amplitude loading.

Attention has been centered mainly on the following methods, namely the non-interactive, Wheeler,|3|,Bell-Eidincff,|4|, and Willenborg,|2|methods.

The growth of a crack under variable amplitude loading is a complicated phenomenon not fully understood at present.

The prediction methods largely rely upon empiricism and their ability to compare with test data. In such conditions any approach for the evaluation of such methods must be founded on comparison

with test data on the basis of some criterium allowing us to evaluate the fit between test and computation data.

A first question in this respect is the fact that crack growth is a random phenomenon whereas prediction methods are deterministic. As a consequence, any comparison must be judged on a statistical basis.

Further, all the prediction methods considered in the present investigation are cycle by cycle computation procedures.They are based on constant amplitude crack propagation data and account for interaction effects by modifying the stress cycle at the crack tip on the basis of set of rules which differ from method to method (no cycle modification for the non-interactive method).

Therefore, if you are interested in evaluating such rules,you need constant amplitude crack growth data which allows you to make an unbiased prediction. In other words, any error in prediction needs to stem from the rule and not from bad constant amplitude data.

As a consequence of the above, the evaluation carried out in the present investigation has been based on:

- a computer program which implements the above mentioned prediction methods. Such a computer program, named CADAV, has already been described in ref.|9|;
- a rationale to produce unbiased constant amplitude crack growth data and to judge on a statistical basis the fit between experimental and computed crack growth data;
- a set of crack growth test data under constant amplitude loading; such data has been used to define the constant of the semiempirical laws (Paris,Forman and Collipriest) which give analytical expression to the K-rate relationship;
- a set of crack growth test data under variable amplitude loading to compare with the results of the prediction methods. Such data has been obtained by testing centrally through cracked flat specimens with standardized load sequences FALSTAFF,|10| and TWIST,|11|, following the test techniques described in appendix 2.

4.1 - THE RATIONALE OF THE PRESENT APPROACH.

Fig.12 shows the main steps of the rationale.

It comprises two main lines which refer to constant amplitude data generation and analysis and variable amplitude data generation and analysis.

The objective of the first line is the determination of the semiempirical laws (Paris,Forman,Collipriest-Walker) for the material used in the variable amplitude tests with sufficient accuracy to allow us to make an unbiased prediction of crack growth under variable amplitude loading.

To this end starting from the crack growth data obtained with the constant amplitude test program, (see sec.4.2), the following main operations have been carried out:

- generation of K-rate relationships in the form given in the Paris,Forman and Collipriest law by means of the SKESA computer program. SKESA selects the constants which define such laws through a regression analysis substantiated by the usual significance tests;
- computation of the number of N_C cycles necessary to reach a given crack length by integration of the best fit curves defined in the previous step;
- comparison of the experimental crack growth data with the data computed by means of a statistical analysis of the random variable n_{ex}/n_C (n_{ex} being the test value of n_C). Such an analysis consists in the determination of the cumulative distributions of n_{ex}/n_C for different crack lengths with data coming from several specimens.

The first attempt at best-fit gives an unbiased prediction only if the medians of the distributions corresponding to different crack lengths have, apart from small differences, always the same value $(n_{ex}/n_C)_M = 1$.

If this is not so,it means that the semiempirical laws do not

follow the same trend as the test data in some part of the growth interval. A typical cause of this state of affairs is unprevented crack lip buckling in the high crack length range which increases the crack growth rate with respect to the unbuckled condition which the SIF solution refers to.

In these cases, some test data must be left out and the steps previously taken must be repeated on the reduced set of a-n data.

Once unbiased constants of the semiempirical laws have been obtained, evaluation of the variable amplitude data can be carried out.

The main steps of the variable amplitude line are the following:

- utilization of data from damage growth tests in specimens subjected to variable amplitude loading.
  These tests must be conducted with specimens made of material taken from the same batch used in constant amplitude test specimens. Different standardized spectra can be used, namely FALSTAFF, TWIST and Gaussian random; tests with different values of reference stress of spectrum can be performed. For each case -assigned specimen and spectrum at a given value of reference stress- a sufficient number of tests are performed to provide a meaningful statistical analysis;
- prediction of damage growth with the non-interactive, Wheeler, Bell-Eidinoff and Willenborg methods for each test case.
  The computer program CADAV is used for this purpose;
- comparison of the experimental damage growth data with the theoretical data. The comparison is obtained by determining the cumulative distribution of the random variable F_{ex}/F_c, F_{ex} being the number of flights in which the damage grows to an assigned value of size and F_c being the same data obtained with the prediction method.Such a distribution is obtained for different intervals of damage propagation, utilizing an adequate number of tests. The median value of F_{ex}/F_c can be used to measure the fit between test data and prediction methods. Median values near one for all the distributions indicate an excellent capability of the method

to predict crack growth under variable amplitude loading.

Scatter around the median value is another important piece of information that can be obtained from inspection of the distributions. In particular, comparison of scatter between constant and variable amplitude data is of fundamental importance.

4.2 - EXPERIMENTAL RESULTS AND ANALYSIS.

4.2.1 - Constant amplitude.

Following the rationale of the previous section, constant amplitude tests have been performed in order to obtain the expression of semiempirical laws.

Twelve flat specimens with central through crack made in 2024-T3 have been tested for various values of the ratio $R=S_{MIN}/S_{MAX}$. The test apparatus and test procedures are shown in appendix 2.

A detailed explanation of data processing is given in ref.|9|.

Here the final results are reported as far as the Forman law determination is concerned. Fig.13 shows data for all the tests and the best-fit straight line as obtained by regression analysis, together with the scatter band of 10%-90%. In the same figure, the values of the typical constants of the law are also shown.

Fig.14 shows the best-fit straight line relevant for tests with different values of parameter R. The three straight lines lie very close to each other and demonstrate the effectiveness of Forman's law to describe damage growth phenomenon at different values of R; this is an important requirement for a law which must be used in prediction methods for variable amplitude loading.

The Forman's law so obtained has been further analyzed with respect to its capability to predict the number of cycles needed to propagate the damage from the initial dimension to an assigned dimension. The results are given in Fig.15a which shows the distribution on normal probability paper of the variable $\log(n_{ex}/n_c)$ for two intervals of cracks growth.

For the propagation from a_o = 6 mm. to a = 30 mm., the distribution is normal with significant accuracy, and the median value is very close to zero; it means that the Forman's law obtained is fairly representative of the crack growth phenomenon in this crack interval.

For the propagation from a_o = 6 mm. to a 18 mm., the law does not work so accurately as in the previous case.

This state of affairs may be ascribed to higher relative error which affects the test data in the low crack length range since the error in measuring crack dimension is constant. Nevertheless, the prediction can still be considered satisfactory and the law so determined has been used in the prediction methods for crack propagation under variable amplitude loading.

4.2.2 - Variable amplitude loading.

For the second aspect of this research, seven tests have been performed using FALSTAFF spectrum, |10|, [1] with S_{MAX} = 235 MPa on flat panels centrally through cracked made with material 2024-T3, drawn from the same batch used for specimens of constant amplitude tests. The test apparatus and procedure are described in appendix 2.

The results of the analysis are shown in Fig.16 and Fig.17.

Fig.16 shows the crack length versus the number of flights as obtained in the tests of the seven specimens and as predicted by the non-interactive, Wheeler, Bell-Eidinoff and Willenborg methods.

Fig.17 shows the distribution on normal probability paper of the variable $\log(F_{ex}/F_c)$ for two intervals of crack damage.

Such a variable conforms to a normal distribution for the two intervals. The scatter of phenomena, measured from the standard deviation of the variable, is pratically the same as that found

---

(1) *Preliminary tests using the TWIST spectrum have been also performed. The results are given in ref.* |9|.

in constant amplitude data. Such a conclusion seems to indicate no particular effects of delay or acceleration effects due to peak load on the scatter.

For each prediction method the median of the distribution (50% value) provides a good indication of the correctness of the method.

The results are still limited and therefore no general conclusions can be drawn, but certain trends in the flat panels are well established. The non-interactive method predicts life in the safe side with a factor of about 6 in accordance with the pronounced delay effects due to the high peak loads typical of the FALSTAFF spectrum.

The Wheeler method, with an adequate selection of the value of its plastic zone characteristics constant, m = 1.9, produces an "exact" prediction, namely the mean value of random variable log (F_{ex}/F_c) equal to zero.

The Willenborg method gives unconservative results with the FALSTAFF spectrum, where the presence of high compressive loads produces crack acceleration which is not taken into account by this method.

The Bell-Eidinoff method does not tally satisfactorily with experimental data. A possible cause of this state of affairs may be ascribed to the fact that the values of the empirical constants which are taken from the existing literature and which are used to characterize the delay and acceleration effects, might not work very well with the material used in the present investigation. The values of such a constant directly determined by ad-hoc tests might improve the prediction.

The test program on stiffened panels under standardized spectra is now in progress and in this case the experimental data obtained so far shows a larger scatter, Fig. 18, with respect to the flat panels.

The data of Fig. 18 is still preliminary and no comparison with the calculation method has yet been made.

5 - CONCLUSIONS

An investigation on fatigue crack growth in aircraft structures is currently being carried out at the Institute of Aeronautics of the University of Pisa, Italy, under contract DA-ERO-78-G-107.

The final goal of the investigation is the development of a reliable method to predict the growth of a crack in built-up structures under operational load conditions.

The first year's results, presented in this paper, mainly concern the two following topics, namely

- crack growth in riveted stiffened panels under constant amplitude loading
- crack growth in plain sheets under variable amplitude loading.

As far as the first topic is concerned, the results are relevant mainly to the evaluation of the rivet flexibility and friction forces between stringer and sheet-cover. The results of crack propagation tests of stiffened panels part of which are riveted with countersunk rivets, the others with round heat rivets, have been analysed with a SKESA computer program developed ad-hoc,which allows us to obtain the average values of the rivet flexibility and friction forces. SKESA computes such quantities by searching for the best regression in correlating the da/dn crack rate with ΔK.

It works with a good degree of accuracy,the errors in final output being generally of the order of 5% and in each case not higher than 10%. They depend mainly on the spline module which computes da/dn from the test data a-n, and could be reduced by a rational thickening of the points (a,n) to be interpolated in the neighbourhood of the flex points in the a-n curves. This state of affairs implies a modification in the test technique with a different selection of the reading spacings in the measurement of the crack length.

Notwithstanding such errors the SKESA computer program represents a valuable device which allows us to obtain quantitative information

on flexibility and friction which can be then confidently used for analysis purpose.

In particular, it has already been possible to obtain conclusive results as far as countersunk rivets are concerned, by defining the cumulative distribution of the flexibility parameter ξ, and finding the range in which the friction parameter η lies. On the contrary, in the case of round head rivets, the pattern is more scattered and there is still not enough data available at present for statistical analysis.

New research in this area will be carried out, in the continuation of the program, by improving, if possible, the spline module and by producing further test data with stiffened panels constructed with different types of fasteners.

As far as the second topic is concerned, four methods for computing crack growth under variable amplitude loading have been evaluated.

Such methods are the non-interactive, Wheeler, Bell-Eidinoff and Willenborg methods.

Evaluation has been carried out firstly by producing constant amplitude crack growth data to obtain unbiased semiempirical laws (of the Paris, Forman and Collipriest type) and then performing variable amplitude crack growth tests with the FALSTAFF spectrum on specimens made with material coming from the same batch as the constant amplitude test specimens. The numbers of flights necessary to increase the crack in a given interval F_{ex} as obtained by testing different specimens, are compared with predictions F_c as obtained from the CADAV computer program, which implements the above mentioned method by utilizing the previously determined semiempirical laws. The comparison is made on a statistical basis by finding the distribution of Log F_{ex}/F_c for the different methods and for different crack growth ranges. The median of the distribution is then used as measurement of the accuracy of each method.

The results obtained up to now indicate that the Wheeler method can be confidently used at least with the FALSTAFF spectrum.

An important conclusion of this analysis concerns the scatter which has been found to be of the same order both in constant and variable amplitude tests.

Further research in this area will be carried out by performing tests both on plain specimens and stiffened panels utilizing new loading spectra (TWIST and Gaussian random loads) and increasing the test data obtained with the FALSTAFF spectrum.

REFERENCES

1 - SCHIJVE J. - Observations on the Prediction of Fatigue Crack Growth Propagation Under Variable Amplitude Loading,in "Fatigue Crack Growth Under Spectrum Loads", ASTM STP 595,American Society for Testing and Materials, 1976,pp.3-23.

2 - WOOD H.A. - The Use of Fracture Mechanics Principles in the Design and Analysis of Damage Tolerant Aircraft Structures, in AGARD Lecture Series n.62 - "Fatigue Life Prediction for Aircraft Structures and Materials", May 1973.

3 - WHEELER O.E. - Spectrum Loading and Crack Growth - J. of Basic Eng., Trans. ASME, Series D, 1962, pp.181-186.

4 - EIDINOFF H.L.,BELL P.D. - Application of the Crack Closure Concept to Aircraft Fatigue Crack Propagation Analysis - The 9th ICAF Symposium, May 1977.

5 - ELBER W. - Crack Growth Under Spectrum Loading, a Crack Closure Model - NASA TM X-72708, National Aeronautics and Space Administration, 1974.

6 - ANTONA E.,GIAVOTTO V.,SALVETTI A.,VALLERANI E. - Fracture Mechanics Approaches in the Design of Aerospace Vehicles. Proceedings of the 11th ICAS Congress, Lisboa, 1978.

7 - SALVETTI A. - Fatigue Crack Propagation in Structures Stiffened with Riveted Stiffeners, Example Problem 3.4.2.8, in "Pratical Applications of Fracture Mechanics", AGARDograph, Preprint.

8 - SWIFT T. - The Application of Fracture Mechanics in the Development of the DC-10 Fuselage, in "Fracture Mechanics of Aircraft Structures", AGARDograph 176, 1974, pp. 227-287.

9 - CAVALLINI G. - Crack Growth Propagation under Variable Amplitude Loading in Aerospace Structures,Convegno di Studi sulla Fatica nelle Strutture Aerospaziali, Torino-1978, ICAF Doc. n.1091.

10 - VAN DIJK G.M.,DE JONGE J.B. - Introduction to a Fighter Aircraft Loading Standard for Fatigue Evaluation, FALSTAFF-NLR MP 75017 U, 1975.

11 - DE JONGE J.B. et alii - Standardized Load Sequence for Flight Simulation Test on Transport Aircraft Wing Structures, NLR TR 73029 C, 1973.

12 - Mc.CARTNEY L.N.,COOPER P.M. - A Numerical Method of Processing Fatigue Crack Propagation Data,Engineering Fracture Mechanics, 1977, Vol.9,pp.265-272.Pergamon Press.

APPENDIX 1 - SPLINE TECHNIQUE

One of the most difficult problems in analysing crack propagation data is the definition of the crack rate, that is how to "differentiate" the discrete raw data obtained in experiments. The problem is of great importance, since the parameters of the semi-empirical laws of crack propagation, which link the crack rate da/dn with the ΔK stress intensity factor range, are strongly influenced by the accuracy with which the derivatives da/dn are computed.

In the past a common solution for the problem, especially for data obtained from simple sheet panels, lying in this case on a smooth curve, has been provided by techniques such as finite difference methods. But the data points are subjected to a degree of scatter which results in large errors of growth rate when using this method. So the technique of fitting a continuous curve to the data points using the least squares concept has been developed, and the crack growth rate can be obtained simply by differentiating the analytical expression of a (n).

At first, a method of fitting a cubic polynomial function was adopted but, for the case of stiffened panels,it was decided to make use of spline function (piece-wise continuous polynomial) and a very good fitting was obtained.

The method adopted, explained in detail in |12|, consists in fitting in the least square sense a curve of the type:

$$n = X - Y \ln(a) - \frac{Z}{a} + \sum_{p=i}^{n} \lambda_p (a-K_p)^{\ell} \qquad (1)$$

to the experimental data points (a_j, n_j). The first part of the expression is a function of a class suggested by a cumulative concept of damage, while the second is the spline function,with polynomials of degree ℓ connected at knots K_p. Following the usual method of minimizing the sum of squares of residuals, a computer program carries out the computations for selecting the best-fit values of the parameters X, Y, Z, λ_p of eq.(1).

Tests have been performed to choose proper values for the number of knots and for the degree of the polynomials and the results show that the values selected of 4 knots for long cracks and 3 for short ones, together with 4 for the exponent, lead to satisfactorily small errors.

Tests have also been carried out by monitoring the errors made when comparing the derivatives of known functions (such as polynomials, trigonometric functions, etc..) with their approximations obtained by using the spline function method.

The results have been considered satisfactory and so the method has been adopted as a standard for getting crack growth rates from experimental points.

Other comparisons have also been made with functions representing propagation curves of ideal stiffened panels under constant amplitude fatigue loading; the results have been discussed in the text, paragraph 3.5.

APPENDIX 2 - TEST APPARATUS

The equipment prepared for the damage propagation tests is composed of two different load machines, of the load spectrum generation system (in variable amplitude loading tests) and the defect growth measuring system.

The first piece of loading equipment is composed of a Servotest hydraulic actuator, controlled in closed loop through a set of six servovalves, capable of ± 500 KN or ± 100 KN (static and dynamic), fed by a 125 HP power pack with an oil flow rate of 190 Lt./min.

For constant amplitude tests, the control unit of the machine directly drives the execution of load; for variable amplitude loading spectra an external input is available. The actuator is mounted on a very stiff rig and the specimen is clamped to the rig and to the load cell of the actuator with grips which hold the specimen by friction. Moreover, anti-buckling guides are available both for flat specimens and stiffened specimens.

The second piece of equipment is composed of a Servotest hydraulic actuator, controlled in closed loop through a set of two servovalves, capable of ± 250 KN or ± 50 KN (static and dynamic). This actuator is in every way similar to the first, is fed from the same power pack and is mounted on a similar rig.

The electric signal, which drives the actuators in the case of variable amplitude loading, is generated from a process computer PDP 11/34. Preliminary tests for determining the maximum working frequency are performed for each condition, loading spectrum and flexibility of specimen.

The input signal in the actuator, representing the desired spectrum, is compared by PDP 11/34 with the response of the actuator, namely the output of the load cell. The working frequency selected is the highest one for which the difference between input and output is not significant. During the tests the output of load cell is also continuously fed to the PDP 11/34. In this way, checks of coincidence of the two signals can be periodically performed. Moreover, if the machine stops because the maximum and

minimum load limits are surpassed or for other reasons, the PDP 11/34 commands the arrest of the input signal and prints the number of flights at that moment.

The defect growth measuring system is formed essentially of a 30 magnification telescope, whose position can be regulated, with a movement parallel to the propagation direction, along a bar, which has a millimetric scale; a vernier is applied to the telescope bearing block, allowing the defect dimension measure to be taken with a 0.1 mm. precision. The number of cycles, or more exactly the number of flights in the "flight-by-flight" spectra case, at which the defect has reached the measured dimension, is written on a printer connected to a counter in which the actuator load cell signal is fed: the printer is activated directly by the operator who makes the observations. In the case in which the spectrum is generated by the process computer, the flight number is directly printed on the telescope type when the operator sends a proper signal to the process computer input. The whole measuring system allows us to take highly accurate measurements, certainly adequate for the purposes of this research.

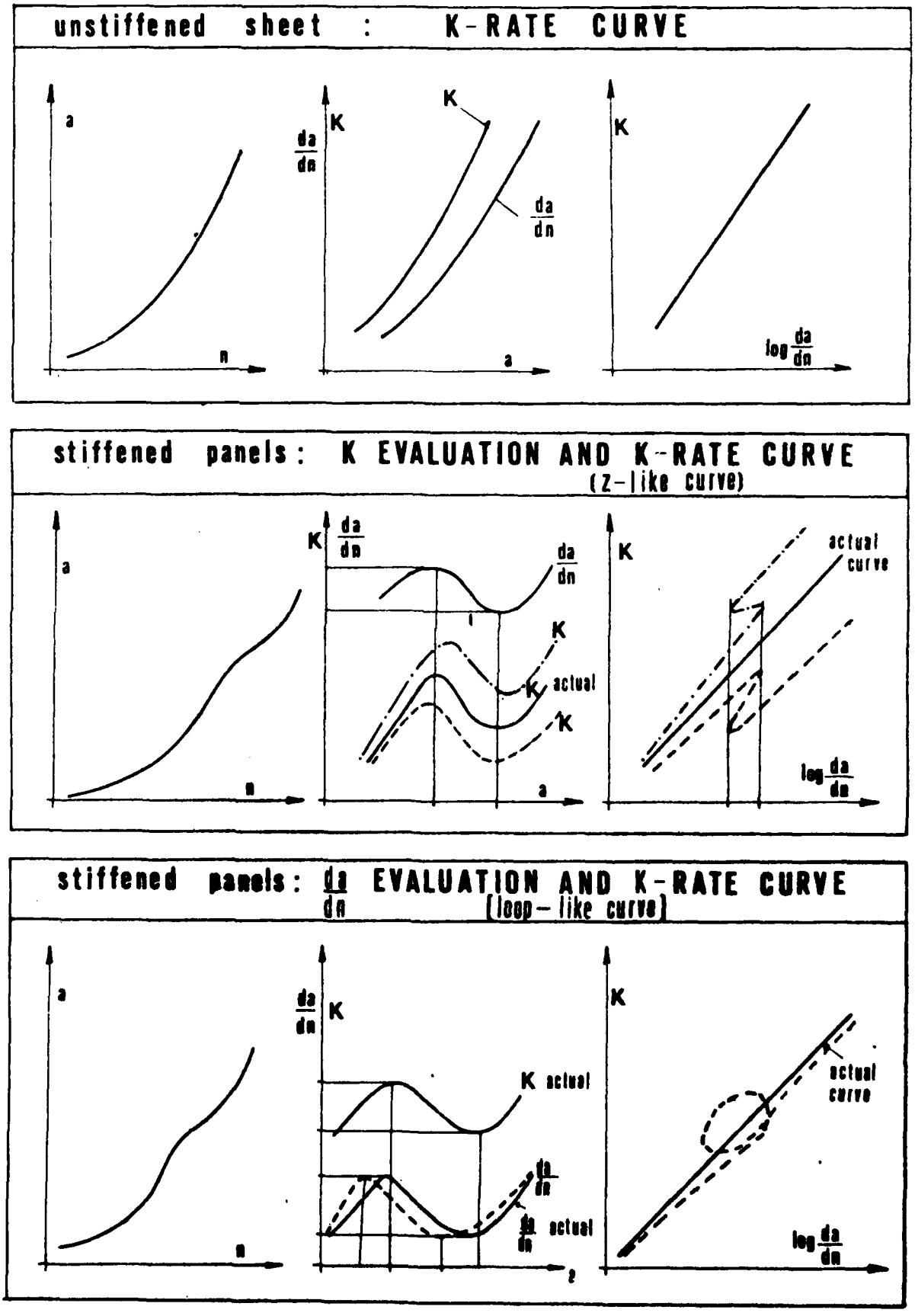

Fig.1 - Typical anomalies in K-rate relationships in stiffened panels due to errors both in SIF and da/dn computation.

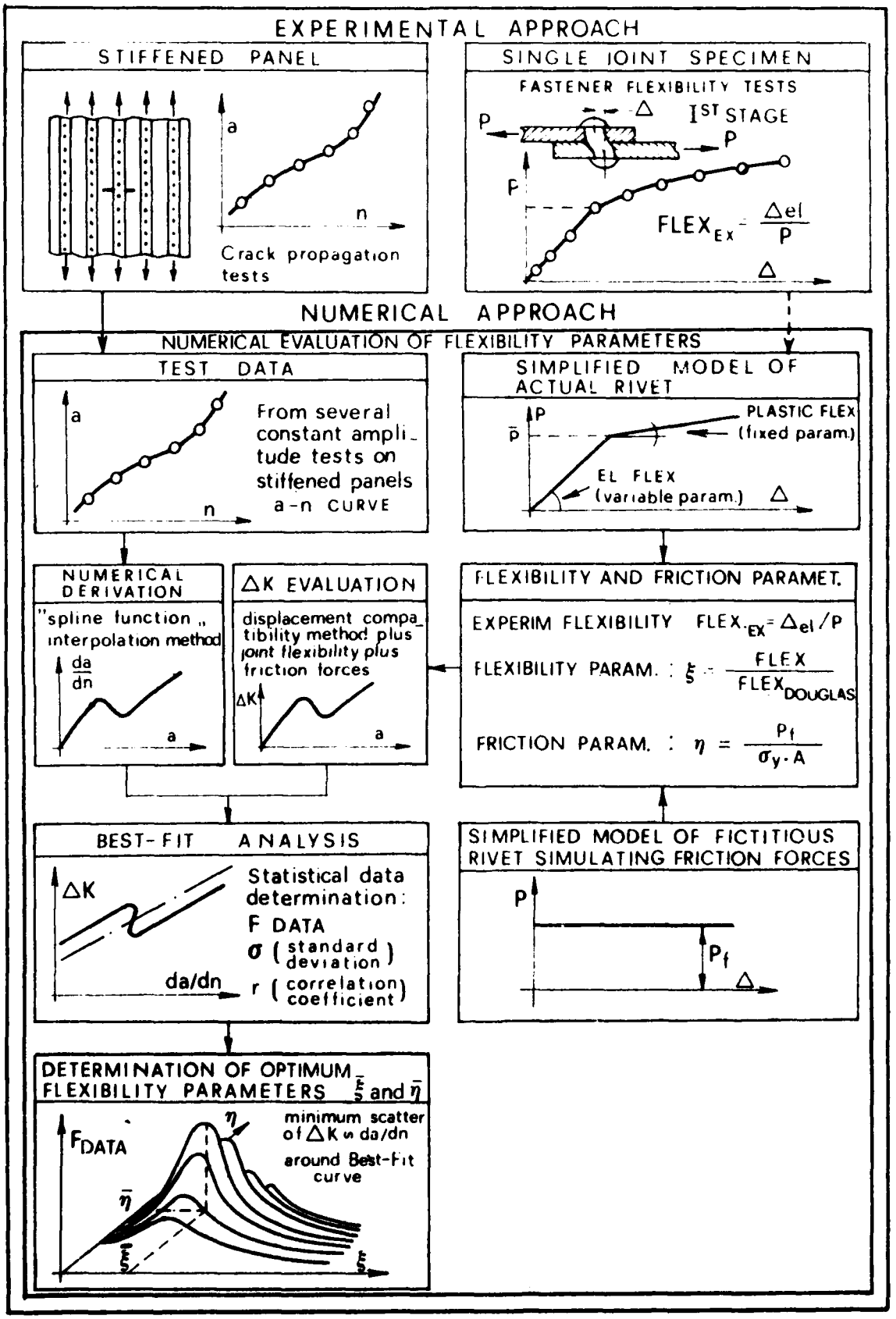

Fig.2 - Rationale for evaluating fastener flexibility and friction forces from test data.

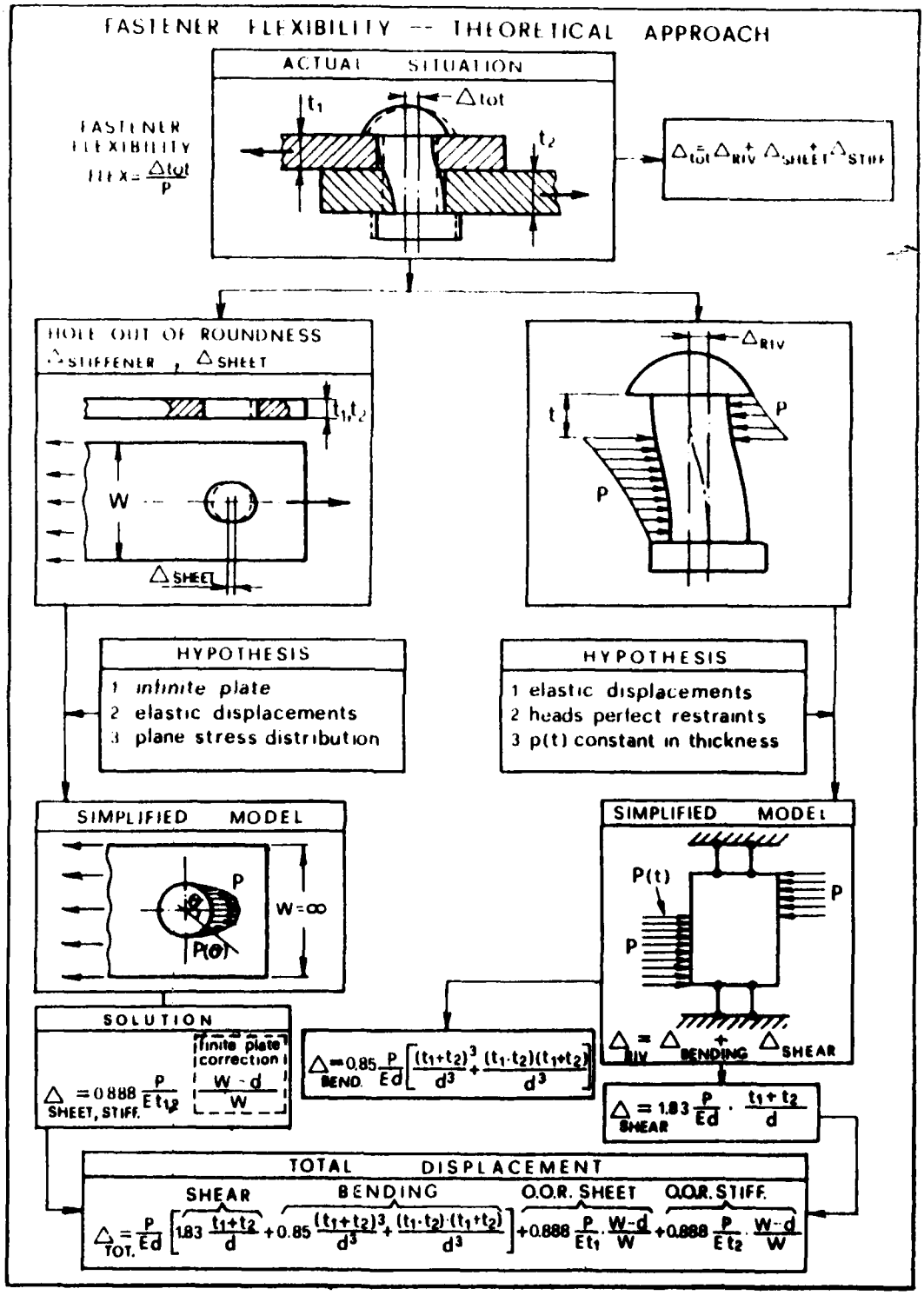

Fig.3 - Simplified method for predicting rivet flexibility.

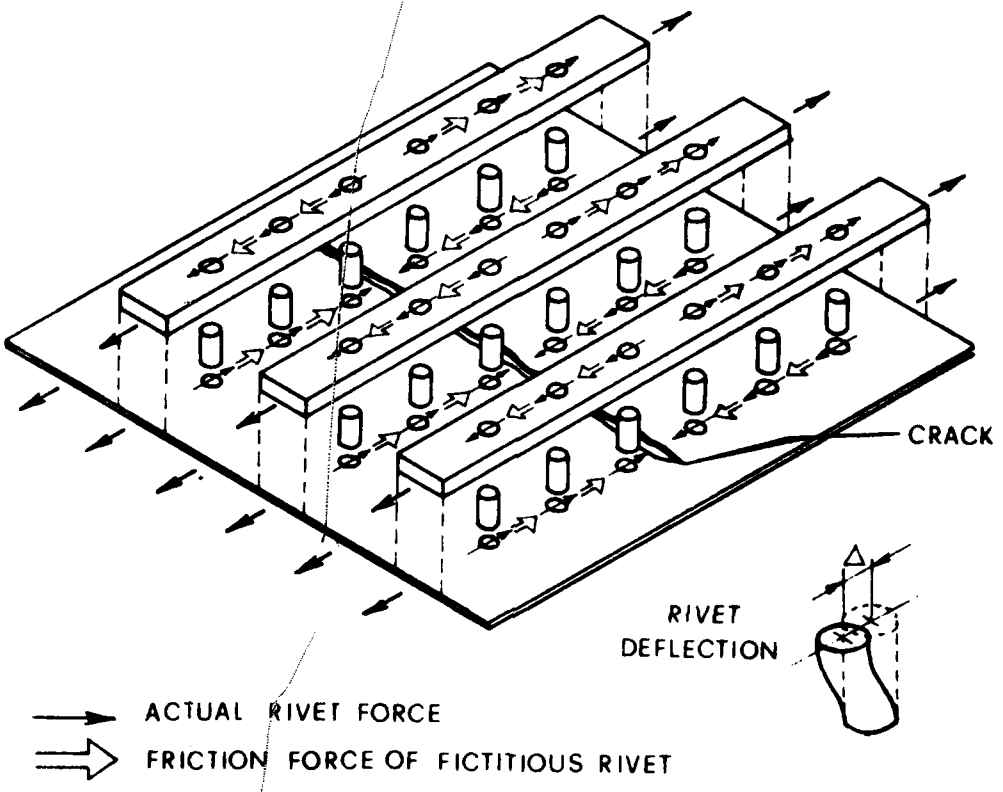

Fig.4 - Idealization of the friction forces by means of fictitious rivets.

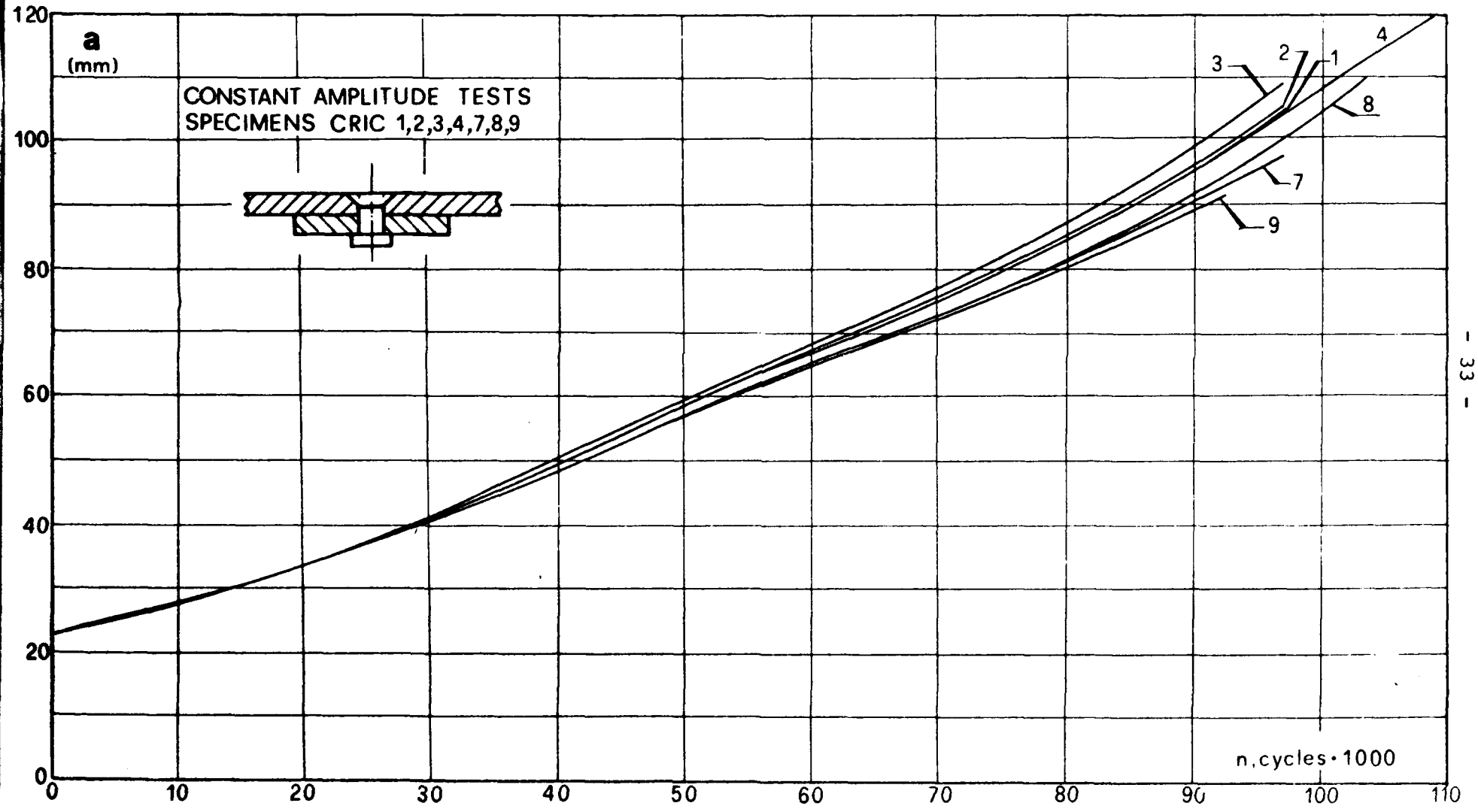

Fig.5a - Crack growth data for stiffened panels riveted with countersunk rivets. New series tests.

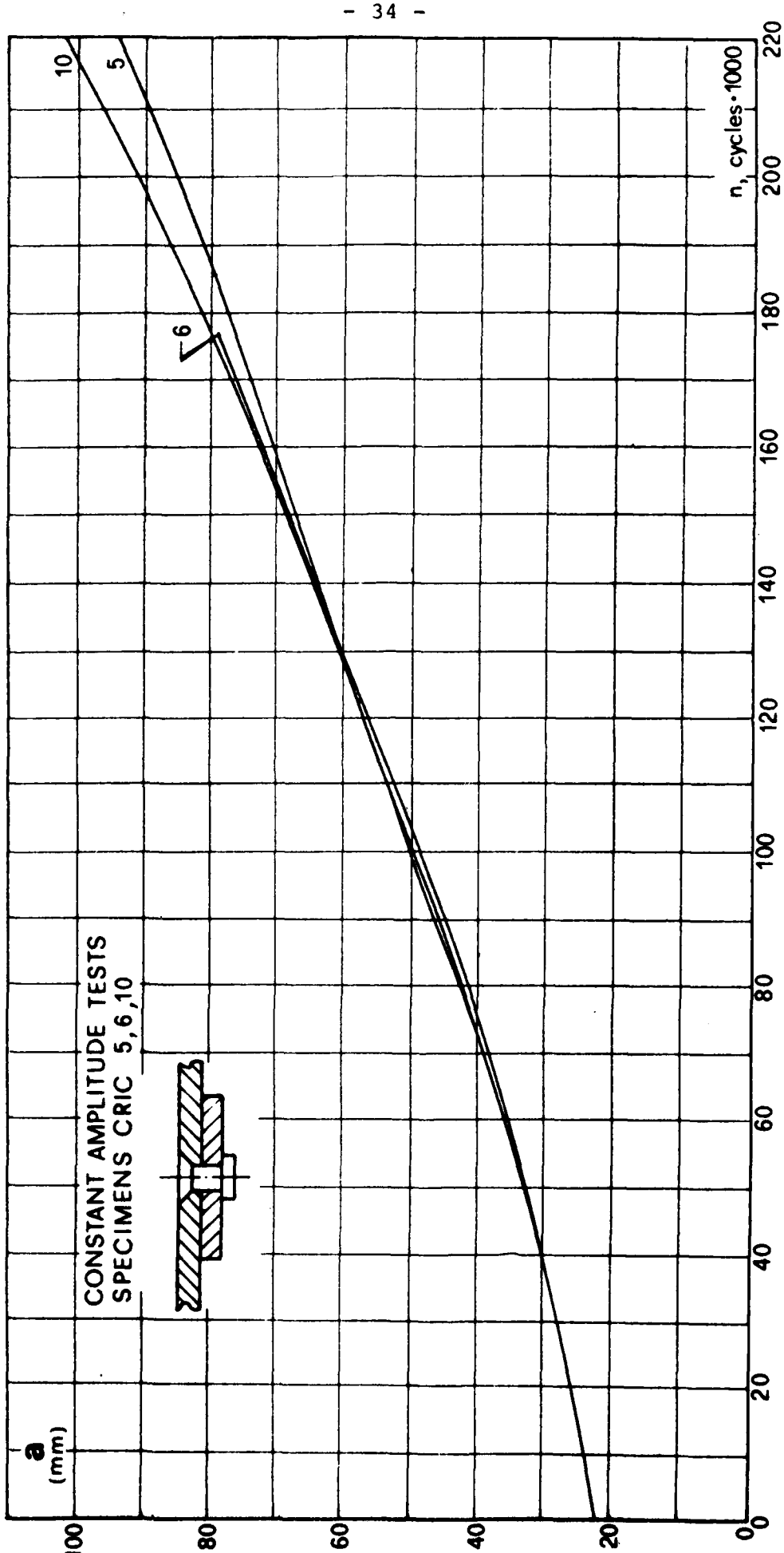

Fig.5a - Continued.

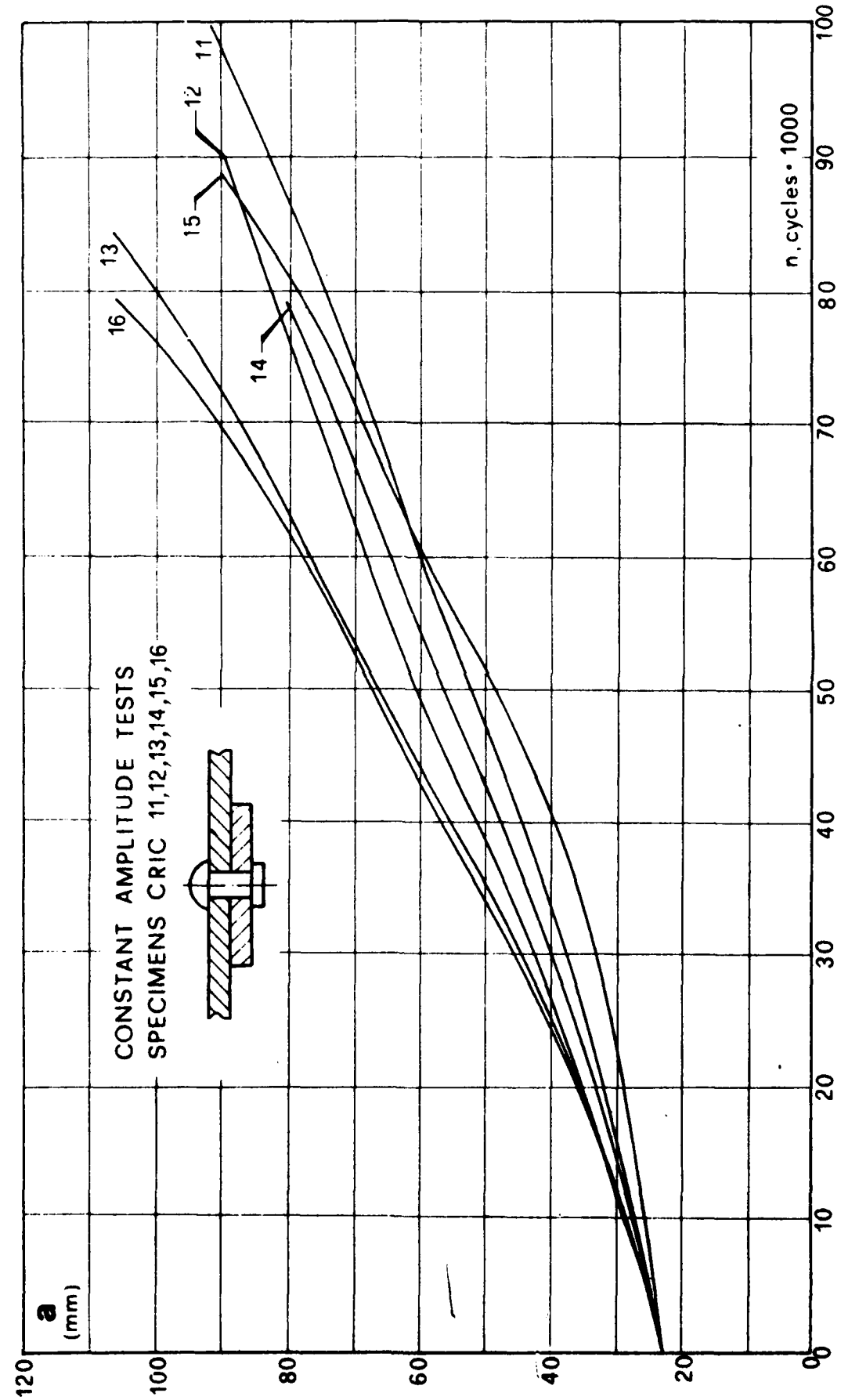

Fig.5b - Crack growth data for stiffened panels riveted with round head rivets. New series tests.

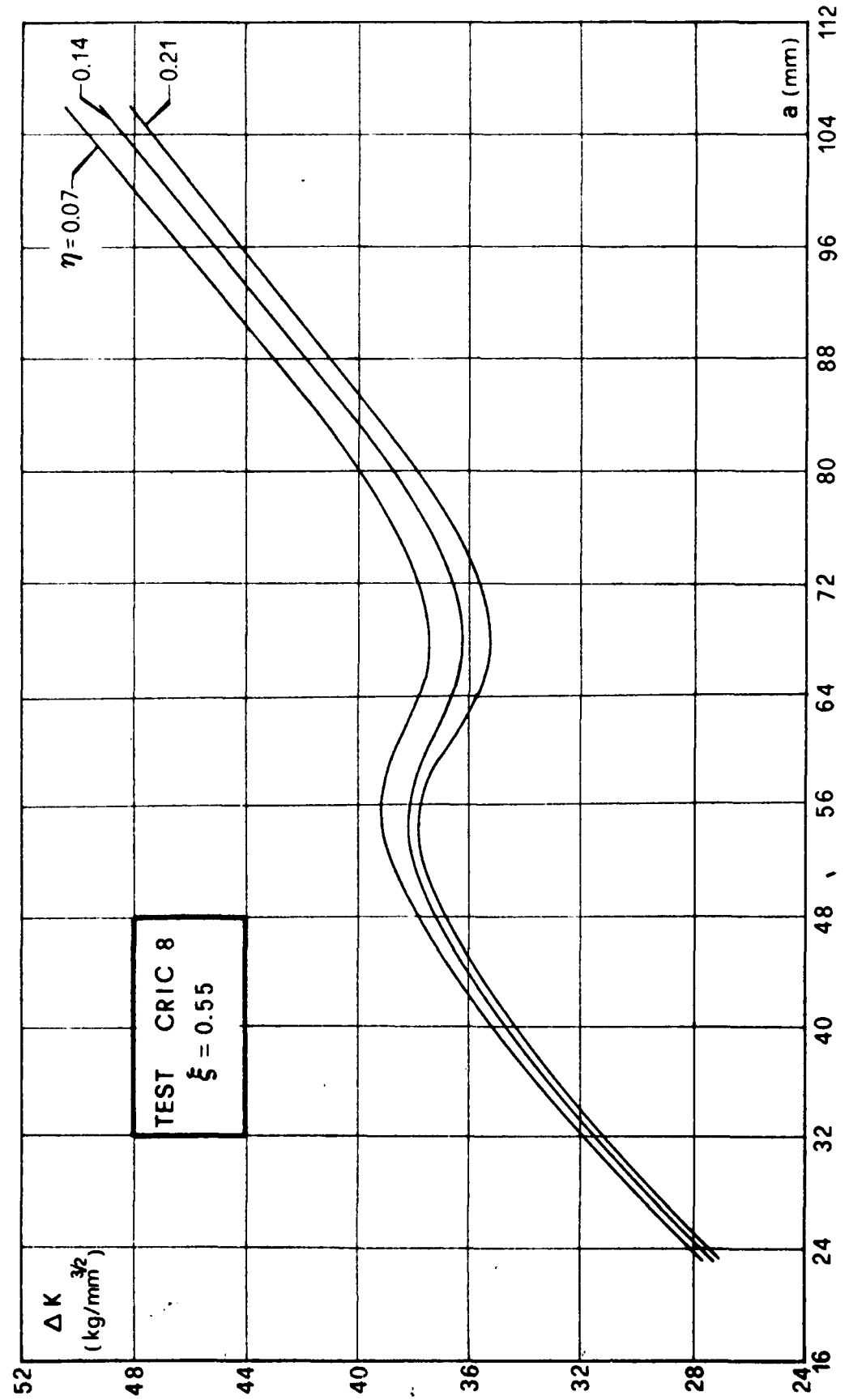

Fig.6a - Influence of the friction forces on the stress intensity factor as computed by SKESA.

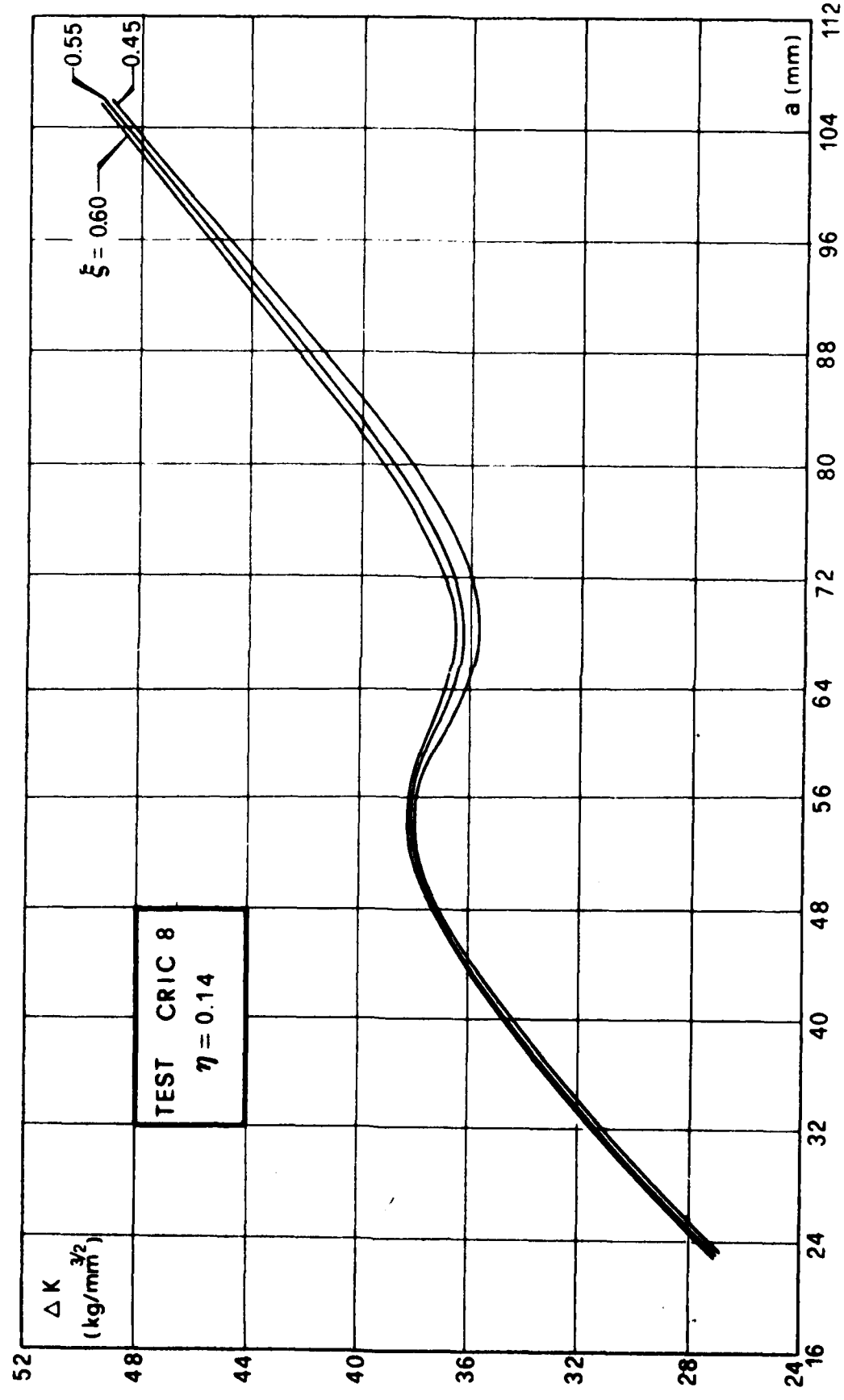

Fig.6b - Influence of the rivet flexibility on the stress intensity factor as computed by SKESA.

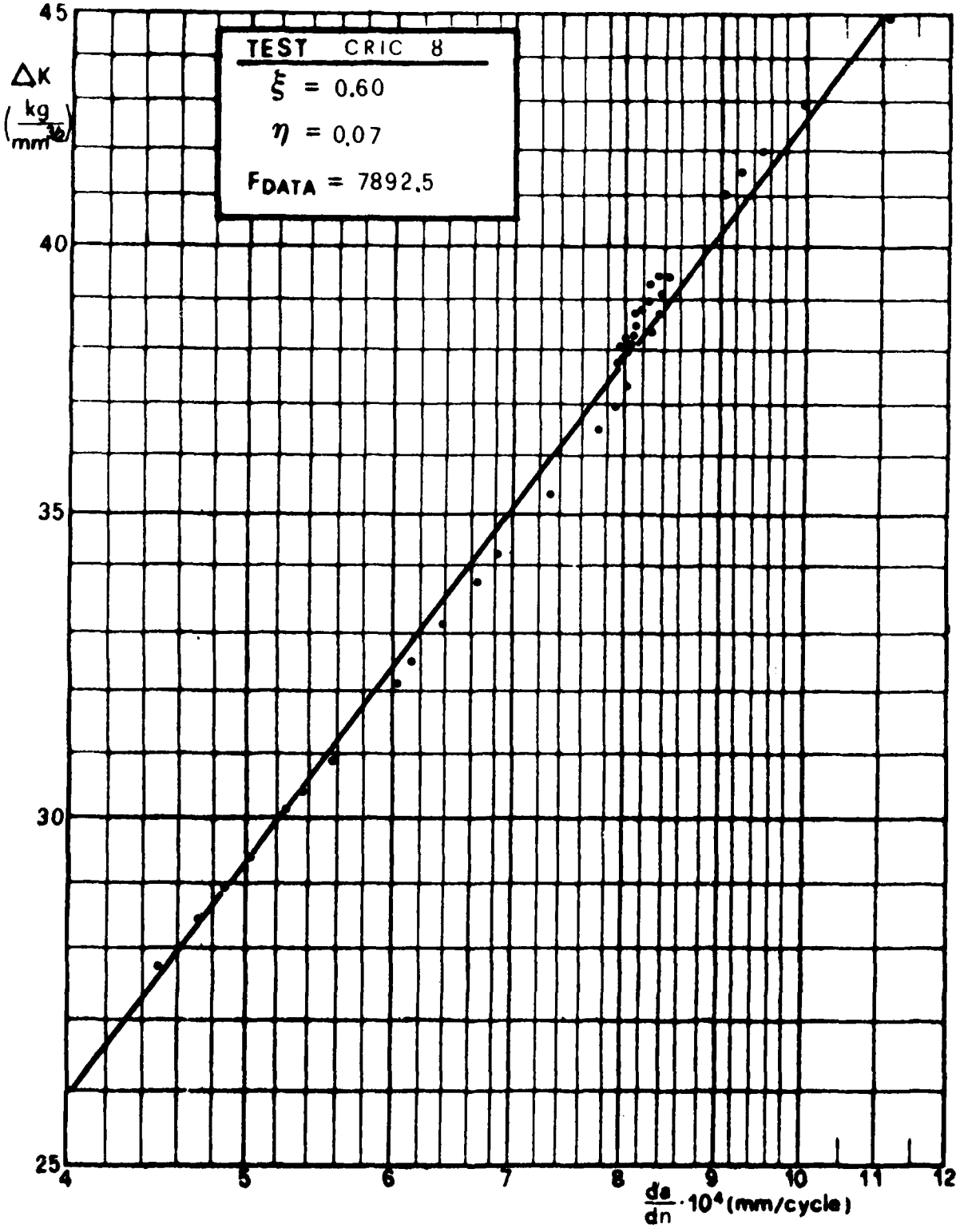

Fig.7a - Test CRIC - 8: shape of da/dn vs. ΔK for different values of ξ and η. The dots correspond to couples of values da/dn, ΔK as obtained by spline and K modules. The continuous line is the best-fit curve.

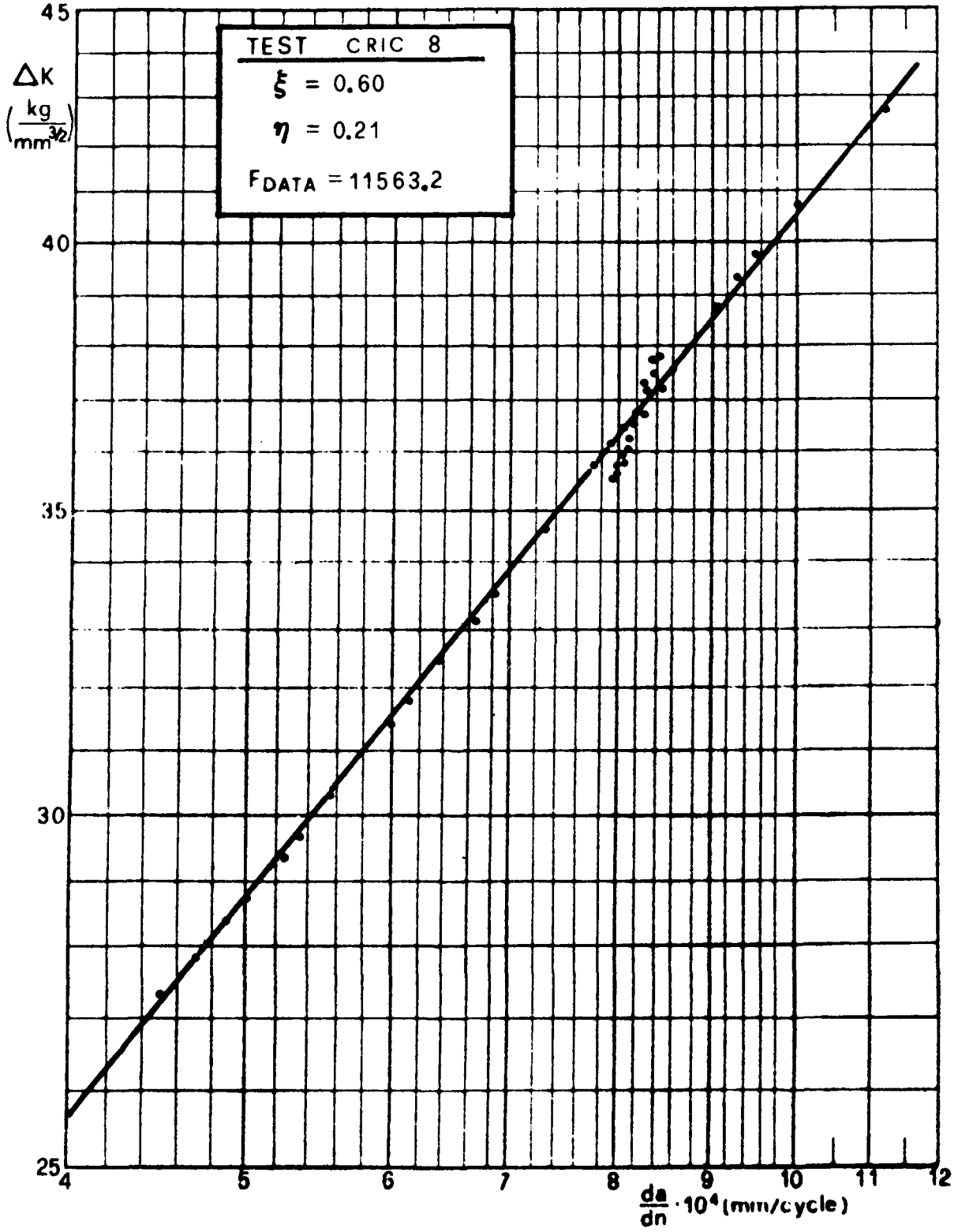

Fig.7a - Continued.

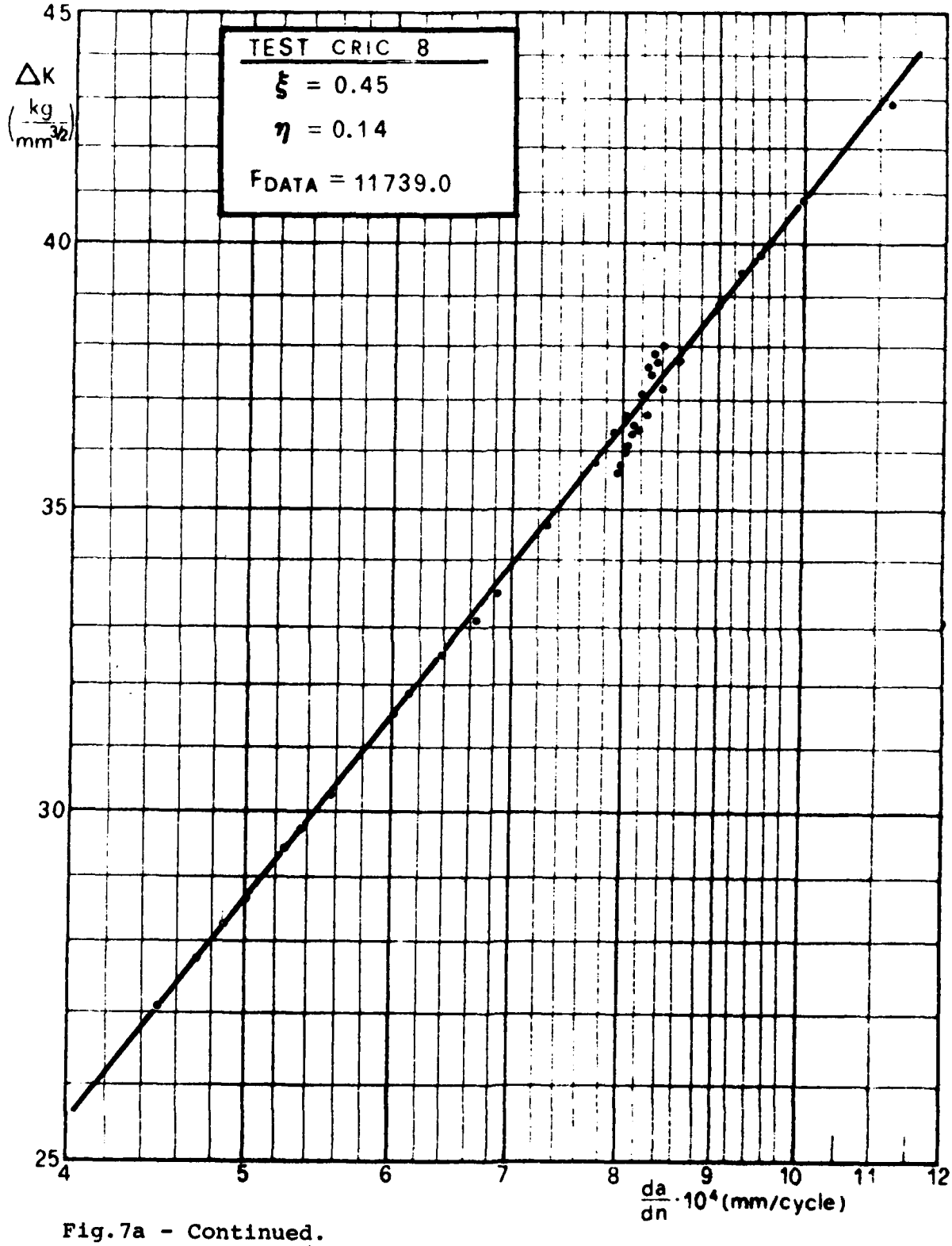

Fig.7a - Continued.

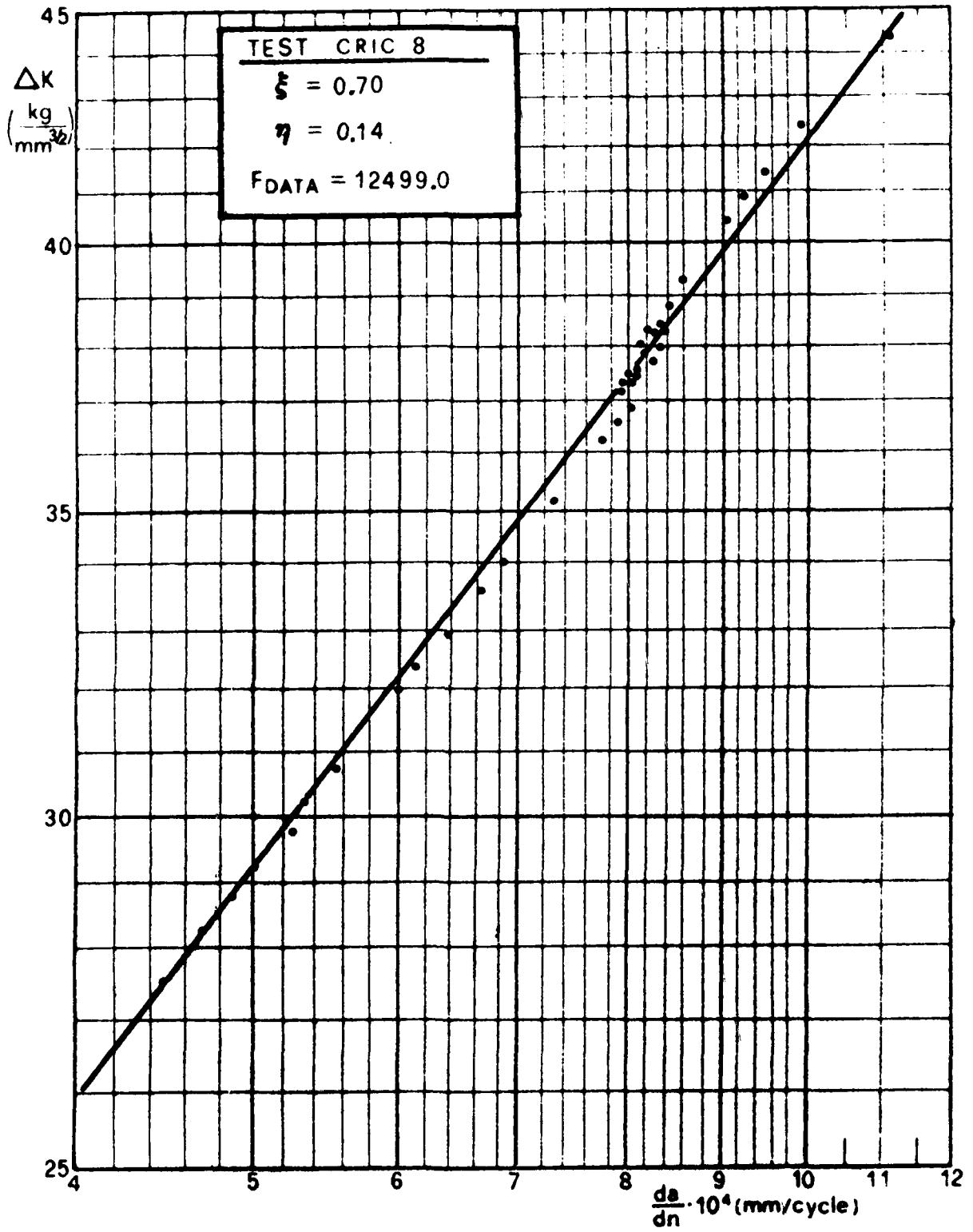

Fig.7a - Continued.

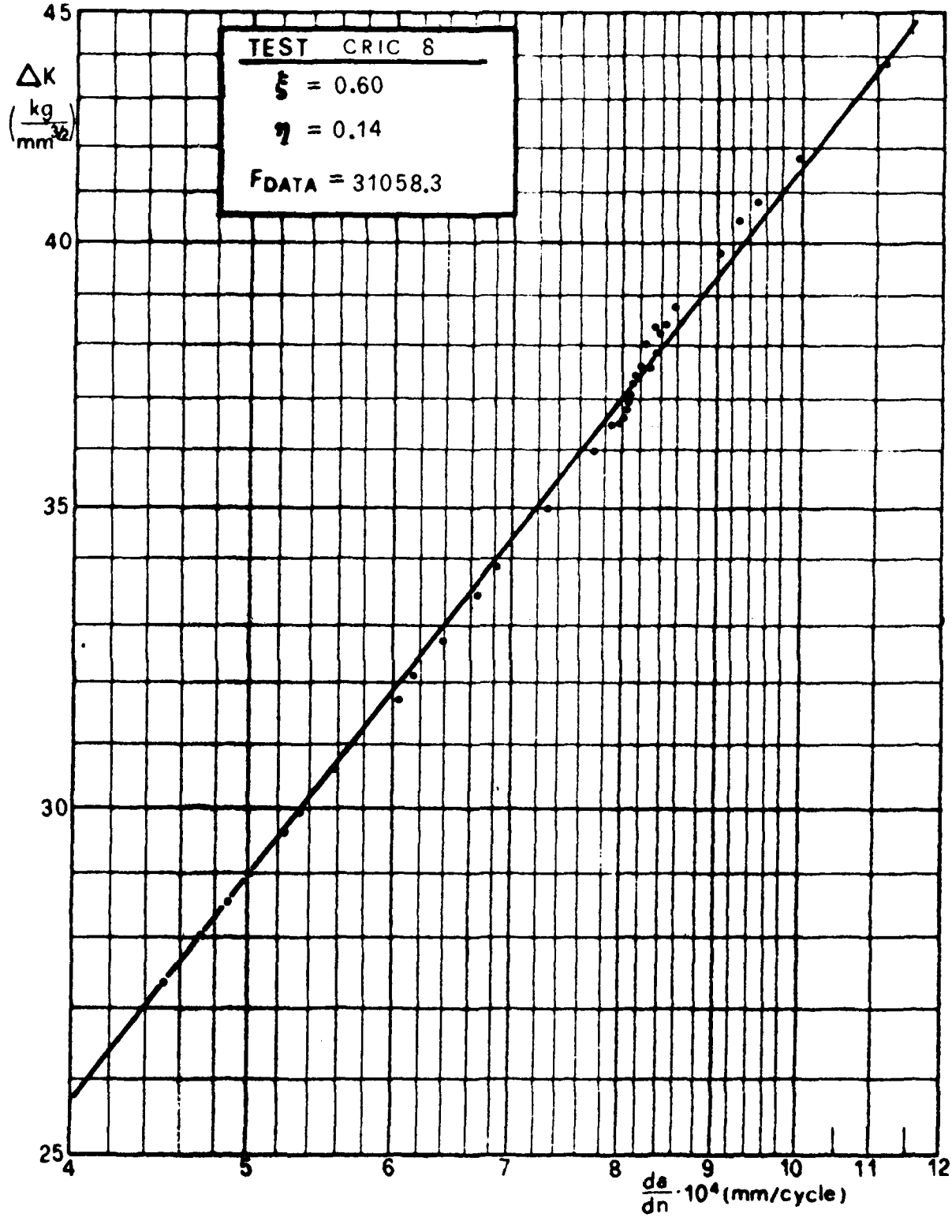

Fig.7a - Continued.

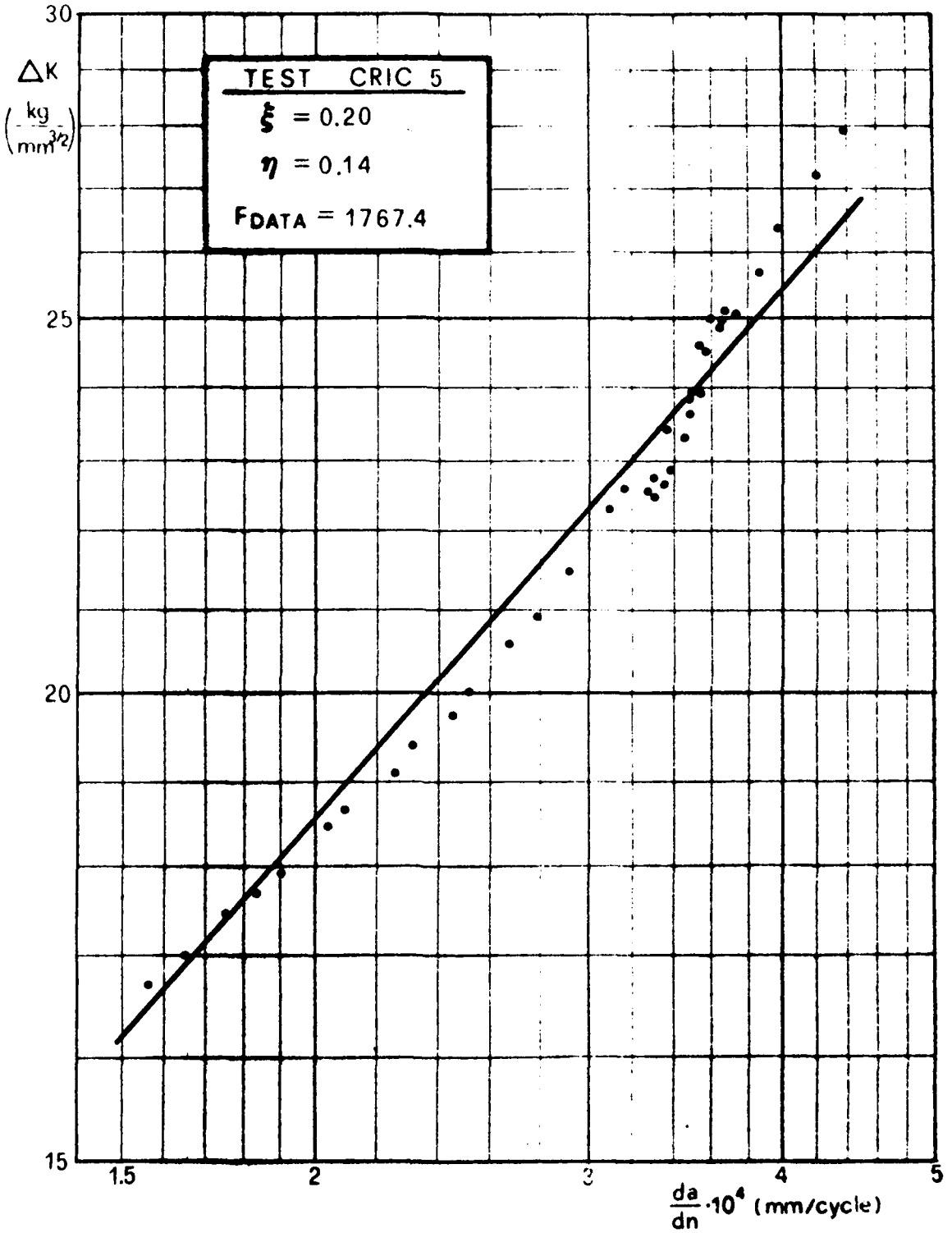

Fig.7b - Test CRIC - 5: da/dn vs. ΔK for different values of ξ and η, plotted as explained in Fig.7a. In this case small loop-type anomalies are present also at the higher values of F_{DATA}.

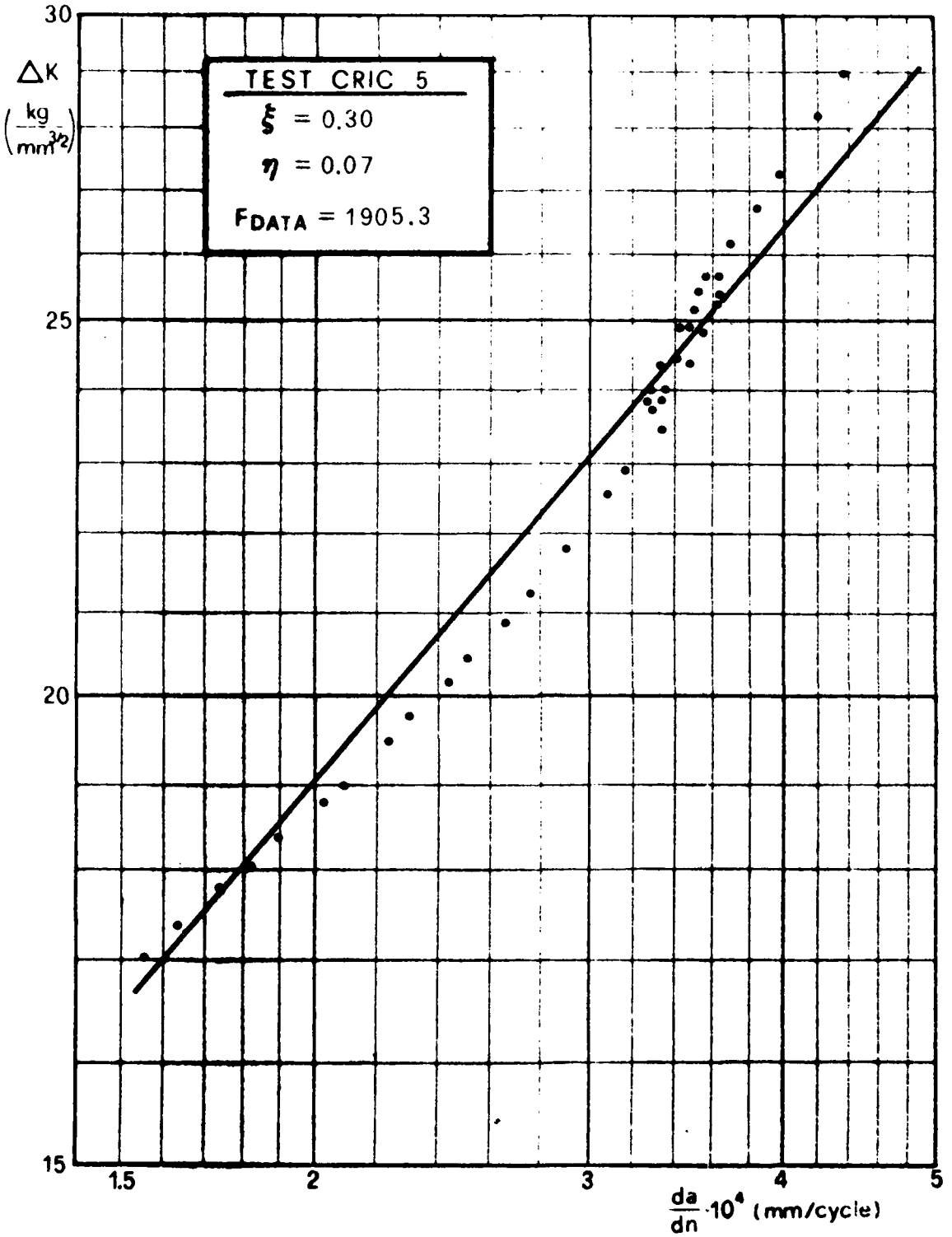

Fig.7b - Continued.

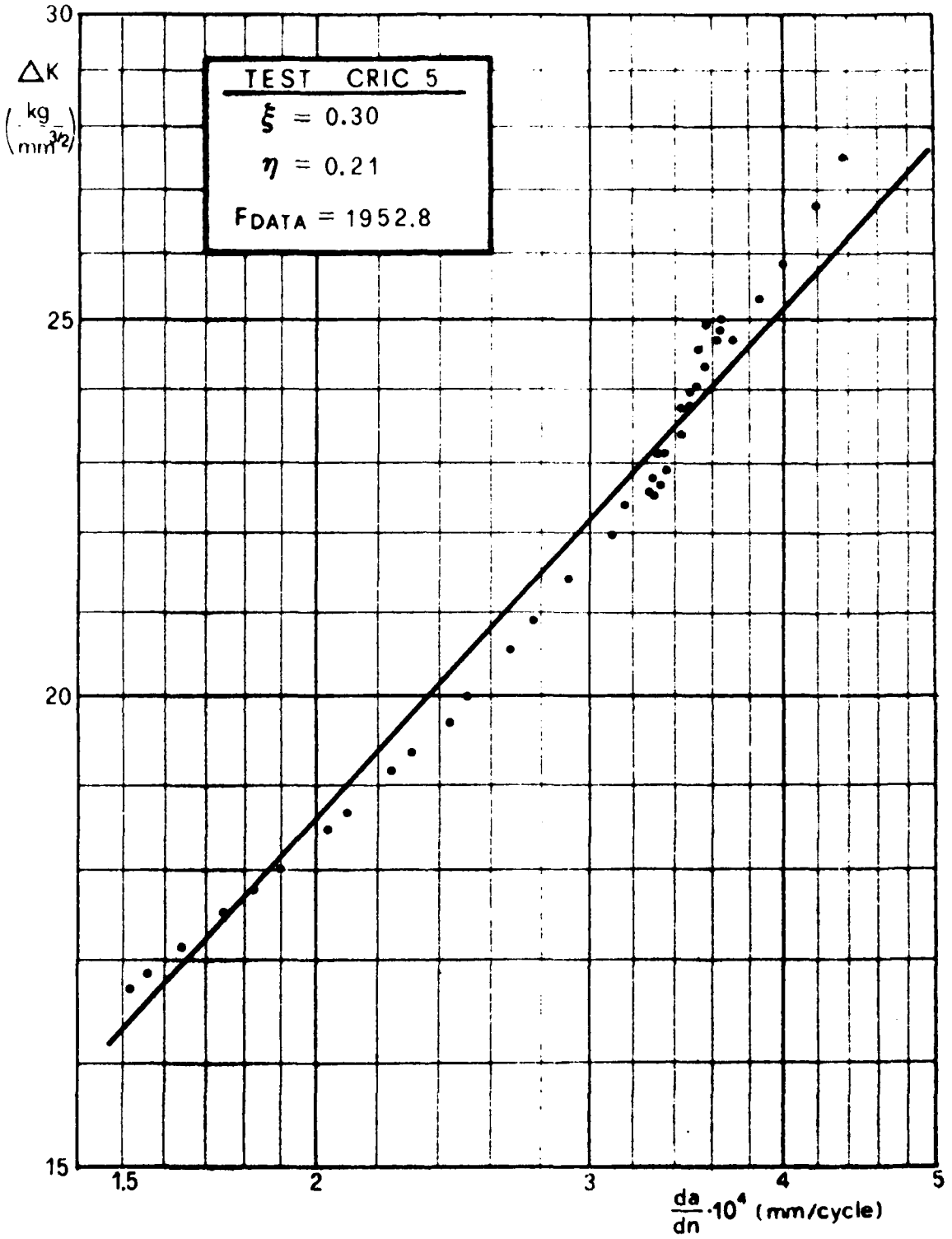

Fig.7b - Continued.

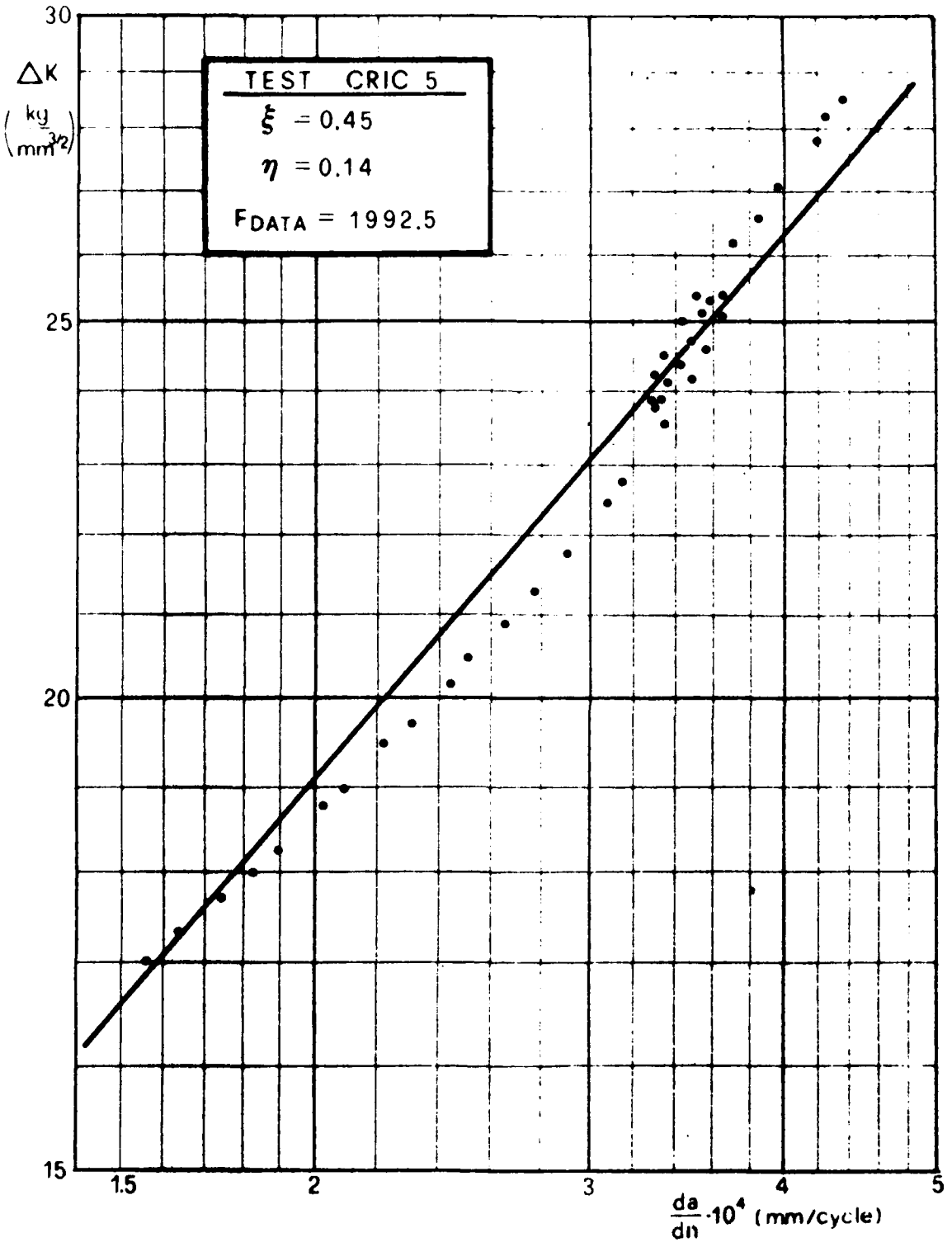

Fig.7b - Continued.

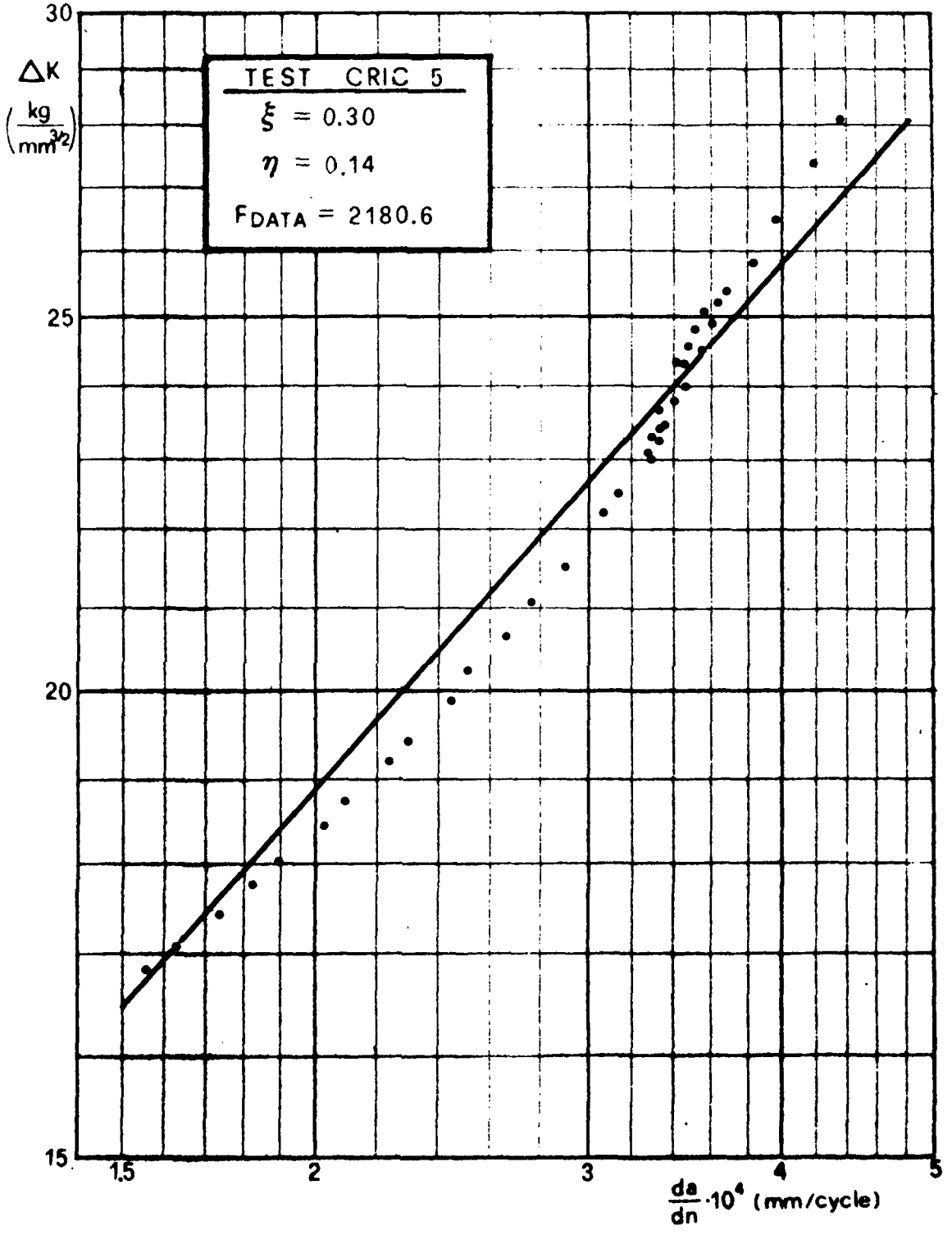

Fig.7b - Continued.

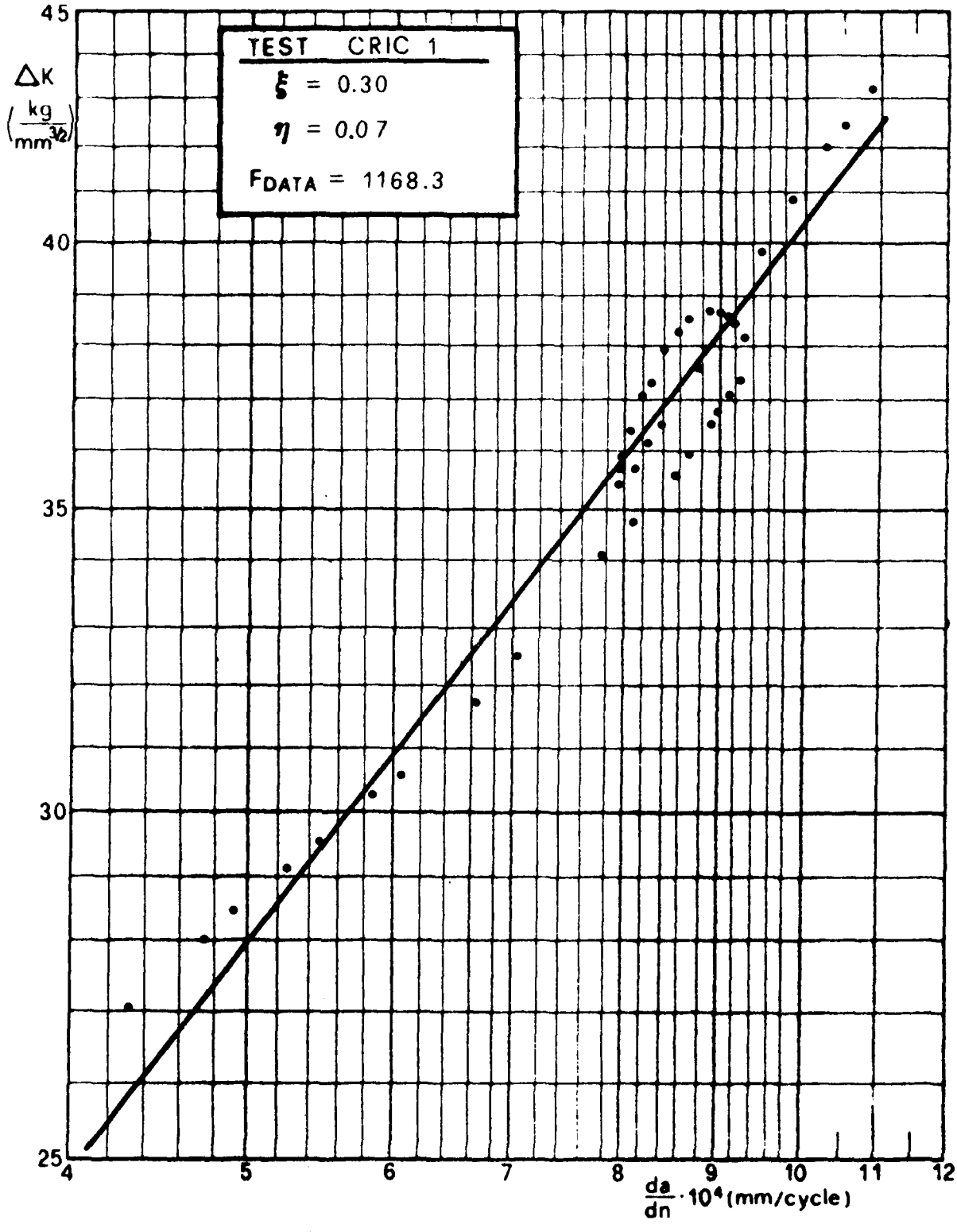

Fig.7c - Test CRIC - 1: da/dn vs. ΔK for different values of ξ and η, plotted as explained in Fig.7a. In this case loop-type anomalies are present also at the higher values of F_{DATA}.

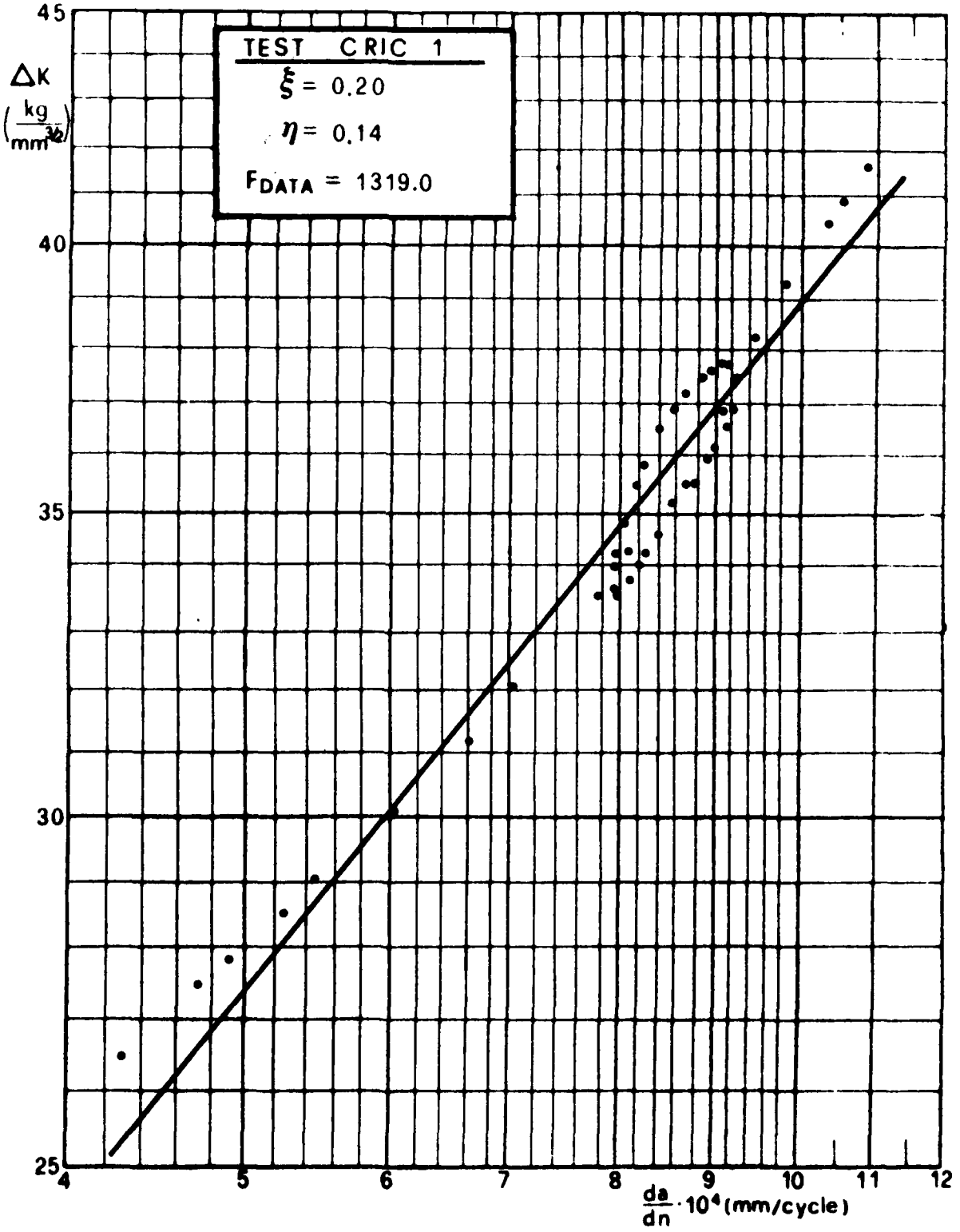

Fig.7c - Continued.

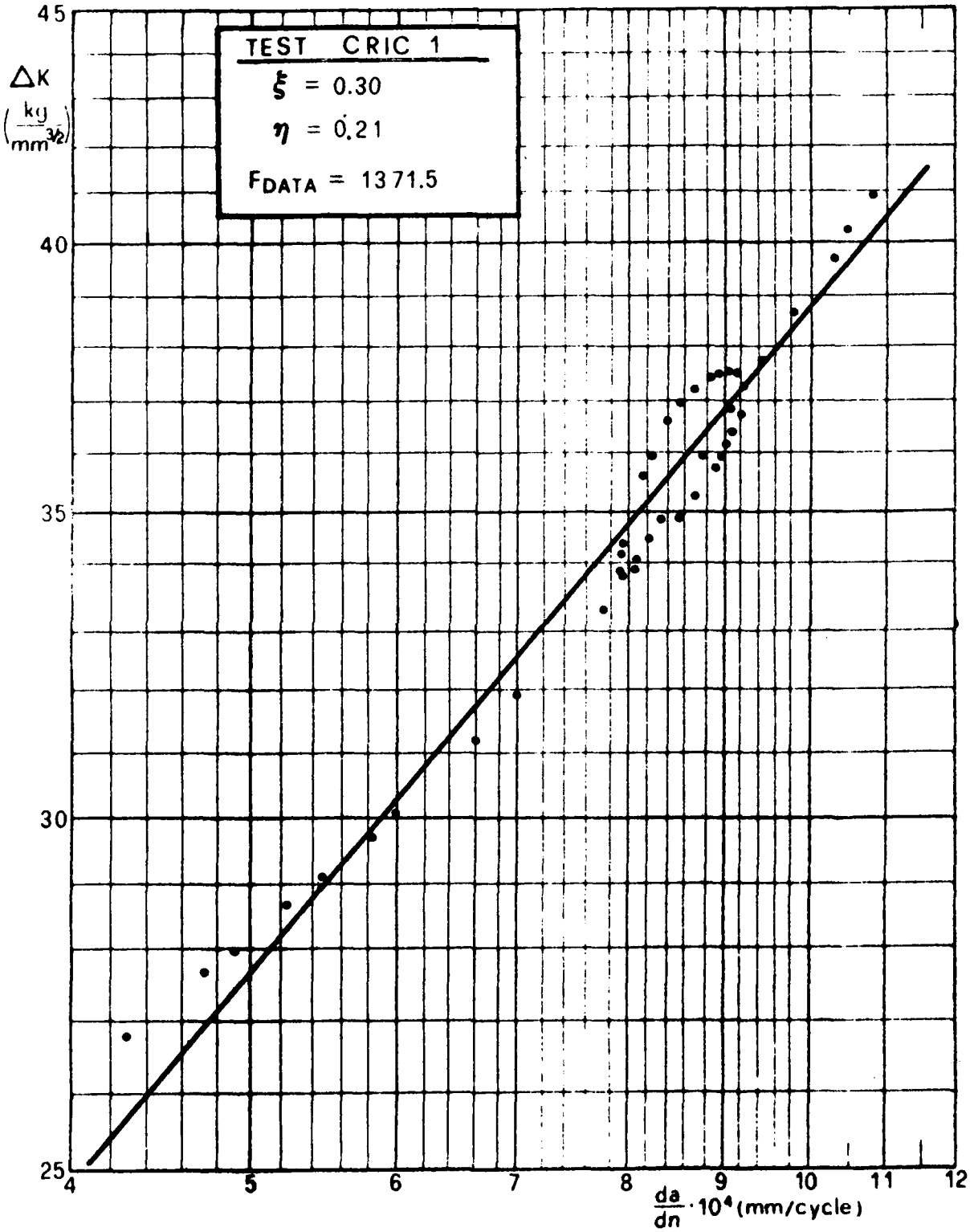

Fig.7c - Continued.

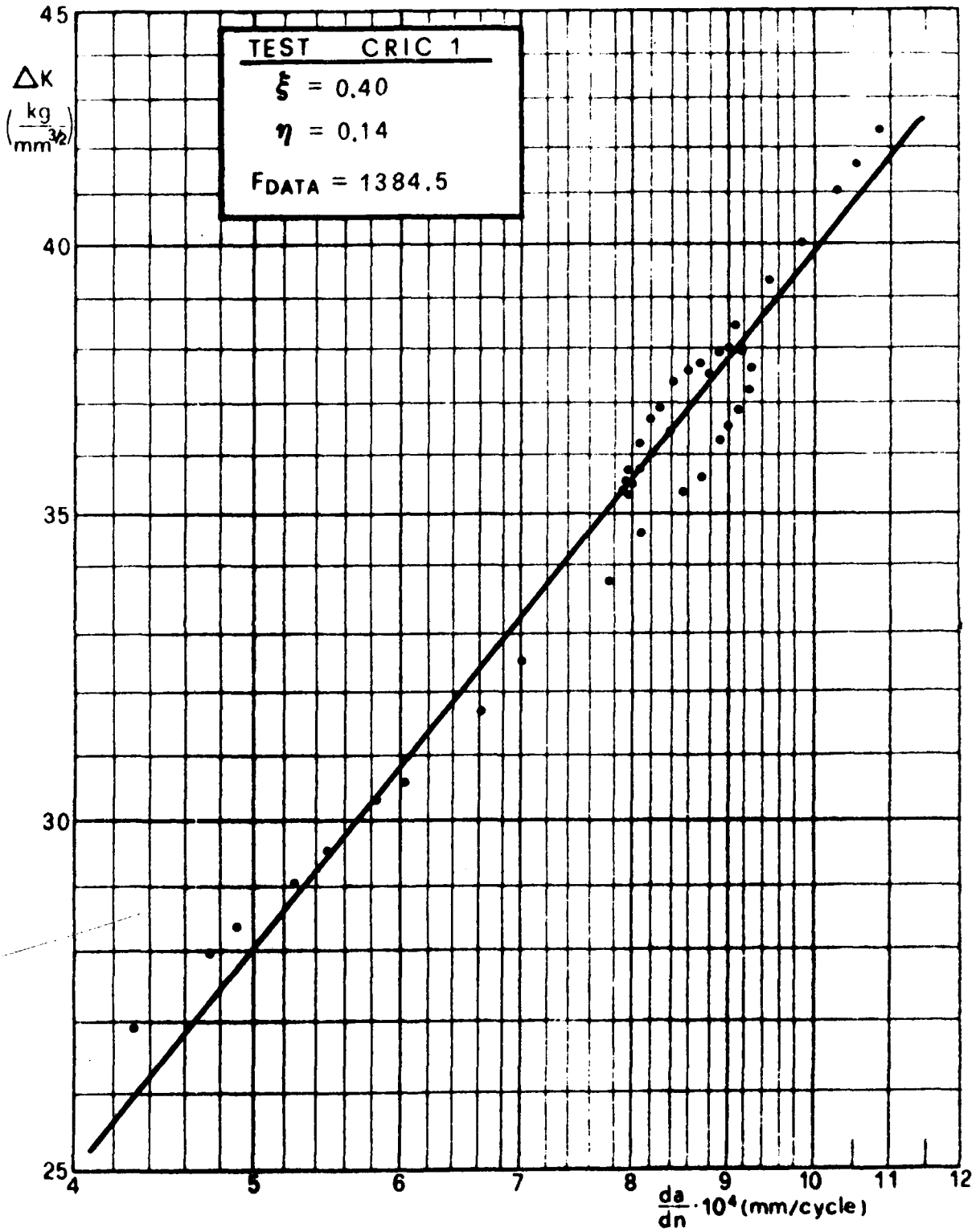

Fig.7c - Continued.

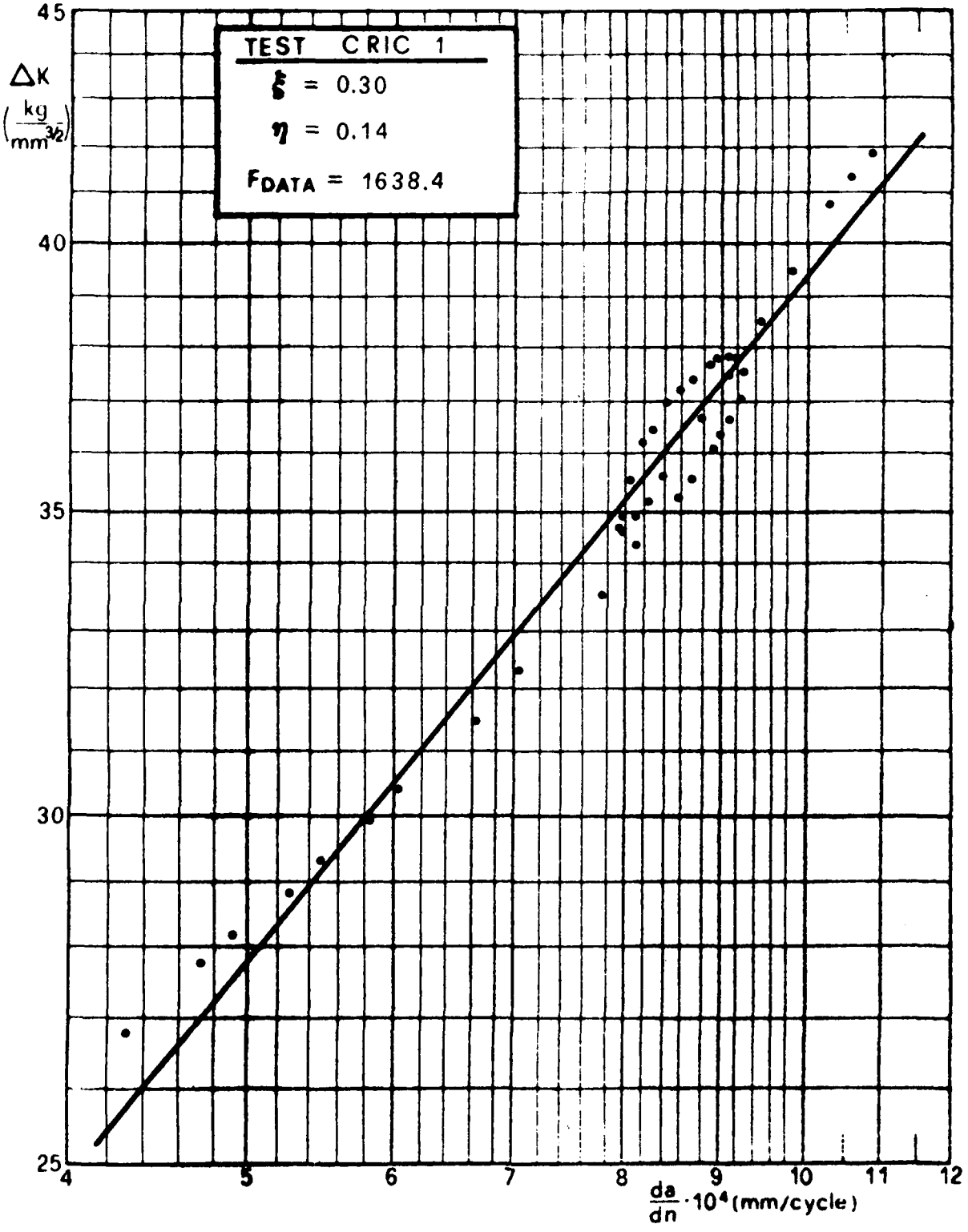

Fig.7c - Continued.

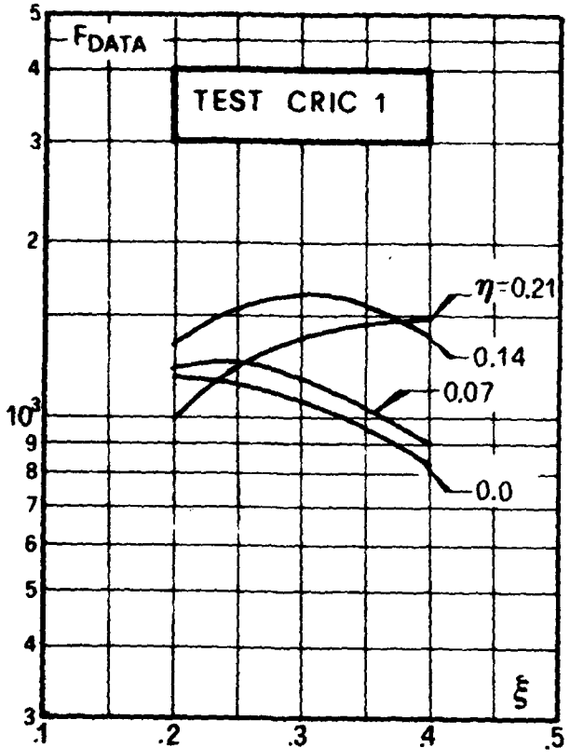

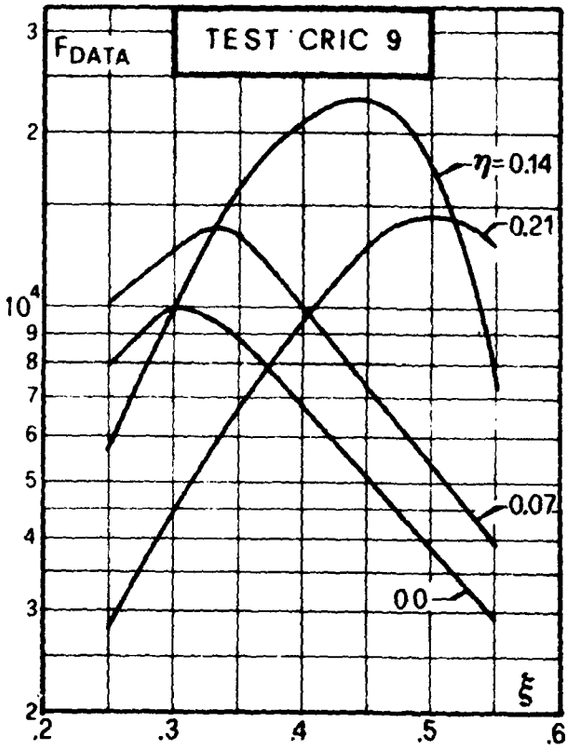

Fig.8a - F_{DATA} versus ξ and η for different stiffened panels. The results well depict the different situations found in the present investigation. Test CRIC-9 and CRIC-8 curves are representative of crack rate data which correlate fairly well with Paris law (negligible anomalies in K-rate relationships $\bar{\xi}$ and $\bar{\eta}$). Test CRIC-1 and CRIC-5 are representative of the worst correlations (small but not negligible anomalies at $\bar{\xi}$ and $\bar{\eta}$).

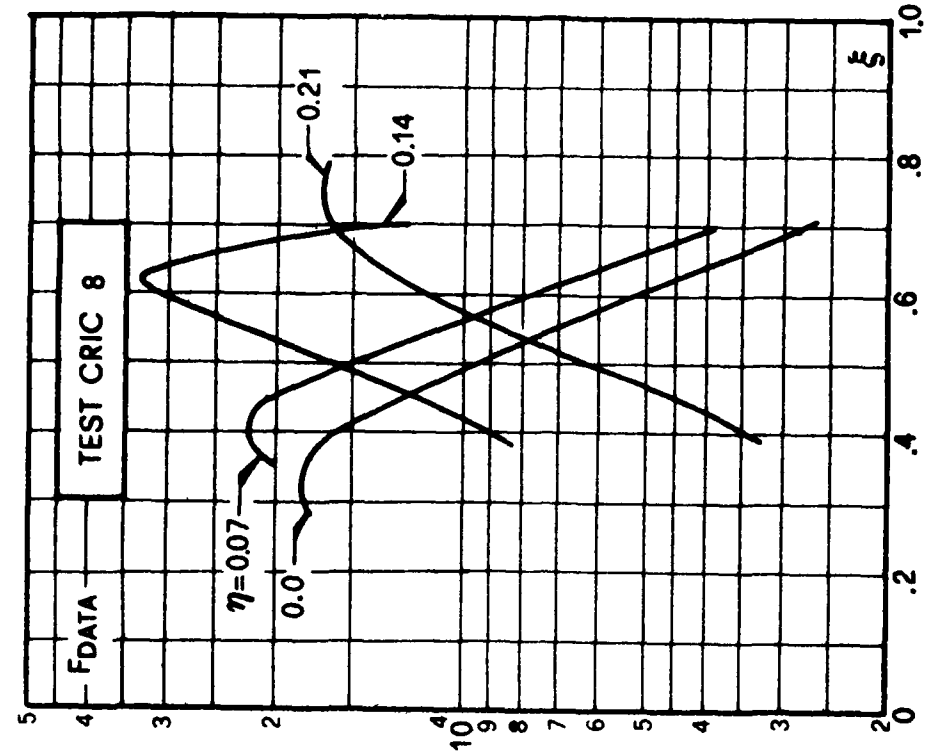

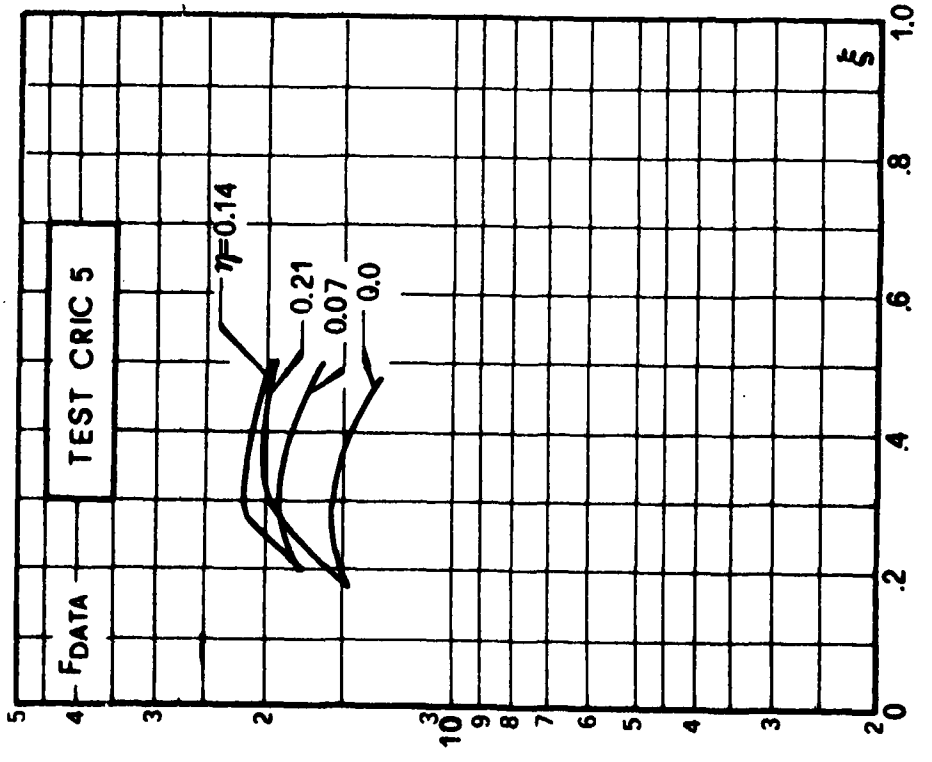

Fig.8a - Continued.

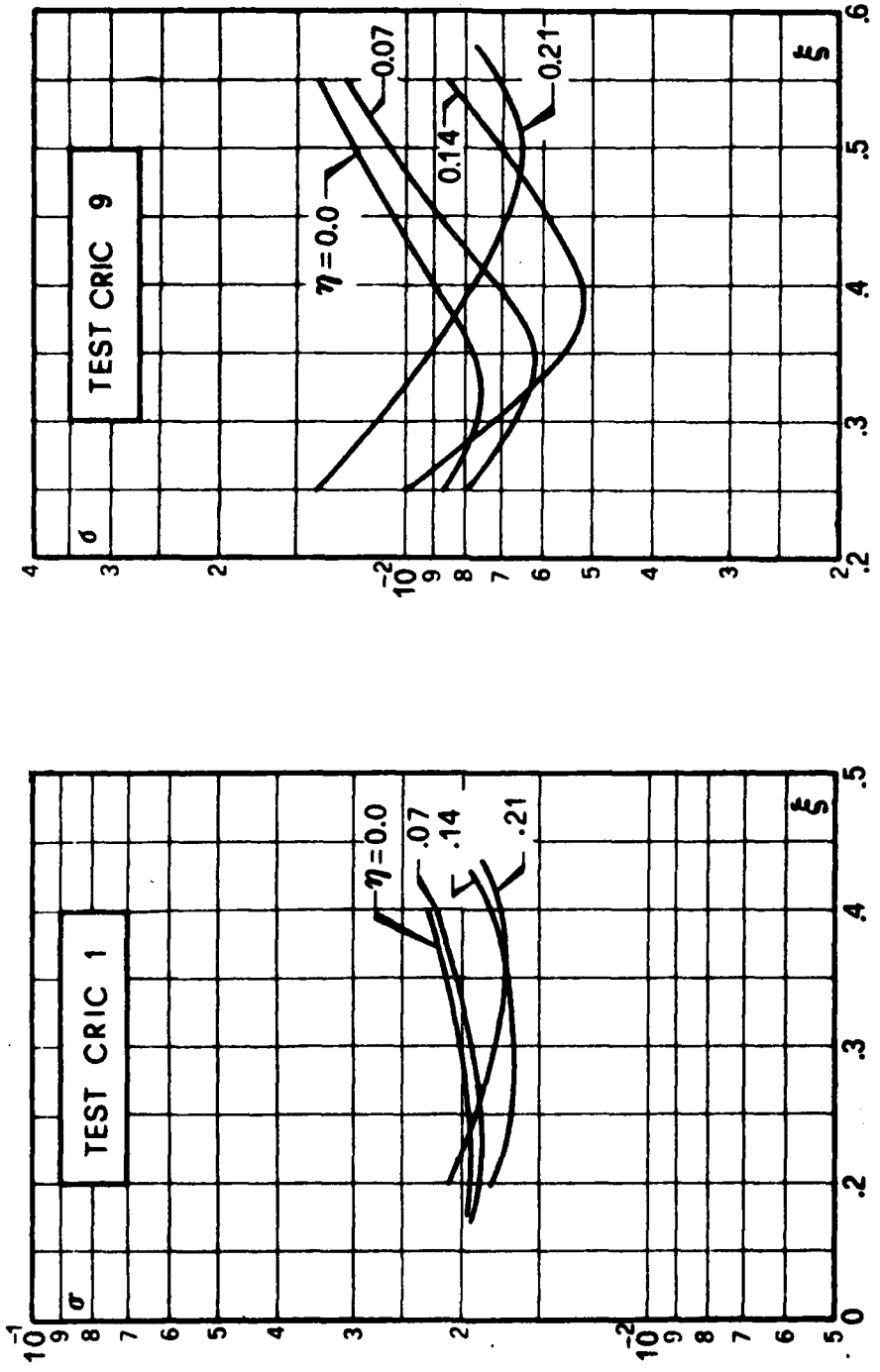

Fig.8b - Standard deviation σ versus ξ and η for different stiffened panels. The same considerations of Fig.8a can be applied.

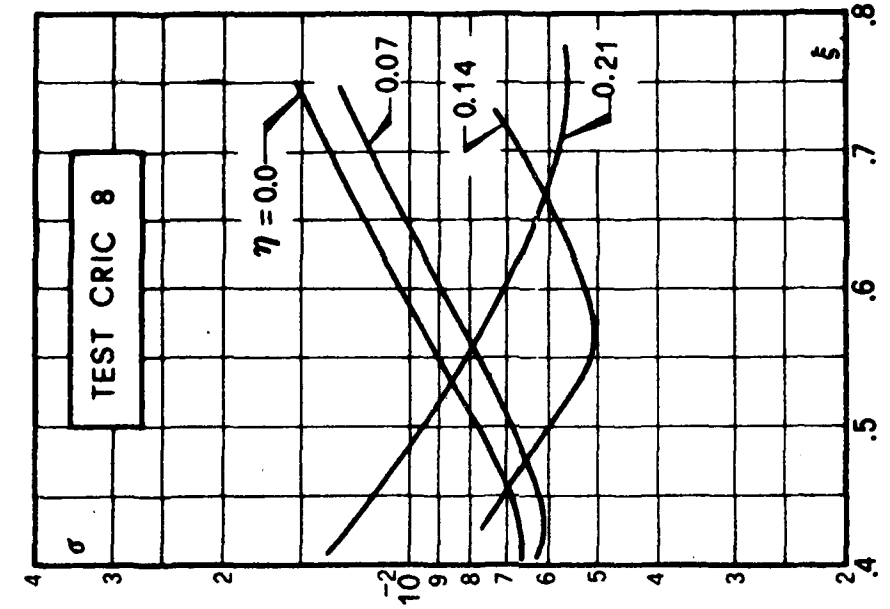

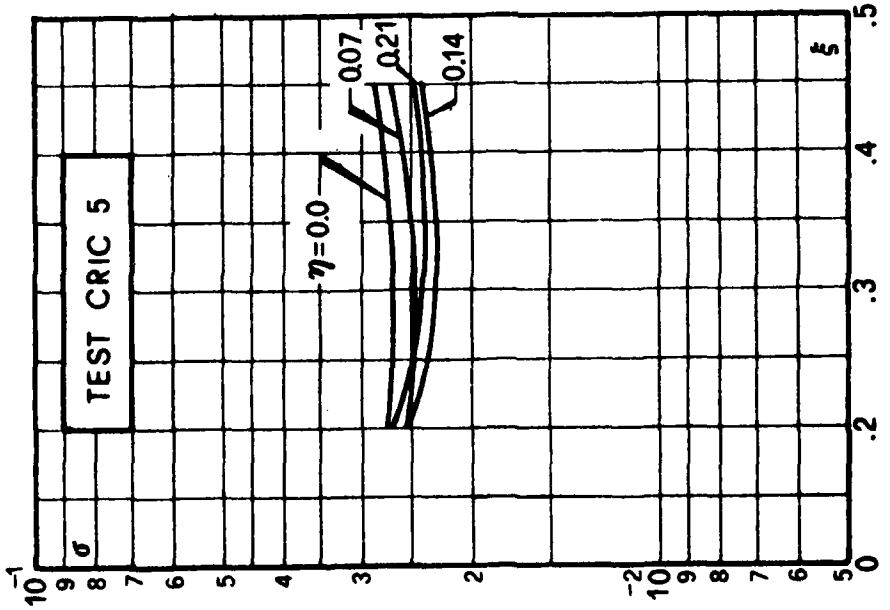

Fig.8b - Continued.

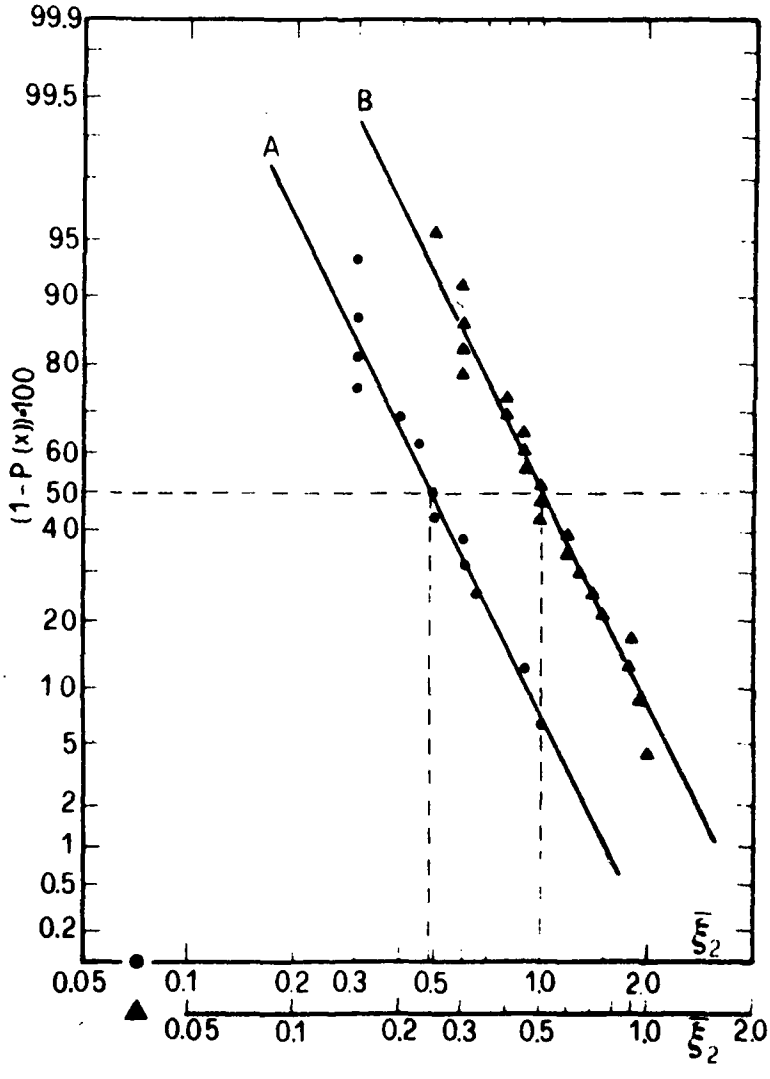

Fig.9 - Log $\bar{\xi}$ distribution. The curve A is relevant to η = 0.14. The median value is $\bar{\xi}_2$= = 0.49 ($\bar{\xi}_1$ = 0.686) and the standard deviation is σ_2=0.219 (σ_1 =0.307). The results indicate that the flexibilities found with this approach are noteworthy lower than those predicted by Fig. 3 or Douglas formula. The curve B has been obtained considering all the $\bar{\xi}$ belonging to the same population irrespective of the values of η .

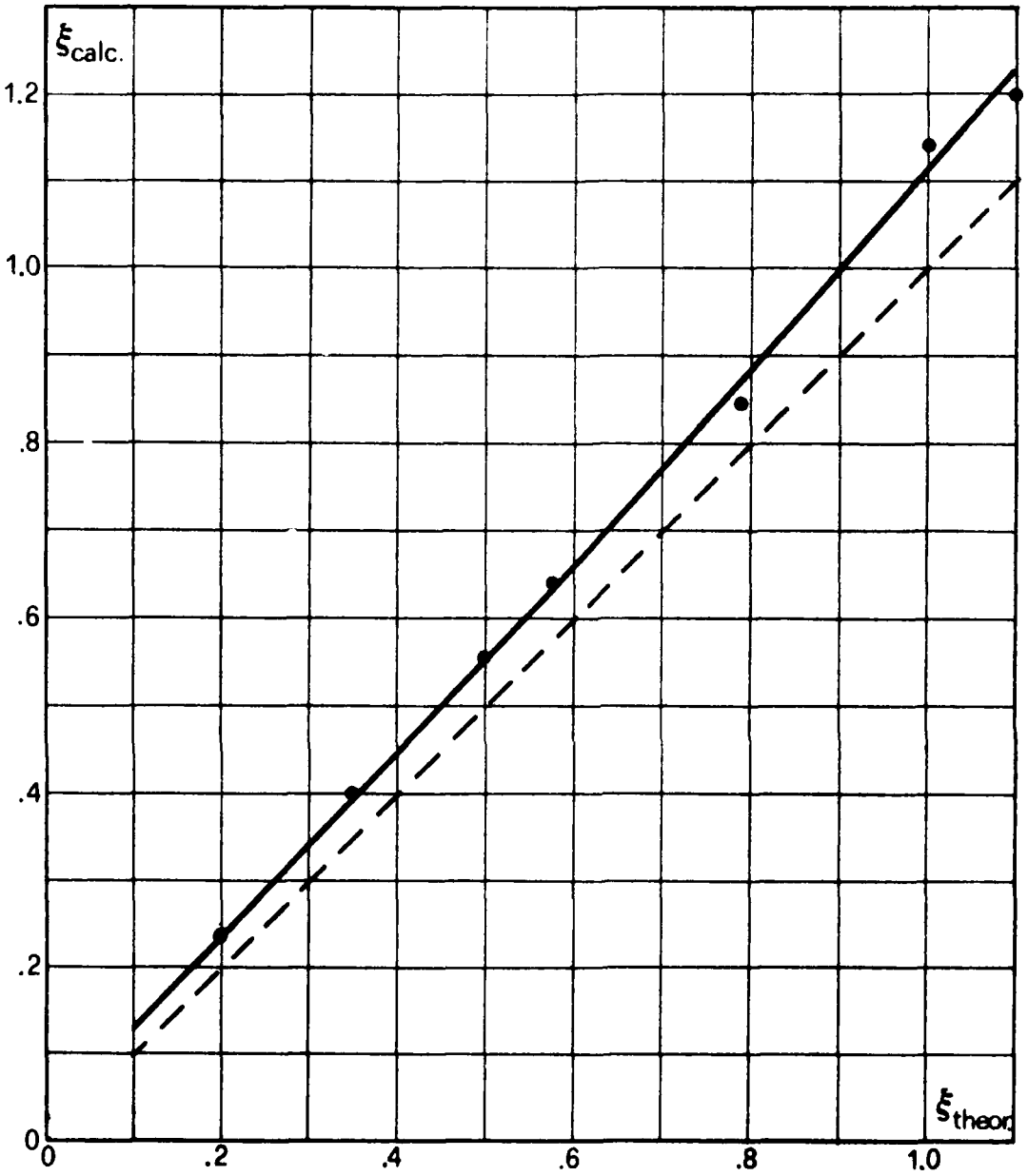

Fig.10 - Errors found in ξ evaluation due to errors in the spline module. Within range of pratical interest $0.2 \leq \xi_2 \leq 0.8$ the absolute error is lower than 0.06 and the relative error is lower than 12%.

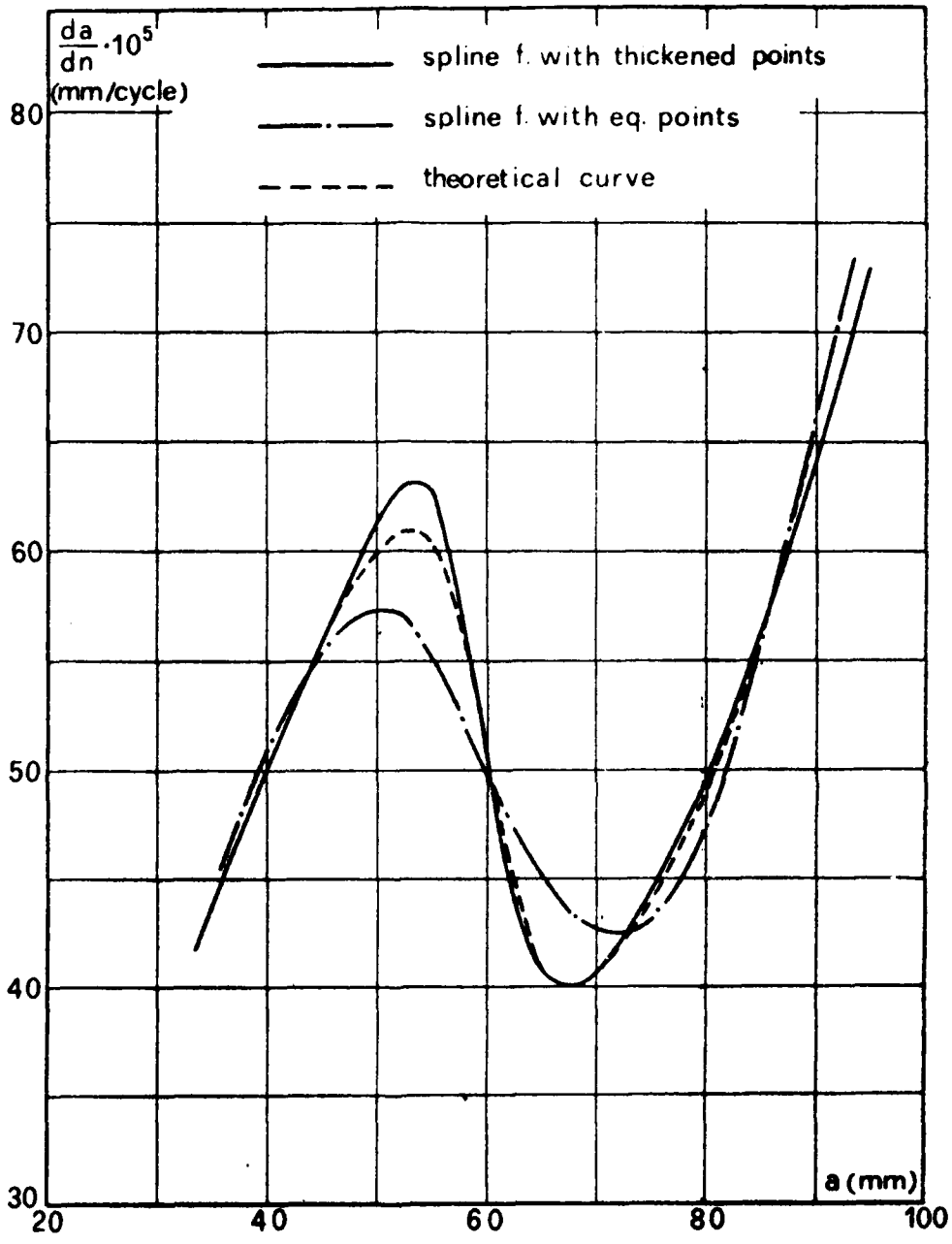

Fig.11 - Typical errors of the spline interpolation technique. The curve with equidistant points is representative of the present approach. The curve with thickened points gives an idea of potential improvements that can be obtained by a modified test technique which provides more information in the neighbourhood of maximum and minimum points.

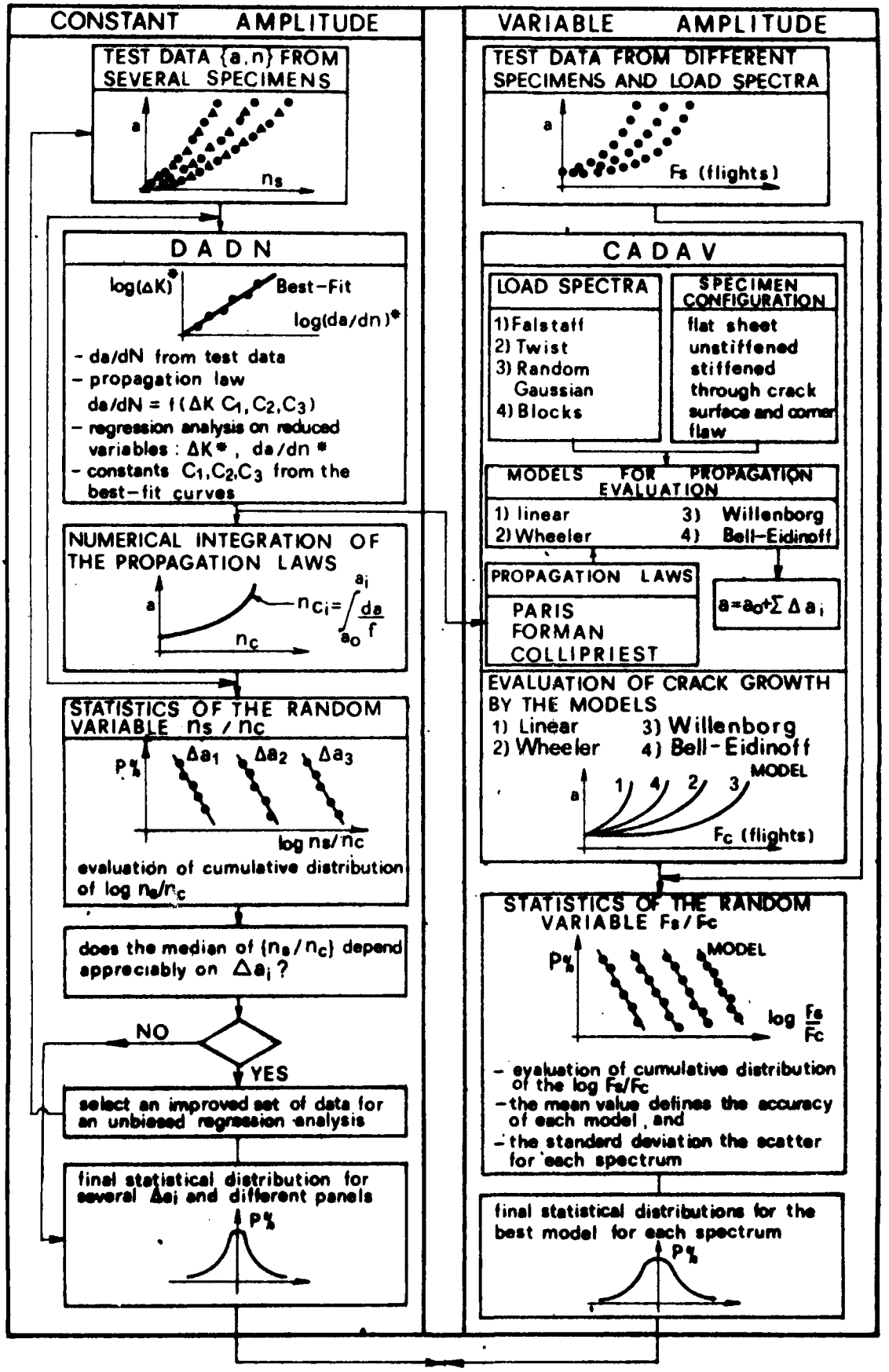

Fig.12 - Fatigue crack propagation under spectrum loading. Approach Logic.

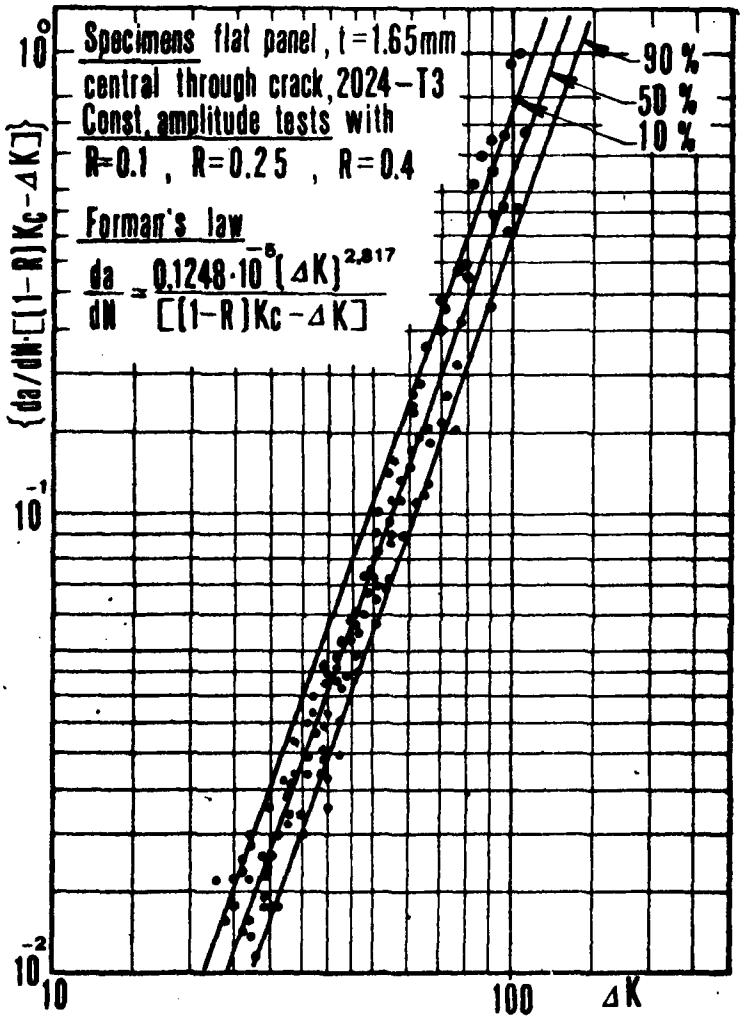

Fig.13 - Regression analysis on experimental data for evaluating Forman's law.

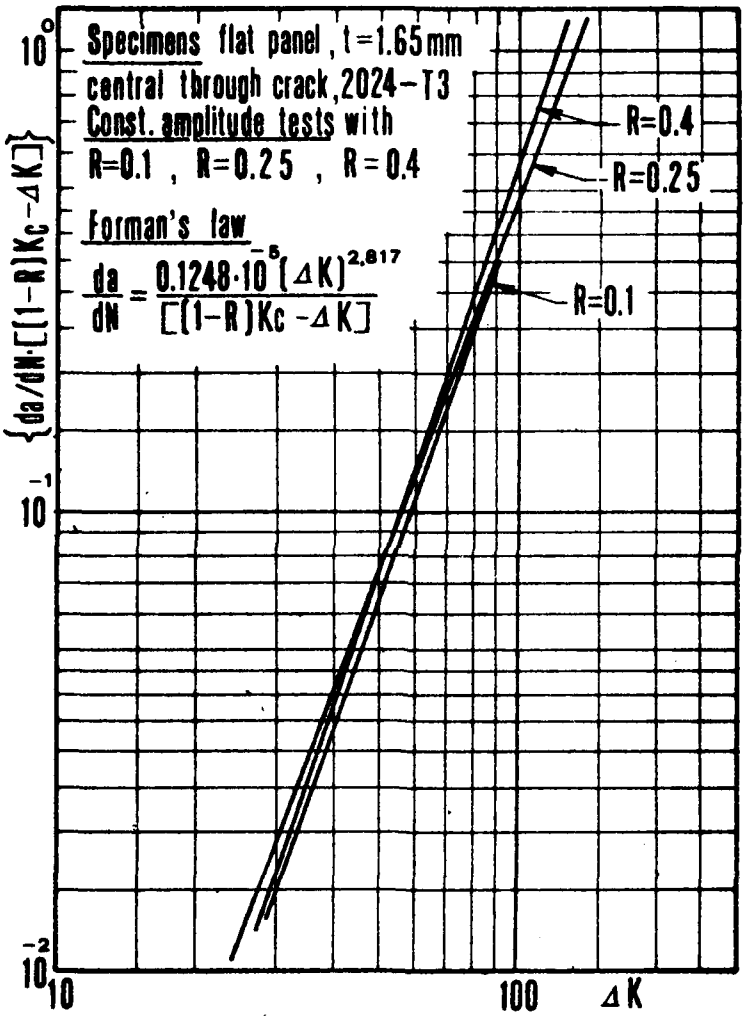

Fig.14 - Regression analysis on experimental data for evaluating Forman's law. Best-fit straigth lines for data relevant to R=cost.

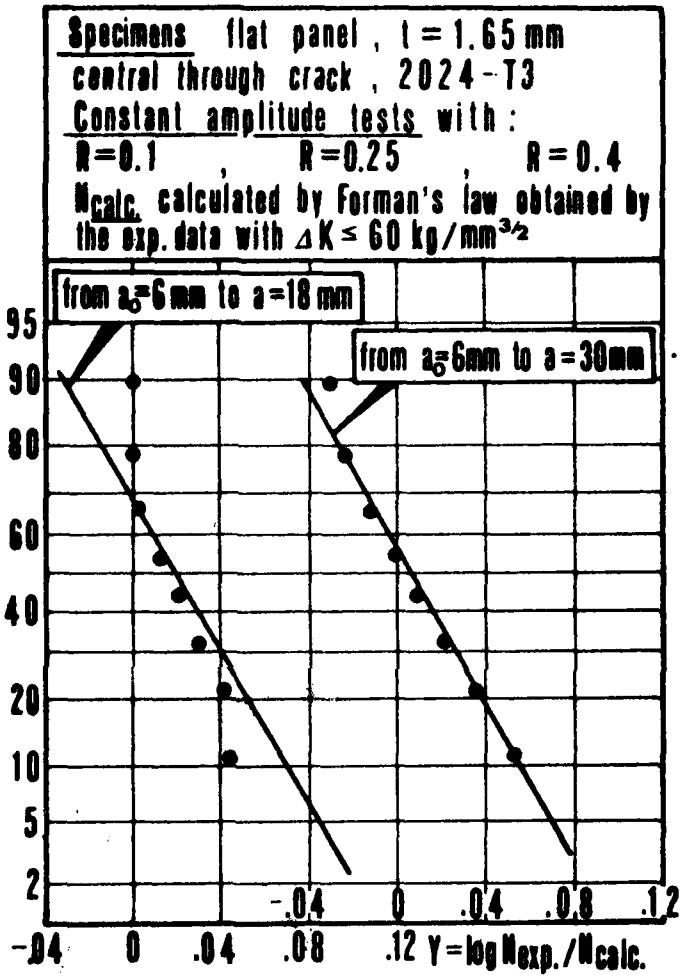

Fig.15 - Lognormal cumulative distributions of the variable n_{ex}/n_c for two ranges of damage growth.

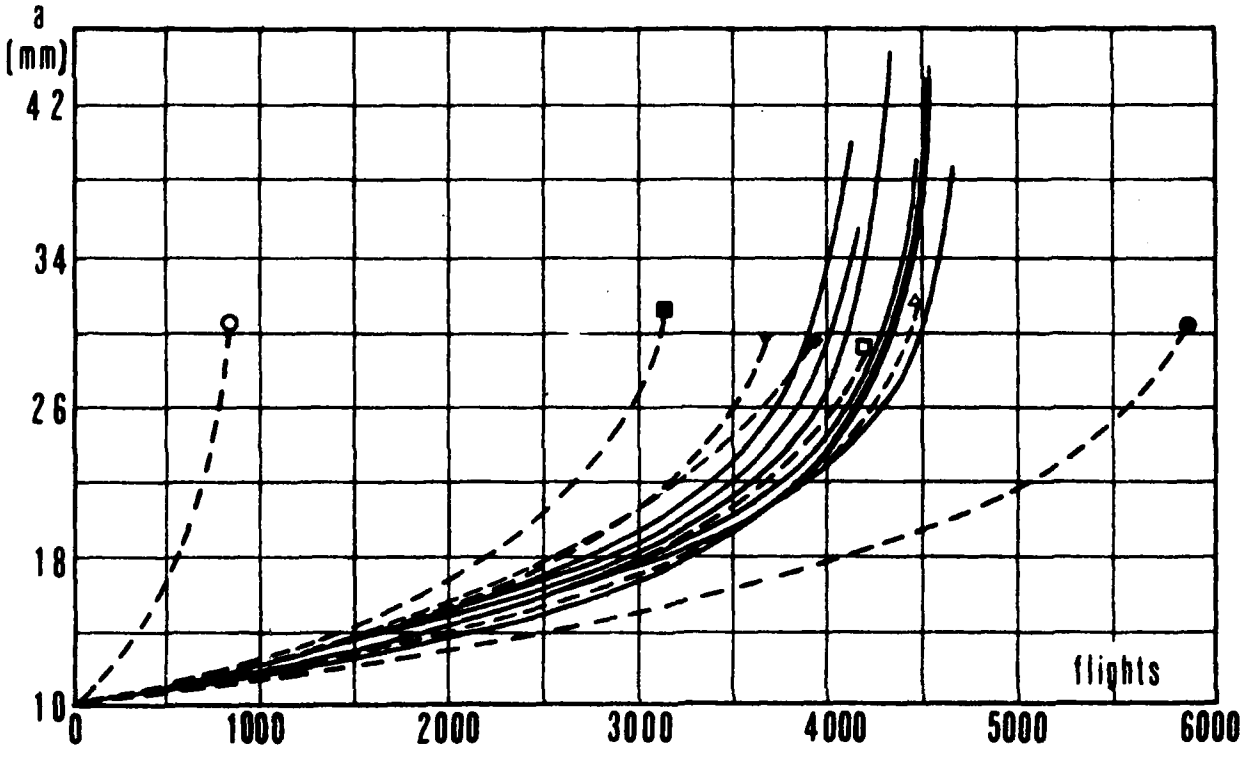

Specimens : flat panels , t = 1.65
Central through crack , 2024-T3
Load spectrum : FALSTAFF S_{max} = 235 MPa (23.9 kg/mm²)

—— experim. data (7 specimens)
o non-interactive method
◆ Bell's method
● Willenborg method
△ m=1.85
□ m=1.8
▼ m=1.6
■ m=1.4
} Wheeler method

Fig.16 - Comparison of test data with prediction.

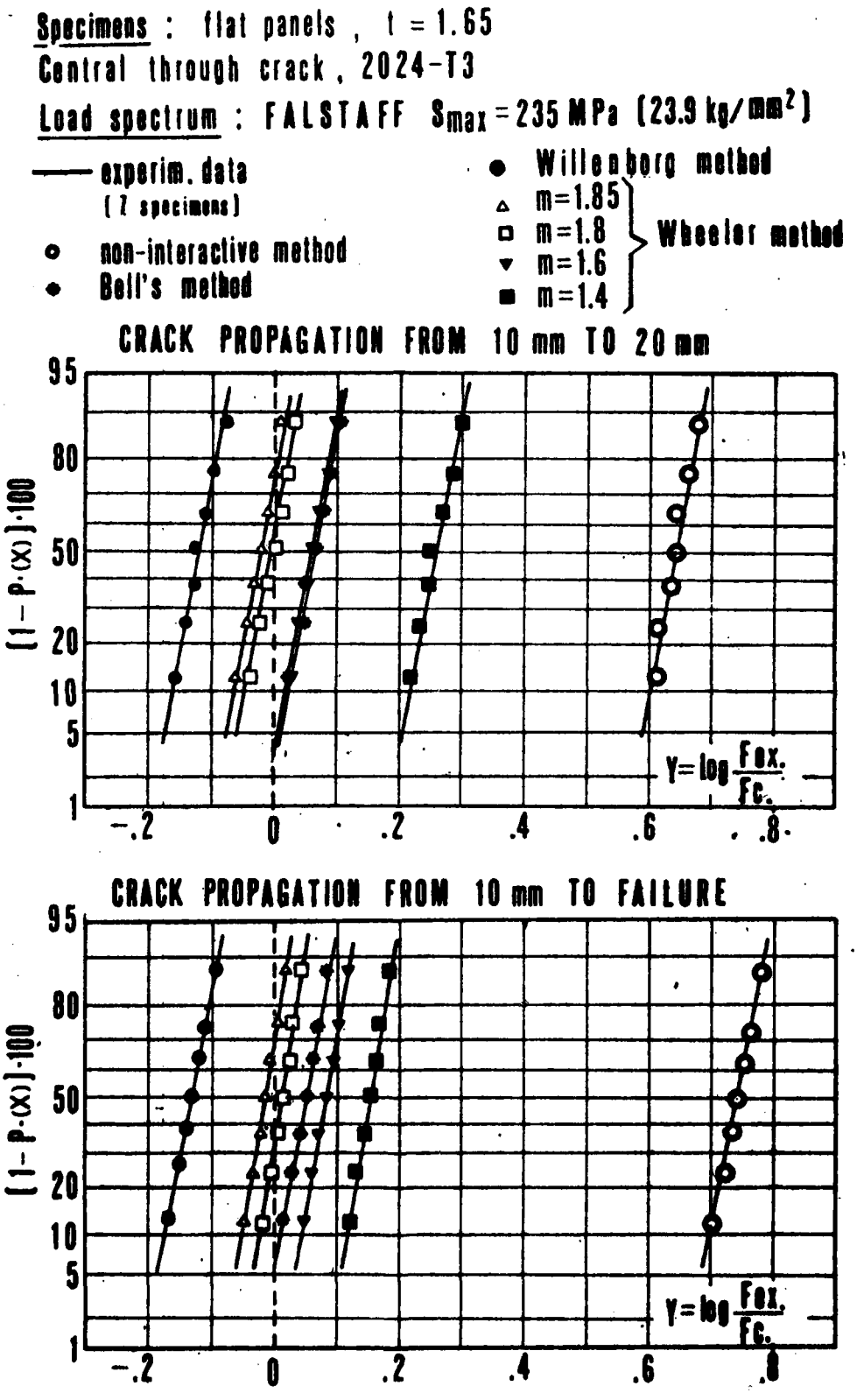

Fig.17 - Fatigue crack propagation under spectrum loading flat panel. FALSTAFF spectrum.

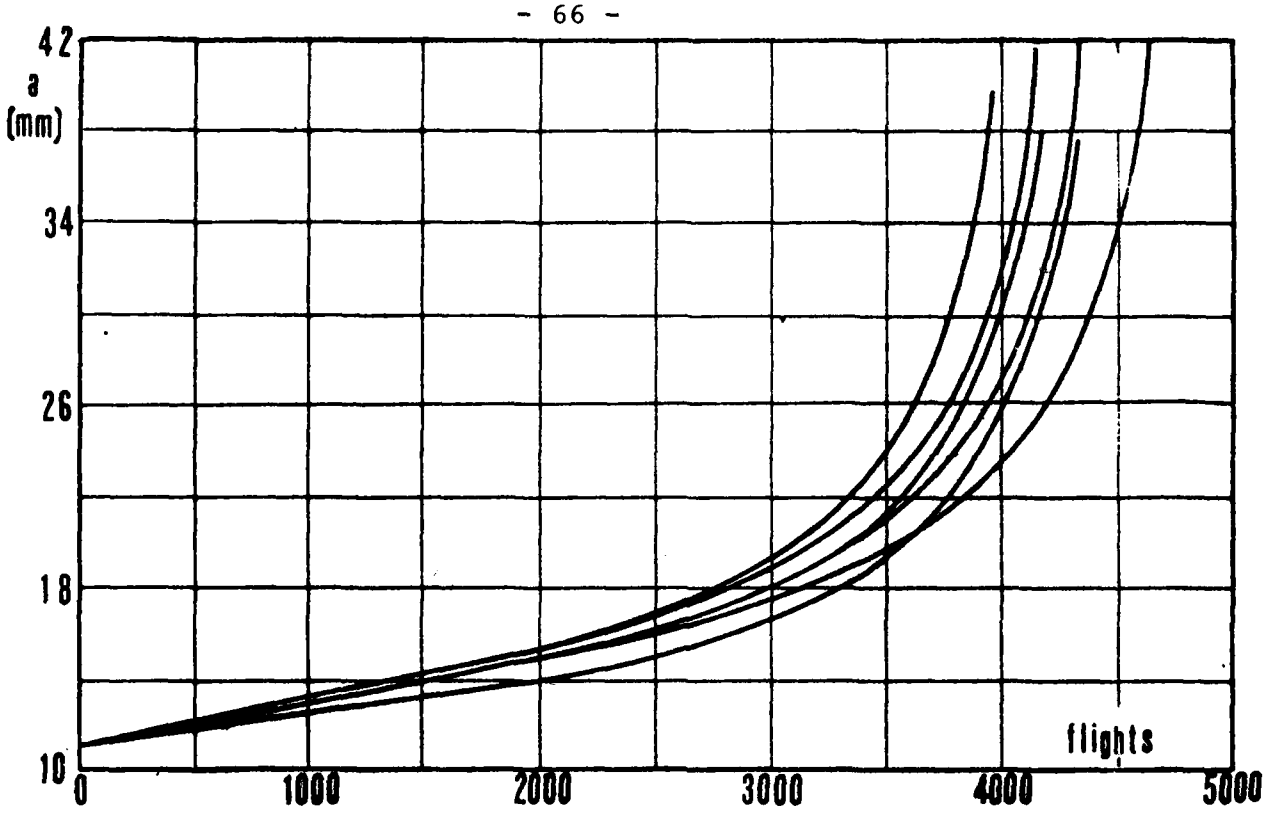

Specimens : stiffened panels, t = 1.65 mm
Central through crack, 7075 - T6
Load spectrum FALSTAFF, S_{max} = 235 MPa (23.9 kg/mm²)
—— experim. data (6 specimens)

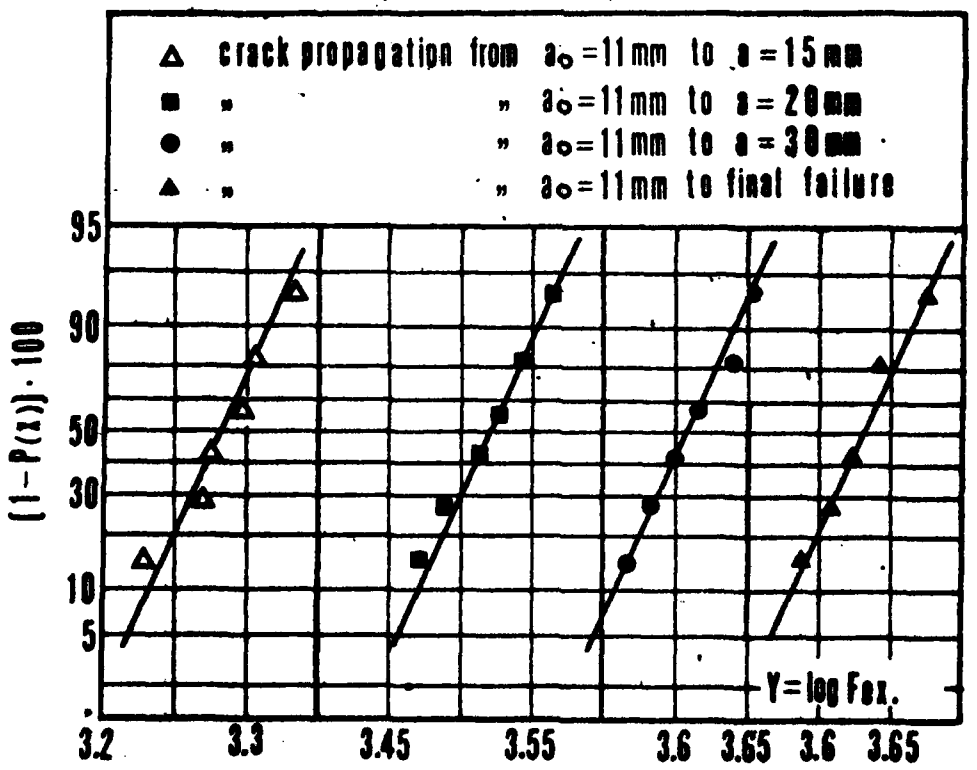

Fig.18 - Fatigue crack propagation under spectrum loading stiffened panels. FALSTAFF spectrum.

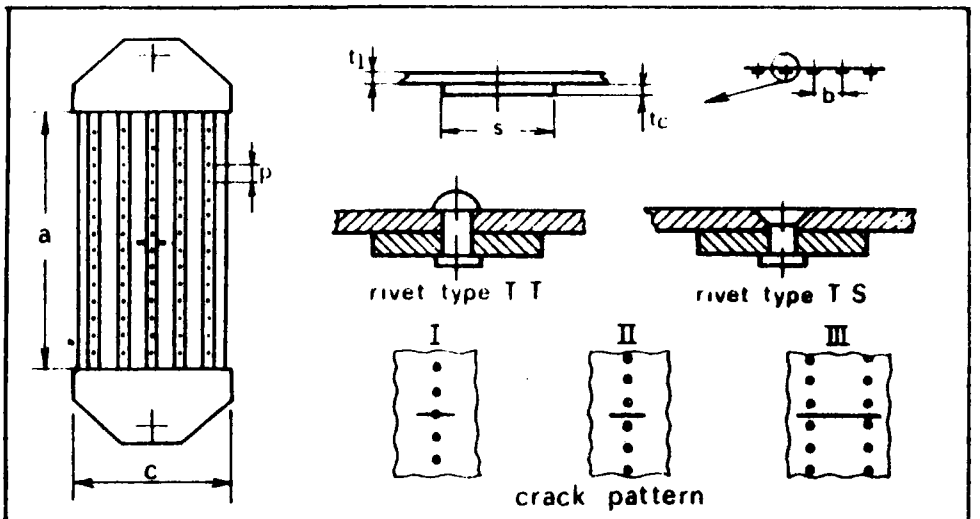

TYPE	a mm	c mm	b mm	p mm	s mm	t_l mm	t_c mm	α_c	n. panels 2024-T3	n. panels 7075 T6
C_1	500	300	60	30	18.5	1.27	0.8	0.20	2	1
C_2	"	"	"	"	21.4	"	1.6	0.45	10	10

$\alpha_c = (t_c \cdot s)/(b \cdot t_l)$

test N	panel type	material	rivet type	crack pattern	α_c	S_{max} kg/mm²	R	a_o mm	$\bar{a}$ mm	$N_o \cdot 10^{-3}$	$\bar{N} \cdot 10^{-3}$
GSF1	C_2	2024-T3	TT	II	0.45	7.0	0.4	14.	59.	4.7	221.91
2	"	"	TS	"	"	"	"	14.2	57.5	8.31	187.07
3	"	"	TT	"	"	"	"	14.	52.	5.81	194.83
4	"	"	"	"	"	6.0	"	20.5	69.5	8.97	314.2
5	"	"	TS	"	"	"	"	20.5	88.25	7.84	305.4
6	"	"	TT	"	"	6.5	"	25.	60.5	8.03	203.37
7	"	7075-T6	"	"	"	"	"	14.2	89.75	4.865	159.27
8	C_1	2024-T3	"	"	0.20	5.5	"	15.0	67.5	20.88	432.46
9	"	"	"	"	"	6.0	"	25.2	67.9	23.42	318.9
10	"	7075-T6	"	"	"	6.0	"	14.0	63.25	3.96	117.48
11	C_2	"	"	"	0.45	6.5	"	14.2	51.5	4.26	119.67
12	"	"	TS	"	"	6.5	"	14.2	71.0	2.79	59.88
13	"	"	"	"	"	6.5	"	25.	78.0	1.225	49.54
GFP1	C_2	2024-T3	"	"	"	7.0	"	14.2	61.0	17.52	200.9
2	"	"	"	"	"	6.5	"	20.5	76.4	9.28	190.24
3	"	7075-T6	"	"	"	6.5	"	25.5	69.7	4.35	72.0
ALP1	"	"	TT	"	"	6.5	"	20.	65.9	6.86	57.46
2	"	"	"	"	"	5.5	"	"	79.4	4.88	79.06
3	"	2024-T3	TS	"	"	5.5	"	"	74.0	17.27	244.30
4	"	"	"	"	"	5.5	"	"	68.6	15.23	269.85
5	"	7075-T6	"	"	"	5.0	"	"	78.7	12.29	111.24
6	"	"	"	"	"	4.5	"	"	98.3	11.43	172.24
7	"	"	"	"	"	4.5	"	"	92.9	10.20	158.50

$\bar{a}$ = Half-crack length when the central stiffener begins to be cracked.

$\bar{N}$ = Number of cycles corresponding to $\bar{a}$.

Tab.I - Main characteristics of the stiffened panels. Old series tests.

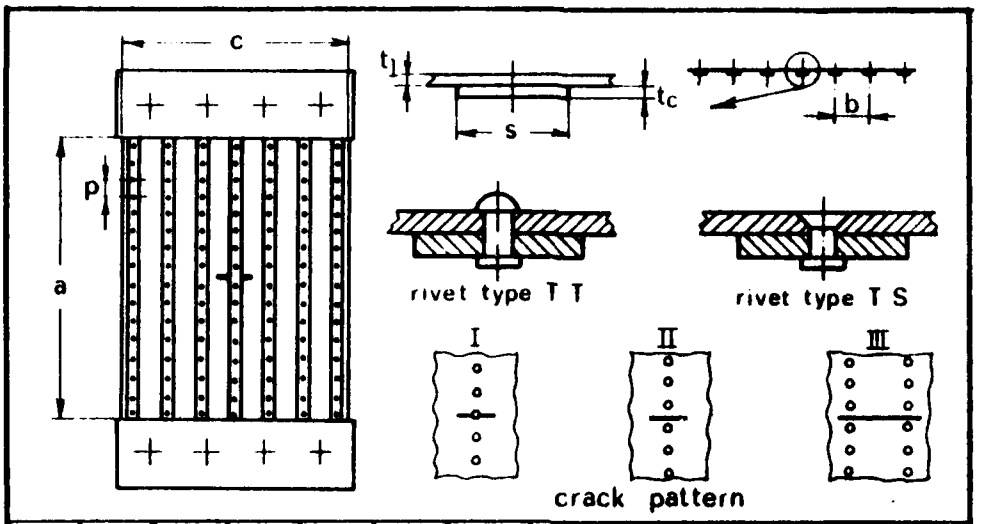

TYPE	a mm	c mm	b mm	p mm	s mm	t_l mm	t_c mm	α_c	n. panels	
									2024-T3	7075-T6
C_3	500	400	60	30	21.4	1.27	1.60	0.45	0	16

$\alpha_c = (t_c \cdot s)/(b \cdot t_\ell)$

test N	panel type	material	rivet type	crack pattern	α_c	S_{max} kg/mm^2	R	a_o mm	$\bar{a}$ mm	$N_o \cdot 10^{-3}$	$\bar{N} \cdot 10^{-3}$
CRIC1	C_3	7075-T6	TS	II	0.45	6.5	0.4	20.7	89.3	8.50	90.02
2	"	"	"	"	"	"	"	21.1	92.1	9.02	93.10
3	"	"	"	"	"	"	"	18.1	92.0	4.76	96.52
4	"	"	"	"	"	"	"	20.6	106.4	4.39	104.68
5	"	"	"	"	"	"	0.6	15.7	95.2	5.35	270.82
6	"	"	"	"	"	"	"	15.0	74.5	4.55	222.83
7	"	"	"	"	"	"	0.4	17.4	85.4	4.26	99.45
8	"	"	"	"	"	"	"	22.7	97.1	5.48	96.23
9	"	"	"	"	"	"	"	15.6	82.5	5.53	100.92
10	"	"	"	"	"	"	0.6	16.9	102.6	7.52	259.08
11	"	"	TT	"	"	"	0.4	19.5	82.0	4.79	103.09
12	"	"	"	"	"	"	"	17.7	77.2	3.29	86.23
13	"	"	"	"	"	"	"	16.6	89.4	5.70	91.22
14	"	"	"	"	"	"	"	16.5	71.5	6.91	88.97
15	"	"	"	"	"	"	"	15.9	74.3	6.82	110.39
16	"	"	"	"	"	"	"	16.7	89.1	3.20	84.29

$\bar{a}$ = Half-crack length when the central stiffener begins to be cracked.

$\bar{N}$ = Number of cycles corresponding to $\bar{a}$.

Tab.II - Main characteristics of the stiffened panels.New series tests.

CRIC-1	
a	n
23.1	13255.
25.0	17510.
25.8	19315.
27.3	22175.
28.3	23745.
29.8	26550.
30.6	28698.
33.2	33500.
35.0	35480.
38.2	39270.
39.8	41035.
42.0	43835.
42.9	44850.
44.3	46510.
44.9	47360.
46.2	48705.
47.7	50550.
50.3	53425.
52.2	55515.
53.0	56235.
54.4	57815.
55.2	58590.
56.7	60230.
57.6	61100.
58.9	62910.
60.3	64680.
61.0	65295.
63.1	67500.
64.9	70355.
65.6	71160.
67.4	73390.
68.4	74635.
70.2	77365.
71.9	79170.
73.8	81335.
75.4	83875.
79.0	87385.
81.3	90050.
83.8	92870.
85.8	94810.
88.3	97340.
89.3	98520.
90.7	99580.
93.5	102000.
96.8	104880.

CRIC-2	
a	n
21.6	13010.
23.8	17220.
24.5	19030.
25.8	22660.
28.0	26950.
29.9	28610.
31.2	31100.
32.7	33605.
34.5	36605.
36.3	38750.
38.3	41000.
40.8	44955.
42.0	46000.
44.9	49310.
47.5	52345.
49.3	54625.
51.9	57330.
54.5	60105.
57.5	63020.
58.5	64510.
59.8	66080.
60.7	67305.
61.8	68710.
63.3	70280.
64.0	71275.
65.7	73100.
67.2	74825.
67.8	76300.
70.0	78750.
71.1	80090.
72.7	82035.
73.9	83255.
75.1	85125.
77.4	87555.
78.0	89750.
81.0	91190.
83.3	93750.
85.4	95805.
87.2	98005.
89.5	100075.
92.1	102125.
93.1	103255.
95.9	105760.
97.6	107020.
100.3	108970.

CRIC-3	
a	n
21.0	11260.
21.6	13550.
23.0	16755.
24.5	20295.
26.0	23765.
27.4	26480.
29.0	29305.
30.6	32205.
32.1	35025.
33.8	37515.
35.8	40410.
37.5	42480.
40.2	45390.
41.3	46765.
43.5	49300.
45.7	51620.
47.7	53980.
50.0	56150.
51.6	57905.
53.0	59495.
54.7	61205.
55.8	62480.
57.5	64190.
59.2	66210.
61.3	68705.
63.3	71215.
64.9	72980.
66.6	74990.
68.9	77815.
71.3	80290.
72.7	81760.
75.0	84275.
76.4	85755.
78.6	88245.
80.4	90190.
82.8	92600.
84.2	93815.
85.8	95635.
88.0	97590.
89.5	99170.
92.0	101280.
95.4	104250.
96.9	105510.
99.2	107205.
101.2	108925.

Tab.III - Results of new series tests.

CRIC-4	
a	n
23.7	11855.
25.3	15435.
26.9	18305.
28.3	21125.
29.1	22680.
30.5	25095.
32.3	27750.
33.7	30160.
35.5	32790.
37.1	35160.
39.1	37695.
42.5	42135.
45.2	45245.
47.8	48130.
50.6	51325.
52.8	53525.
54.5	55475.
57.0	58390.
58.6	60100.
60.8	62460.
61.7	63610.
63.2	65165.
65.6	68065.
66.8	69605.
68.8	72145.
70.4	74125.
73.1	77425.
75.0	79685.
78.9	84100.
81.5	86840.
83.4	88835.
85.4	90770.
87.8	93140.
90.6	95795.
92.3	97415.
95.7	100425.
98.4	102660.
100.8	104675.
103.6	106965.
106.4	109075.
109.4	111280.
111.5	112750.

CRIC-5	
a	n
16.1	7930.
16.5	11950.
17.5	19985.
18.1	25390.
19.1	31600.
19.7	34920.
20.1	37885.
21.0	45415.
22.1	49070.
23.0	55000.
23.8	58460.
25.3	66020.
25.9	69415.
27.4	76240.
28.1	79135.
29.5	85440.
30.5	88990.
32.2	96010.
33.6	101605.
35.1	106700.
37.5	115010.
38.6	118535.
41.7	127960.
44.3	135295.
46.5	141605.
49.1	148595.
49.8	150895.
52.9	159065.
55.9	167390.
58.3	173900.
60.5	180450.
62.8	186890.
64.5	192625.
65.8	196335.
68.8	205510.
70.5	210720.
73.1	218535.
75.0	223920.
77.9	232495.
79.3	236495.
82.6	245590.
84.3	249965.
86.2	255000.
88.9	261935.
91.2	267085.

CRIC-6	
a	n
16.4	17570.
17.1	21305.
18.1	29670.
19.5	38845.
20.7	49420.
21.5	53800.
22.8	60360.
23.5	66010.
24.3	70120.
25.7	77070.
27.5	85500.
29.7	94450.
30.5	98555.
31.5	102675.
32.5	106825.
33.6	111260.
34.5	115705.
36.0	120230.
36.8	123405.
38.2	128000.
39.3	131640.
40.6	136750.
43.0	143500.
44.9	149650.
46.2	153070.
47.3	156160.
49.4	161650.
50.4	164890.
52.2	169065.
54.5	175105.
55.5	177775.
56.7	180840.
58.4	184490.
59.5	187805.
60.5	190655.
61.2	192200.
62.7	196485.
64.1	199945.
65.3	203185.
66.5	208520.
68.6	212015.
70.4	216985.
71.3	219000.
73.0	223625.
74.5	227380.

Tab.III - Continued.

CRIC-7	
a	n
18.3	7100.
19.5	11000.
20.7	13730.
22.0	16870.
24.0	20845.
26.0	25820.
28.0	29515.
29.4	32830.
32.0	36400.
33.5	38885.
34.5	40695.
35.8	42540.
37.0	44705.
39.1	47030.
40.6	49090.
42.0	50885.
44.0	53350.
46.7	56695.
48.7	59160.
50.0	60780.
52.0	63020.
53.7	64640.
54.9	66005.
56.2	67400.
57.2	68600.
58.1	69810.
59.2	71255.
60.5	72495.
62.0	74645.
63.3	77055.
64.8	78255.
65.7	79660.
66.8	80935.
67.8	82160.
69.1	83460.
70.5	86195.
72.4	88510.
75.6	92455.
78.2	95625.
80.7	98570.
83.0	101125.
85.4	103710.
87.3	105720.
88.9	107280.
90.6	108890.

CRIC-8	
a	n
23.3	6765.
24.5	9210.
25.6	11430.
26.5	13215.
27.9	16115.
28.5	17245.
29.8	19730.
32.5	24915.
33.2	26135.
34.8	28105.
36.3	30700.
37.5	32180.
40.5	36435.
43.5	40615.
44.9	42320.
46.0	43705.
49.2	47620.
50.5	49300.
52.6	52850.
56.4	56275.
59.0	59255.
60.3	60235.
62.4	62845.
63.2	64160.
64.3	65705.
66.3	68260.
67.8	70205.
70.5	73665.
71.7	75160.
74.3	78335.
75.2	79430.
77.0	81715.
78.7	83595.
81.8	86790.
83.2	88890.
84.3	91025.
86.8	92180.
91.8	95735.
93.2	98755.
94.3	99855.
97.1	101710.
102.6	105820.
106.1	108570.

CRIC-9	
a	n
16.4	7430.
17.6	10850.
18.8	13085.
19.3	15820.
20.4	18235.
22.0	22005.
23.0	23675.
24.1	25950.
25.9	28675.
27.4	31760.
28.4	33830.
29.3	35260.
30.4	37305.
31.2	38910.
32.7	41580.
34.0	43635.
35.3	45895.
36.8	48215.
39.3	51610.
41.0	54325.
42.8	56780.
44.4	58880.
46.0	60995.
47.5	62835.
51.7	67740.
53.5	69835.
55.0	71785.
57.2	74490.
58.8	76045.
60.3	77980.
62.2	80130.
63.7	82145.
65.1	84125.
66.3	85590.
68.1	88065.
69.7	90265.
70.8	91775.
71.9	93290.
73.4	95380.
75.3	97675.
76.8	99585.
78.4	101575.
81.1	104865.
82.5	106450.
84.7	108980.

Tab.III - Continued.

CRIC-10	
a	n
17.6	13410.
18.5	18820.
19.4	26740.
20.6	34100.
22.0	41500.
22.8	47320.
24.1	53610.
25.3	59420.
26.8	66390.
27.8	73780.
30.3	82500.
31.7	89310.
34.0	96650.
36.8	103090.
37.5	108510.
39.8	115430.
42.0	121020.
43.1	125580.
46.2	139070.
48.8	140180.
51.8	148810.
54.0	155200.
56.7	162450.
58.4	166630.
60.3	171380.
62.1	176210.
63.6	180770.
65.5	185040.
67.3	190070.
69.8	197030.
71.0	200560.
72.9	205540.
74.8	210390.
76.2	214000.
77.7	217820.
79.6	221610.
81.4	226180.
83.1	229740.
84.9	233520.
86.9	238500.
89.8	244490.
92.6	250110.
94.7	254880.
97.2	259510.
99.8	263590.

CRIC-11	
a	n
20.5	7645.
21.5	11700.
23.3	17115.
24.1	18745.
25.4	21855.
26.4	24670.
28.0	26705.
28.6	28135.
29.5	31285.
30.3	33000.
31.4	35100.
32.8	38160.
34.4	41095.
36.5	44705.
38.3	47610.
39.8	50140.
41.1	52105.
42.3	54150.
43.9	56480.
46.2	59565.
47.5	61595.
49.3	63890.
52.1	67640.
53.8	70010.
56.0	72585.
57.7	74855.
59.5	77475.
61.3	79880.
63.3	82725.
65.3	85505.
66.9	87575.
69.6	91420.
71.2	94750.
73.9	96975.
75.3	99505.
76.6	100895.
77.9	102715.
78.8	103865.
79.9	105195.
82.0	107880.
83.3	109680.
85.0	111230.
86.3	112830.
87.3	113920.

CRIC-12	
a	n
18.8	7000.
20.5	10700.
21.7	13485.
23.0	16135.
24.8	19670.
26.9	22910.
28.3	25190.
29.6	27365.
30.9	29010.
32.3	31175.
33.7	33380.
35.4	35860.
36.5	37390.
37.8	39200.
39.0	40805.
41.2	43715.
43.1	45980.
44.2	47385.
45.7	49160.
47.7	51570.
49.7	53590.
51.7	55890.
53.4	57855.
55.2	59945.
57.3	62115.
58.7	63665.
60.2	65505.
61.8	67000.
63.3	69165.
64.8	71080.
65.9	72590.
67.3	74695.
68.3	76260.
69.3	78045.
71.0	80775.
71.7	83245.
73.4	84615.
74.1	85810.
75.8	87505.
77.2	89525.
78.2	90920.
79.1	92250.
80.8	94550.
82.8	96220.
83.8	97265.

Tab.III - Continued.

CRIC-13	
a	n
18.1	10500.
19.9	15730.
22.2	21995.
24.2	25915.
25.8	29075.
27.1	31285.
28.4	33420.
30.4	36945.
31.8	38990.
34.5	42875.
36.2	45015.
37.6	46525.
39.8	49015.
42.5	51855.
43.5	53090.
45.5	55175.
47.7	57355.
49.6	59435.
50.9	60805.
52.9	62635.
55.2	64775.
56.9	66395.
58.5	67690.
60.4	69570.
61.4	70570.
63.3	72275.
65.0	73805.
66.6	75350.
68.8	77665.
69.7	78490.
70.7	79415.
71.9	80520.
72.8	81505.
74.2	82905.
75.6	84065.
76.8	85220.
78.8	86675.
80.4	88750.
83.7	91765.
85.9	93715.
89.4	96920.
97.9	103755.

CRIC-14	
a	n
16.5	6915.
17.5	10695.
18.9	14650.
20.4	18830.
21.6	21945.
22.5	24140.
25.6	31375.
27.1	34595.
28.2	36605.
29.5	39145.
30.7	41230.
31.7	43150.
33.0	45265.
33.8	46560.
34.5	47860.
36.8	51255.
37.7	52715.
39.3	55005.
40.7	56890.
42.5	59300.
45.3	63000.
48.0	66490.
49.7	68500.
51.1	70140.
52.9	72280.
54.3	73820.
55.9	75720.
58.2	78475.
59.5	80190.
61.3	82500.
63.6	85425.
65.2	87200.
66.1	88720.
67.6	90450.
70.1	94130.
71.5	95880.
73.7	98705.
75.3	100940.
76.1	101870.

CRIC-15	
a	n
16.5	10715.
16.9	13875.
17.5	17140.
17.9	19455.
18.5	21890.
19.5	25745.
20.2	29570.
20.9	32660.
21.9	35565.
22.7	38095.
24.0	42625.
25.3	46910.
26.5	50915.
27.5	54995.
28.7	58595.
29.6	61625.
30.7	64615.
32.3	67650.
34.0	70970.
35.6	73715.
37.8	76895.
41.3	81130.
43.3	83965.
45.8	86555.
49.6	90810.
52.4	93665.
54.8	95895.
56.7	97715.
57.8	98875.
59.3	100240.
60.4	101230.
61.6	102370.
62.7	103365.
64.1	104695.
65.1	105600.
66.9	107550.
70.0	110770.
72.3	113260.
74.3	117215.
78.4	119800.
79.7	120945.
80.5	121685.
81.2	122285.
83.2	124045.

Tab.III - Continued.

CRIC-16	
a	n
18.6	8385.
20.0	11345.
21.9	15375.
23.7	18915.
26.2	23400.
28.4	26750.
32.5	33175.
35.0	36405.
37.0	38700.
40.9	43340.
42.9	45525.
45.3	47935.
47.3	49910.
50.3	52640.
53.4	55675.
55.4	57585.
56.7	58845.
58.7	60560.
60.7	62355.
64.2	65300.
65.9	67365.
68.1	69395.
68.8	70125.
70.0	71210.
71.1	72175.
72.1	73060.
73.3	74245.
74.3	75165.
76.2	76880.
76.8	77630.
77.3	78000.
78.4	78830.
79.4	79640.
80.8	80855.
82.3	82030.
85.4	84405.
86.3	85075.
87.8	86555.
89.1	87495.
92.7	90030.
94.6	91330.
95.3	91765.
95.9	92230.
96.8	92755.
97.8	93415.

Tab.III - Continued.

TEST	$\bar{\xi}_2$	η	TEST	$\bar{\xi}_2$	$\bar{\eta}$
CRIC-4	0.7	0.21	CRIC-9	0.45	0.14
CRIC-8	0.6	0.14	CRIC-5	0.3	0.14
CRIC-10	0.75	0.14	CRIC-6	1.0	0.14
CRIC-2	0.45	0.21	CRIC-1	0.3	0.14
CRIC-3	0.5	0.14	CRIC-7	0.4	0.14
GSF-13	0.6	0.14	GFP-3	0.3	0.14
ALP-6	0.5	0.21	ALP-5	0.25	0.21
GFP-2	0.9	0.21	ALP-3	0.65	0.14
ALP-4	0.5	0.14	GSF-12	0.3	0.14
ALP-7	0.9	0.14	GSF-2	0.4	0.07
GSF-5	0.45	0.14	GFP-1	0.95	0.07

ξ_2 = Flex./Flex. Douglas

$\eta = P_f/A_r \cdot S_y$ $\qquad$ $S_y = 36$ Kg/mm^2

Tab.IVa - Optimum values of ξ and η parameters for countersunk rivets tests.

TEST	$\bar{\xi}_2$	$\bar{\eta}$	TEST	$\bar{\xi}_2$	$\bar{\eta}$
GSF-1	0.65	0.14	GSF-4	0.08	0.14
GSF-3	0.2	0.14	GSF-7	0.2	0.21
ALP-2	0.6	0.07	GFP-8	0.05	0.07
ALP-1	0.2	0.21	GSF-11	0.5	0.21
GSF-8	0.7	0.07	GSF-9	0.02	0.07
GSF-10	0.22	0.21	CRIC-11	0.6	0.14
CRIC-12	0.	0.21	CRIC-13	0.6	0.07
CRIC-14	0.4	0.14	CRIC-15	0.5	0.07
CRIC-16	0.7	0.07			

ξ_2 = Flex./Flex. Douglas

$\eta = P_f/A_r \cdot S_y$ $\qquad S_y = 36$ Kg/mm^2

Tab.IVb - Optimum values of ξ and η parameters for round head rivets tests.